

## 1 Synthesis of data products for ocean carbonate chemistry

2  
3 Li-Qing Jiang<sup>1,2</sup>, Amanda Fay<sup>3</sup>, Jens Daniel Müller<sup>4,5</sup>, Luke Gregor<sup>4,6</sup>, Alizée Roobaert<sup>7</sup>, Lydia  
4 Keppler<sup>8</sup>, Dustin Carroll<sup>9,10</sup>, Siv K. Lauvset<sup>11</sup>, Tim DeVries<sup>12</sup>, Judith Hauck<sup>13,14</sup>, Christian  
5 Rödenbeck<sup>15</sup>, Nicolas Metzler<sup>16</sup>, Andrea J. Fassbender<sup>17</sup>, Jean-Pierre Gattuso<sup>18,19</sup>, Peter  
6 Landschützer<sup>7</sup>, Rik Wanninkhof<sup>20</sup>, Christopher Sabine<sup>21</sup>, Simone R. Alin<sup>17</sup>, Mario Hoppema<sup>12</sup>,  
7 Are Olsen<sup>22</sup>, Matthew P. Humphreys<sup>23</sup>, Kunal Chakraborty<sup>24</sup>, Ana C. Franco<sup>25,26</sup>, Kumiko  
8 Azetsu-Scott<sup>27</sup>, Dorothee C. E. Bakker<sup>28</sup>, Leticia Barbero<sup>20,29</sup>, Nicholas R. Bates<sup>30,31</sup>, Nicole  
9 Besemer<sup>20</sup>, Henry C. Bittig<sup>32</sup>, Albert E. Boyd<sup>20,29</sup>, Daniel Broullón<sup>33</sup>, Wei-Jun Cai<sup>34</sup>, Brendan R.  
10 Carter<sup>35,17</sup>, Thi-Tuyet-Trang Chau<sup>36,37</sup>, Chen-Tung Arthur Chen<sup>38</sup>, Frédéric Cyr<sup>39,40</sup>, John E.  
11 Dore<sup>41</sup>, Ian Enochs<sup>20</sup>, Richard A. Feely<sup>17</sup>, Hernan E. Garcia<sup>2</sup>, Marion Gehlen<sup>36</sup>, Prasanna Kanti  
12 Ghoshal<sup>24</sup>, Lucas Gloege<sup>3</sup>, Melchor González-Dávila<sup>42</sup>, Nicolas Gruber<sup>4</sup>, Debby Ianson<sup>43</sup>,  
13 Yosuke Iida<sup>44</sup>, Masao Ishii<sup>45</sup>, A.P. Joshi<sup>24</sup>, Esther Kennedy<sup>46</sup>, Alex Kozyr<sup>1,2</sup>, Nico Lange<sup>10</sup>,  
14 Claire Lo Monaco<sup>16</sup>, Derek P. Manzello<sup>47</sup>, Galen A. McKinley<sup>3</sup>, Natalie M. Monacci<sup>48</sup>, Xose A.  
15 Padin<sup>33</sup>, Ana M. Palacio-Castro<sup>20,29</sup>, Fiz F. Pérez<sup>33</sup>, J. Magdalena Santana-Casiano<sup>42</sup>, Jonathan  
16 Sharp<sup>35,17</sup>, Adrienne Sutton<sup>17</sup>, Jim Swift<sup>49</sup>, Toste Tanhua<sup>50</sup>, Maciej Telszewski<sup>51</sup>, Jens Terhaar<sup>52</sup>,  
17 <sup>53</sup>, Ruben van Hooidonk<sup>54</sup>, Anton Velo<sup>33</sup>, Andrew J. Watson<sup>55</sup>, Angelique E. White<sup>21</sup>, Zelun  
18 Wu<sup>34</sup>, Liang Xue<sup>56</sup>, Hyelim Yoo<sup>1,2</sup>, Jiye Zeng<sup>57</sup>, Guorong Zhong<sup>58</sup>.

20 <sup>1</sup>Cooperative Institute for Satellite Earth System Studies, Earth System Science Interdisciplinary Center, University  
21 of Maryland, College Park, Maryland 20740, United States.

22 <sup>2</sup>NOAA/NESDIS National Centers for Environmental Information, Silver Spring, Maryland 20910, United States.

23 <sup>3</sup>Columbia University and Lamont-Doherty Earth Observatory, Palisades, New York 10964, United States.

24 <sup>4</sup>Environmental Physics, Institute of Biogeochemistry and Pollutant Dynamics, ETH Zürich, Zürich, Switzerland.

25 <sup>5</sup>Carbon to Sea Initiative, Washington, ~~D.C.~~, United States.

26 <sup>6</sup>Swiss Data Science Center, ETH Zurich and EPFL, Zurich, Switzerland.

27 <sup>7</sup>Flanders Marine Institute (VLIZ), Jacobsenstraat 1, 8400 Ostend, Belgium.

28 <sup>8</sup>Vycarb Inc., Brooklyn, New York, United States.

29 <sup>9</sup>Moss Landing Marine Laboratories, San José State University, Moss Landing, California, United States.

30 <sup>10</sup>Jet Propulsion Laboratory, California Institute of Technology, Pasadena, California, United States.

31 <sup>11</sup>NORCE Research AS, Bjerknes Centre for Climate Research, Bergen, Norway.

32 <sup>12</sup>Department of Geography and Earth Research Institute, University of California, Santa Barbara, California, United  
33 States.

34 <sup>13</sup>Alfred Wegener Institute Helmholtz Centre for Polar and Marine Research, Bremerhaven, Germany

35 <sup>14</sup>University of Bremen, Department 02 Biology/Chemistry Bremen, Germany.

36 <sup>15</sup>Max Planck Institute for Biogeochemistry, Jena, Germany.

37 <sup>16</sup>Laboratoire LOCEAN/IPSL, Sorbonne Université-CNRS-IRD-MNHN, 75005 Paris, France.

38 <sup>17</sup>NOAA/OAR Pacific Marine Environmental Laboratory, Seattle, Washington 98115, United States.

39 <sup>18</sup>Sorbonne Université, CNRS, Laboratoire d'Océanographie de Villefranche, 06230 Villefranche-sur-Mer, France.

Deleted: <sup>6</sup>

Deleted: District of Columbia

- 42 <sup>19</sup>Institute for Sustainable Development and International Relations, Paris, France.
- 43 <sup>20</sup>NOAA/OAR Atlantic Oceanographic and Meteorological Laboratory, Miami, Florida 33149, United States.
- 44 <sup>21</sup>Department of Oceanography, University of Hawai'i at Mānoa, 1000 Pope Rd., Honolulu, Hawaii 96822, United  
45 States.
- 46 <sup>22</sup>Geophysical Institute, University of Bergen and Bjerknes Centre for Climate Research, Bergen, Norway.
- 47 <sup>23</sup>Department of Ocean Systems, NIOZ Royal Netherlands Institute for Sea Research, Texel, the Netherlands.
- 48 <sup>24</sup>Indian National Center for Ocean Information Services, Ministry of Earth Sciences, Hyderabad, India.
- 49 <sup>25</sup>Department of Earth, Ocean and Atmospheric Sciences, University of British Columbia, Vancouver, BC, Canada.
- 50 <sup>26</sup>Current affiliation: Earth Sciences Department, Barcelona Supercomputing Center, Barcelona, Spain.
- 51 <sup>27</sup>Fisheries and Oceans, Canada, Bedford Institute of Oceanography, Dartmouth, Nova Scotia, Canada.
- 52 <sup>28</sup>Centre for Ocean and Atmospheric Sciences, School of Environmental Sciences, University of East Anglia,  
53 Norwich NR4 7TJ, United Kingdom.
- 54 <sup>29</sup>Cooperative Institute for Marine and Atmospheric Studies, Rosenstiel School of Marine and Atmospheric Science,  
55 University of Miami, Miami, Florida 33149, United States.
- 56 <sup>30</sup>Bermuda Institute of Ocean Sciences, ASU-BIOS, 17 Biological Lane, St. Georges, GEO1, Bermuda.
- 57 <sup>31</sup>School of Ocean Futures, Arizona State University, Tempe, Arizona 85281, United States.
- 58 <sup>32</sup>Leibniz Institute for Baltic Sea Research Warnemünde (IOW), Rostock, Germany.
- 59 <sup>33</sup>Instituto de Investigaciones Mariñas, IIM – CSIC, Vigo, Spain.
- 60 <sup>34</sup>School of Marine Science and Policy, University of Delaware, Newark, Delaware 19716, United States.
- 61 <sup>35</sup>Cooperative Institute for Climate, Ocean, and Ecosystem Studies, University of Washington, Seattle, Washington,  
62 United States.
- 63 <sup>36</sup>Laboratoire des Sciences du Climat et de l'Environnement, LSCE-IPSL, CEA-CNRS-UVSQ, Université Paris-  
64 Saclay, 91191 Gif-sur-Yvette, France.
- 65 <sup>37</sup>Laboratoire Interdisciplinaire des Sciences du Numérique (LISN), Centre de recherches INRIA, Université Paris-  
66 Saclay, René Thom, F-91190, Gif-sur-Yvette, France.
- 67 <sup>38</sup>Department of Oceanography, National Sun Yat-Sen University, Kaohsiung, Taiwan.
- 68 <sup>39</sup>Northwest Atlantic Fisheries Centre, Fisheries and Oceans Canada, St. John's, Newfoundland and Labrador,  
69 Canada.
- 70 <sup>40</sup>Current affiliation: Centre for Fisheries Ecosystems Research, Fisheries and Marine Institute of Memorial  
71 University of Newfoundland, St. John's, Canada.
- 72 <sup>41</sup>Department of Land Resources and Environmental Sciences, Montana State University, Bozeman, Montana,  
73 United States.
- 74 <sup>42</sup>Instituto de Oceanografía Cambio Global, IOCAG, Universidad de Las Palmas de Gran Canaria, 35017 Las  
75 Palmas de Gran Canaria, Spain.
- 76 <sup>43</sup>Institute of Ocean Sciences, Fisheries and Oceans Canada, Sidney, British Columbia, Canada.
- 77 <sup>44</sup>Atmosphere and Ocean Department, Japan Meteorological Agency, 3-6-9 Toranomon, Minato City, Tokyo, Japan.
- 78 <sup>45</sup>Meteorological Research Institute, Japan Meteorological Agency, Tsukuba, Japan.
- 79 <sup>46</sup>University of California Davis, Bodega Marine Laboratory, Davis, California, United States.

Deleted: o

81 <sup>47</sup>Coral Reef Watch, U.S. National Oceanic and Atmospheric Administration, College Park, Maryland, United  
82 States.  
83 <sup>48</sup>College of Fisheries and Ocean Sciences, University of Alaska Fairbanks, Fairbanks, Alaska, United States.  
84 <sup>49</sup>Scripps Institution of Oceanography, La Jolla, California, United States.  
85 <sup>50</sup>GEOMAR Helmholtz Centre for Ocean Research Kiel, Kiel, Germany.  
86 <sup>51</sup>International Ocean Carbon Coordination Project, Institute of Oceanology of Polish Academy of Sciences, Sopot,  
87 Poland.  
88 <sup>52</sup>Climate and Environmental Physics, Physics Institute, University of Bern, Bern, Switzerland.  
89 <sup>53</sup>Oeschger Centre for Climate Change Research, University of Bern, Bern, Switzerland.  
90 <sup>54</sup>Science for Climate Change Resilience, Boulder, Colorado 80302, United States.  
91 <sup>55</sup>Global Systems Institute, University of Exeter, Exeter, United Kingdom.  
92 <sup>56</sup>First Institute of Oceanography, and Key Laboratory of Marine Science and Numerical Modeling, Ministry of  
93 Natural Resources, Qingdao, China.  
94 <sup>57</sup>National Institute for Environmental Studies, Tsukuba, Japan.  
95 <sup>58</sup>Institute of Oceanology, Chinese Academy of Sciences, Qingdao, China.  
96 *Correspondence to:* Li-Qing Jiang (liqing.jiang@noaa.gov)

97 **Abstract.** As the largest active carbon reservoir on Earth, the ocean is a cornerstone of the global carbon cycle,  
98 playing a pivotal role in modulating ocean health and the Earth's climate system. Understanding these crucial roles  
99 requires access to a broad array of data products documenting the changing chemistry of the global ocean as a vast  
100 and interconnected system. This review article provides an overview of 68 existing ocean carbonate chemistry data  
101 products and data product sets, encompassing compilations of cruise datasets, derived gap-filled data products,  
102 model simulations, and compilations thereof. It is intended to help researchers identify and access data products that  
103 best align with their research objectives, thereby advancing our understanding of the ocean's evolving carbonate  
104 chemistry. The list will be updated periodically to incorporate new data products. The most up-to-date list is  
105 available at <https://oceanco2.github.io/co2-products/>. New data products can be submitted through  
106 <https://forms.gle/g8hYm37Wg1Uifg8E8>.

## 107 1 Introduction

108 Since the onset of the Industrial Revolution in 1750, human activities, such as the burning of fossil fuels, cement  
109 production, and land-use change, have emitted ~2600 Gt carbon dioxide (CO<sub>2</sub>) (1 Gt = 10<sup>15</sup> g, 1 Gt CO<sub>2</sub> = 0.273 Gt  
110 Carbon, or Gt C) into the atmosphere, causing the atmospheric CO<sub>2</sub> levels to increase by ~50% (DeVries, 2022a;  
111 Friedlingstein et al., 2025; Tans and Keeling, 2025). The global carbon cycle, encompassing the exchange of CO<sub>2</sub>  
112 among the atmosphere, oceans, terrestrial ecosystems, and geosphere, plays a critical role in regulating atmospheric  
113 CO<sub>2</sub> levels (Archer, 2010; DeVries, 2022a; Friedlingstein et al., 2025). As the largest dynamic CO<sub>2</sub> reservoir, the  
114 ocean holds approximately 45 times the amount of carbon found in the atmosphere currently and actively exchanges

Deleted: 3.667

116 it with the air above and sediments below. On timescales from decades to millennia, the ocean imposes a dominant  
117 control over atmospheric CO<sub>2</sub> levels (Revelle and Suess, 1957; Broecker, 1982; Archer et al., 2009; DeVries,  
118 2022a).

119 The ocean currently absorbs about a quarter of human-caused CO<sub>2</sub> emissions (Sabine et al., 2004a; Gruber et al.,  
120 2019a; Carroll et al., 2022; Crisp et al., 2022; Terhaar et al., 2022a; Gruber et al., 2023; DeVries et al., 2023; Müller  
121 et al., 2023a; Schimel and Carroll, 2024; Terhaar, 2025). The chemistry of the ocean has been shifting as a result of  
122 anthropogenic CO<sub>2</sub> increase in the ocean (Feely et al., 2023; Ma et al., 2023; Müller et al., 2023a; Fassbender et al.,  
123 2023; Keppler et al., 2023a; Jiang et al., 2023; Müller and Gruber, 2024a; Terhaar et al., 2020, 2021a, and 2024).  
124 Since the beginning of the Industrial Revolution, the total amount of dissolved inorganic carbon (DIC) in the layer  
125 from 0 to 200 m has risen from 1690 to 1730 Gt of Carbon, and from 35,400 to 35,560 Gt C below 200 m (Sabine et  
126 al., 2004a; Müller et al., 2023a). The seemingly small increase of 0.5% results in a substantial drop of the oceans'  
127 buffer capacity (DeVries, 2022a). Buffer capacity refers to the ocean's ability to resist changes in pH, and thus also  
128 the partial pressure of CO<sub>2</sub> ( $p\text{CO}_2$ ), when CO<sub>2</sub> or any other acid or base is added or removed.

129 As anthropogenic CO<sub>2</sub> enters seawater, it reacts with water to form carbonic acid. This is the first in a series of  
130 rapid acid-base reactions that release protons (H<sup>+</sup>) and decrease the availability of carbonate ions, which are building  
131 materials that many marine organisms, such as mollusks, crustaceans, and corals, use to construct their shells and  
132 skeletons (Gattuso and Hansson, 2011). This process, referred to as "ocean acidification (OA)", has already  
133 decreased surface ocean pH by roughly 0.11 (~30% increase in acidity) since 1750 (Orr et al., 2005; Jiang et al.,  
134 2019a; Kwiatkowski et al., 2020; Jiang et al., 2023; IPCC, 2023). In some parts of the subsurface ocean, the trends  
135 of some acidification variables, e.g., pH, and total hydrogen ion content ( $[\text{H}^+]_{\text{total}}$ ), can be even greater due to the  
136 increasing sensitivity of  $[\text{H}^+]$  to DIC changes at depth (Chen et al., 2017; Perez et al., 2021; Fassbender et al., 2023;  
137 Müller and Gruber, 2024a). This ongoing acidification threatens critical ocean ecosystem services, including food  
138 security, fisheries, aquaculture, and the broader Blue Economy, for billions of people globally (Cooley and Doney,  
139 2009; Perez et al., 2018; Doney et al., 2020).

140 In some parts of the ocean, OA is driven not only by the uptake of carbon but also by other processes (Delaigue  
141 et al., 2024), for example via alkalinity changes driven by freshening of the Arctic Ocean (Terhaar et al., 2021a) or  
142 changes in the carbon and alkalinity export from the Pacific Ocean and Arctic rivers (Terhaar et al., 2019; Qi et al.,  
143 2017 and 2022; Bertin et al., 2023). Local anthropogenic inputs through rivers or from air pollution also contribute  
144 to OA (e.g. Sarma et al., 2015; Sridevi and Sarma, 2021). Furthermore, eutrophication and hypoxia in coastal  
145 regions may exacerbate OA in oxygen-deficient bottom waters, as biologically produced CO<sub>2</sub> weakens the natural  
146 buffering capacity of seawater (Cai et al., 2011). If anthropogenic CO<sub>2</sub> emissions continue without mitigation, as per  
147 the shared socioeconomic pathway (SSP5-8.5) scenario, surface ocean pH could decrease by a further 0.3 to 0.4 by  
148 2100, equivalent to a 100–150% increase in acidity (Kwiatkowski et al., 2020; Jiang et al., 2023). If society,  
149 however, succeeds in reducing emissions, the future acidity level becomes highly uncertain as it sensitively depends  
150 on the transient response of the Earth system and the amount of reductions of non-CO<sub>2</sub> radiative agents (Terhaar et  
151 al., 2023).

Deleted: termed

Deleted: in DIC with

Deleted: lead

Deleted: .

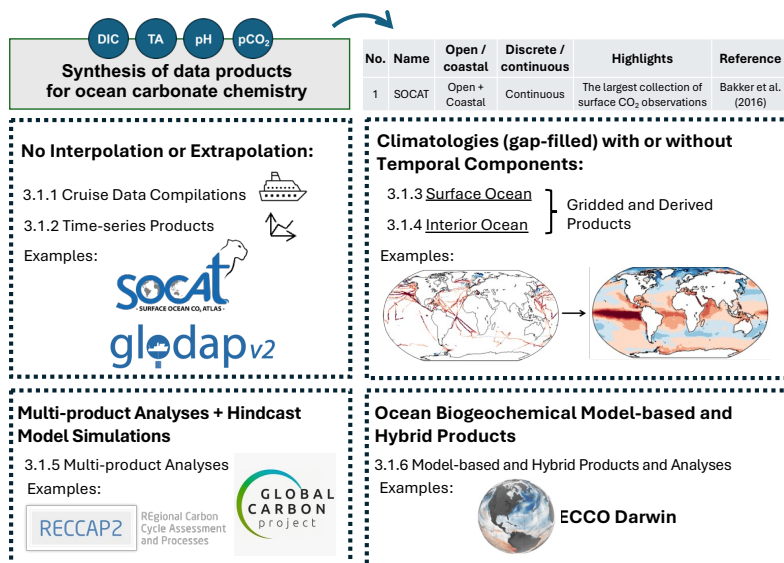
Deleted: at

157 In summary, monitoring ocean carbonate chemistry is essential for (a) tracking the evolving ocean carbon sink,  
 158 and (b) understanding OA and its ecological impacts. Additionally, monitoring ocean carbonate chemistry is crucial  
 159 when considering marine carbon dioxide removal (mCDR) strategies such as ocean alkalinity enhancement (OAE),  
 160 artificial upwelling, ocean fertilization, and electrochemical ocean CO<sub>2</sub> removal (Kheshgi, 1995; Bach et al., 2019;  
 161 Schimel and Carroll, 2024; Oeschies et al., 2025). The ocean's vast and interconnected nature necessitates that data  
 162 from individual oceanographic cruises be meticulously preserved, subject to rigorous quality-control, and uniformly  
 163 formatted to promote their usability (Brett et al., 2020; Schoderer et al., 2024). Following Lange et al. (2023), we  
 164 curate an exhaustive catalogue of synthesis products pertaining to ocean carbonate chemistry, including cruise data  
 165 compilations, gridded gap-filled data products, and other derived data products. This compilation spans both global  
 166 and regional scales, providing a holistic view of the current state of ocean biogeochemistry data aggregation.

Deleted: quality control

## 167 2 Methods

168 In this paper, data products are defined as outputs that quality-control, aggregate, and transform individual  
 169 datasets from multiple sources into a unified, structured format to support research, decision-making, or operational  
 170 needs for specific end users. The data products included in this study were identified through a literature review and  
 171 discussions with researchers via the Ocean Acidification Information Exchange (OAIE) platform.



173 **Figure 1.** An overview diagram outlining the paper's structure and flow.

175 The products are organized into six categories based on end-user needs and listed within each class with no  
176 particular order (Figure 1):

- 177 1. Cruise data compilations (no interpolation or gap-filling).
- 178 2. Time-series data products (no interpolation or gap-filling).
- 179 3. Derived gap-filled (e.g., interpolated) products for the surface ocean, starting with products offering a cli-  
180 matological snapshot of the ocean, followed by those showing temporal changes.
- 181 4. Derived gap-filled (e.g., interpolated) products for the interior ocean, also starting with products offering a  
182 climatological snapshot of the ocean, followed by those showing temporal changes.
- 183 5. Multi-product analyses of 3 and 4. These compilations also include hindcast model simulations of the  
184 ocean carbon cycle and biogeochemistry.
- 185 6. Model and hybrid data products projecting ocean carbonate system variables into the future [Note: Here the  
186 term 'model' refers to ocean biogeochemical models (Fennel et al., 2022). If a statistical model or machine  
187 learning model is used for gap-filling, the product is not categorized as a model output product in this com-  
188 pilation.]

189 Each category includes numbered descriptions of each data product in that class, as well as a summary table of  
190 the data products with corresponding IDs so the user can easily jump to the associated product description. For each  
191 data product, the description is followed by its access links. Persistent identifiers (e.g., digital object identifiers, or  
192 DOIs) and links to all data products are also summarized in the table in Section 4. Data availability.

193 Although some data products, such as Surface Ocean CO<sub>2</sub> Atlas (SOCAT) and Lamont-Doherty Earth  
194 Observatory (LDEO) surface *p*CO<sub>2</sub> Database report only one ocean carbonate system variable, i.e., fugacity of  
195 carbon dioxide (*f*CO<sub>2</sub>) or *p*CO<sub>2</sub>, they provide a foundation from which additional variables can be derived using  
196 empirical algorithms. For instance, total alkalinity content (TA) can be estimated from salinity and temperature and  
197 other factors (Lee et al., 2006) and by neural network approaches such as those developed by Velo et al. (2013) and  
198 Broullón et al. (2019). Beyond TA, neural network algorithms have been extended to estimate DIC as demonstrated  
199 by Broullón et al. (2020a), and even the full marine carbonate system (MCS) through frameworks like CANYON-  
200 B/CONTENT (Bittig et al., 2018) and Empirical Seawater Property Estimation Routines (ESPERs) (Carter et al.,  
201 2021). While these methods primarily employ neural networks, both Velo et al. (2013) and Carter et al. (2021)  
202 provide alternative estimation approaches based on local interpolation, through their 3-dimensional moving window  
203 multilinear regression algorithm (3DwMLR) and locally interpolated regression (LIR) methods, respectively.  
204 Utilizing such derived data, the complete suite of ocean carbonate system variables can then be calculated using  
205 computer software, such as CO2SYS (Lewis and Wallace, 1998; van Heuven et al., 2011; Orr et al., 2018; Sharp et  
206 al., 2023) or its Python implementation PyCO2SYS (Humphreys et al., 2022). An in-depth explanation of the  
207 methods employed for these calculations can be found in the Supplementary material of Jiang et al. (2022a).

208 **3 Results and Discussion**

209 **3.1 Data products for ocean carbonate chemistry**

210 **3.1.1 Cruise Data Compilations (no interpolation or gap-filling):**

211 The data compilations described in this section standardize datasets collected from individual research vessels,  
212 ships of opportunity, and uncrewed platforms, presenting them in a uniform format for easy access. These datasets  
213 typically undergo both primary QC (identifying outliers and obvious errors within an individual cruise dataset) and  
214 secondary QC (when possible, to objectively compare data from one cruise against another or a previously  
215 synthesized dataset to quantify systematic differences in reported values). It is important to note that data providers  
216 are expected to carry out rigorous QC prior to data submission.

Deleted: '

217 **1) SOCAT:** The Surface Ocean CO<sub>2</sub> Atlas features surface *f*CO<sub>2</sub> measurements from both the open ocean and  
218 the coastal ocean, predominantly sourced from research vessels, ships of opportunity, and autonomous  
219 platforms including fixed moorings and uncrewed surface vehicles (USVs) (Bakker et al., 2016). It  
220 represents the most extensive collection of observational ocean CO<sub>2</sub> data for the global surface ocean. Since  
221 2013, SOCAT has been updated annually. Dataset flags indicate the estimated uncertainty and  
222 completeness of metadata in SOCAT synthesis products. The SOCAT gridded product (monthly 1° x 1°)  
223 contains *f*CO<sub>2</sub> values with an estimated uncertainty of less than 5 μatm. To access the latest version of the  
224 SOCAT data product (with 40 million data points), visit <https://socat.info/> (Bakker et al., 2025).

225 **2) LDEO Surface pCO<sub>2</sub> Database:** Dr. Taro Takahashi at LDEO in Palisades, New York started  
226 synthesizing global surface ocean CO<sub>2</sub> data in 1997, compiling three decades of observations (~250,000  
227 measurements) to create inaugural monthly global surface pCO<sub>2</sub> maps (Takahashi et al., 1997; Takahashi et  
228 al., 2002). The most recent version (V2019) expanded this dataset to approximately 14.2 million surface  
229 water pCO<sub>2</sub> measurements spanning 1957–2019. Distinct from the SOCAT database, the LDEO database  
230 reports pCO<sub>2</sub> instead of *f*CO<sub>2</sub>, exclusively from equilibrator-CO<sub>2</sub> analyzer systems, with an average  
231 estimated uncertainty of ± 2.5 μatm. The database is also interpolated onto a global surface ocean 4° × 5°  
232 grid for a reference year 2000 (Takahashi et al., 2009) and 2010 (Fay et al., 2024). Access to the LDEO  
233 Surface pCO<sub>2</sub> database (Version 2019) is provided by the Ocean Carbon and Acidification Data System  
234 (OCADS) at <https://www.ncei.noaa.gov/data/oceans/nci/ocads/metadata/0160492.html> (Takahashi et al.,  
235 2017). Additionally, a dedicated webpage for the LDEO Database is available at  
236 [https://www.ncei.noaa.gov/access/ocean-carbon-acidification-data-](https://www.ncei.noaa.gov/access/ocean-carbon-acidification-data-system/oceans/LDEO_Underway_Database/)  
237 [system/oceans/LDEO\\_Underway\\_Database/](https://www.ncei.noaa.gov/access/ocean-carbon-acidification-data-system/oceans/LDEO_Underway_Database/).

Deleted: [

Deleted: ,

Deleted: ]

Deleted:

Deleted: from

Deleted: s

Deleted: at:

Deleted: there is

Deleted: OCADS:

238 **3) GLODAPv2:** The Global Ocean Data Analysis Project Version 2 (GLODAPv2) aggregates  
239 biogeochemical data collected from discrete bottle samples, offering extensive global coverage from the  
240 surface to depth (Key et al., 2015; Olsen et al., 2016; Lauvset et al., 2024). While GLODAP is primarily a

Deleted: s

252 product for basin-scale hydrographic data, it also includes coastal datasets and observations from a few  
253 time-series. The GLODAPv2 data product provides rigorously quality-controlled measurements for 14  
254 essential oceanographic variables: temperature, salinity, dissolved oxygen (DO), nitrate, silicate, phosphate,  
255 DIC, TA, pH, chlorofluorocarbons (CFC-11, CFC-12, CFC-113), carbon tetrachloride (CCl<sub>4</sub>), and sulfur  
256 hexafluoride (SF<sub>6</sub>). These variables, excluding temperature, undergo both primary and secondary quality-  
257 control procedures to detect outliers and adjust for significant measurement biases. GLODAPv2 was first  
258 published in 2016 and was updated annually through a living data process in Earth System Science Data  
259 from 2019 through “v2023,” which was published in 2024. For these updates, new data (including historical  
260 data not previously included in the data product) are quality-controlled and adjusted to the 2016 version  
261 (Olsen et al., 2019; Olsen et al., 2020; Lauvset et al., 2021; Lauvset et al., 2022; Lauvset et al., 2024). Since  
262 the global repeat hydrography programs operate with decadal repetitions, the aim is to produce a  
263 completely new version of GLODAP, where all cruise datasets will be reevaluated, every decade. Release  
264 of the GLODAPv3 data product is planned for 2026, and is expected to evolve the secondary data quality-  
265 control practices relative to those used in GLODAPv2. For more information on the secondary quality-  
266 control process, refer to Tanhua et al. (2010) and Lauvset and Tanhua (2015). GLODAPv2 offers two kinds  
267 of products: the compilation of quality-controlled data from discrete bottle samples taken at sampling  
268 location (Key et al., 2015; Olsen et al., 2016; Olsen et al., 2019; Olsen et al., 2020; Lauvset et al., 2021;  
269 Lauvset et al., 2022; Lauvset et al., 2024), and a gridded product, interpolated to a 1° × 1° grid and the 33  
270 standard depth levels of World Ocean Atlas (WOA) (Lauvset et al., 2016). All versions of the GLODAPv2  
271 data product can be accessed at <https://glodap.info/>.

272 GLODAPv2 builds upon three foundational data products: the original GLODAP (Sabine et al., 2004a),  
273 CARbon dioxide IN the Atlantic Ocean (CARINA, Key et al., 2010), and PACIFIC ocean Interior Carbon  
274 (PACIFICA, Suzuki et al., 2013). These data products remain available at NCEI:  
275 <https://www.ncei.noaa.gov/data/oceans/ncei/ocads/metadata/0001644.html> (GLODAP, Sabine et al.,  
276 2004b), <https://www.ncei.noaa.gov/data/oceans/ncei/ocads/metadata/0113899.html> (CARINA, Tanhua et  
277 al., 2013), and <https://www.ncei.noaa.gov/data/oceans/ncei/ocads/metadata/0110865.html> (PACIFICA,  
278 Suzuki et al., 2013), respectively.

279 **4) Quality Edited Hydrographic Data:** The Quality Edited Hydrographic Data product offers both a user-  
280 friendly application and a library of ocean profile data curated by Jim Swift (Scripps Institution of  
281 Oceanography, La Jolla, California, United States). Similar to GLODAPv2, this data product serves as a  
282 comprehensive repository of quality-controlled discrete bottle-based measurements (and limited CTD),  
283 spanning from the surface to the depths of the global ocean. Unlike GLODAPv2, this data product does not  
284 apply offset corrections. It encompasses a range of oceanographic variables including temperature, salinity,  
285 DO, DIC, TA, silicate, phosphate, nitrate, nitrite, CFC-11, CFC-12, and SF<sub>6</sub>. To access the application and  
286 data, visit: <https://joa.ucsd.edu/>. Currently, there is not a peer-reviewed paper or public-accessible report for

**Deleted:** quality control

**Deleted:** ,

**Deleted:** quality control

**Deleted:** quality control

**Deleted:** quality control

**Deleted:** collection

**Deleted:** no

**Deleted:** were applied to this data product

295 this data product. Cite the data product itself as: “Swift, J. (2022), Quality Edited Hydrographic Data,  
296 [https://joa.ucsd.edu/Data\\_homepage](https://joa.ucsd.edu/Data_homepage)”, or cite the entire data product as: “Swift, J. and Osborne, J. (2022),  
297 The Quality Edited Hydrographic Data, <https://joa.ucsd.edu>”.

298 **5) WOD:** In addition to the GLODAPv2 (No. 3) and Quality Edited Hydrographic Data (No. 4), users can  
299 also access historical and recent original biogeochemical data collected from discrete bottle samples in a  
300 uniform format and units, along with their originator ~~quality-control~~ (QC) flags, through the World Ocean  
301 Database (WOD) (Mishonov et al., 2024). Like the Quality Edited Hydrographic Data, these measured data  
302 remain unaltered. The WOD allows users to filter and subset data ~~by~~ specific variables, platforms,  
303 institutions, projects, regions, or time periods (Garcia et al., 2024). Users can visualize sampling locations  
304 on a “distribution plot” and access a cruise list for all selected data and variables. Users also have the  
305 option of exporting data in NetCDF or Comma-Separated Values (CSV) formats. Additionally, all data in  
306 the WOD are reproducible and traceable to their original data sources archived at NOAA’s National  
307 Centers for Environmental Information (NCEI). The WOD is accessible at  
308 <https://www.ncei.noaa.gov/products/world-ocean-database>.

309 **6) SNAPO-CO<sub>2</sub>:** Metzl et al. (2024) aggregated over 44,400 measurements of DIC and TA from a series of  
310 research cruises and ships of opportunity across various oceanic regions from 1993 ~~2022~~, under several  
311 French research programs, to create a product called “Service National d’Analyse des Paramètres  
312 Océaniques du CO<sub>2</sub> (SNAPO-CO<sub>2</sub>)”. The majority of the samples were analyzed by the Service National  
313 d’Analyse des Paramètres Océaniques du CO<sub>2</sub> (SNAPO-CO<sub>2</sub>) at the LOCEAN laboratory in Paris, France.  
314 Sampling was performed either from CTD-rosette casts (Niskin bottles) or collected from the ship’s flow-  
315 through system (intake at roughly 5\_m depth). DIC and TA determinations were conducted simultaneously  
316 through potentiometric titration in a closed-cell setup, calibrated with certified reference material to achieve  
317 an accuracy of  $\pm 4 \mu\text{mol kg}^{-1}$  for both variables, ~~following~~ Edmond (1970). This methodology was also  
318 applied for real-time measurements during OISO cruises, with data from the South Indian Ocean for 1998-  
319 ~~2018~~ included in this compilation. The data ~~are~~ split into two sets: one for the global ocean and coastal  
320 zones, and another for the Mediterranean Sea, both accessible in the same format at  
321 <https://doi.org/10.17882/95414>. Additionally, this data product is available at OCADS:  
322 <https://www.ncei.noaa.gov/data/oceans/ncei/ocads/metadata/0285681.html> (Metzl et al., 2023)

323 **7) CODAP-NA:** Jiang et al. (2021) synthesized two decades of discrete measurements of carbonate system  
324 variables, DO, and nutrient data from the North American continental shelves to generate the first version  
325 of Coastal Ocean Data Analysis Data Product in North America (CODAP-NA). The 2021 release  
326 encompasses 3,391 oceanographic profiles from 61 research cruises spanning the North American  
327 continental shelves from Alaska to Mexico in the west and from Canada to the Caribbean in the east. It  
328 includes 14 key variables, including temperature, salinity, DO, DIC, TA, pH, carbonate ion,  $f\text{CO}_2$ , silicate,  
329 phosphate, nitrate, all of which have undergone rigorous ~~quality-control~~. Note that certain datasets meeting

**Deleted:** quality control

**Deleted:** with

**Deleted:** -

**Deleted:** as per

**Deleted:** -

**Deleted:** is

**Deleted:** quality control

337 the GLODAPv2 QC standards are also included in the GLODAPv2 since its 2022 release (No. 3 above).  
338 CODAP-NA is available at <https://www.ncei.noaa.gov/data/oceans/ncei/ocads/metadata/0219960.html>  
339 (Jiang et al., 2020).

Deleted: OCADS:

340 8) **AZMP Carbon:** Gibb et al. (2023) compiled ocean carbonate system variables data from the Canadian  
341 Atlantic Zone Monitoring Program (AZMP Carbon) since 2014. More than 100 seagoing missions are  
342 represented in this dataset. The sampling strategy generally corresponds to full-depth water samples mostly  
343 collected along standardized hydrographic sections. The majority of these data were collected as part of the  
344 Atlantic Zone Monitoring Program (AZMP) of Fisheries and Oceans Canada (DFO). Implemented in 1998,  
345 the AZMP aims to characterize and understand the causes of oceanic variability at the seasonal, interannual  
346 and decadal scales in support of, among other things, fisheries management in the Atlantic Zone (including  
347 the Gulf of St. Lawrence, the Scotian shelf and the Newfoundland and Labrador shelf). Since 2014, a  
348 minimum of two of the three following carbonate system variables, DIC, TA, and pH, are also acquired by  
349 the program at standardized hydrographic stations across the zone (sampled up to three times a year). Each  
350 measurement is completed with corresponding temperature, salinity and, when available, nutrients and DO  
351 concentration data. This dataset also includes samples collected as part of ships of opportunity, fishing and  
352 other scientific trips. The entire dataset comprises 19,531 discrete samples [last updated 21 August 2024].  
353 Among this number, 18,085 have at least two of the three carbonate system variables (e.g., TA, DIC and  
354 pH), allowing the derivation of other variables such as the saturation state relative to aragonite and calcite  
355 ( $\Omega_{\text{arag}}$  and  $\Omega_{\text{calc}}$ ) and  $p\text{CO}_2$  (in  $\mu\text{atm}$ ). The full dataset of measured and derived variables is available from  
356 the Federated Research Data Repository: <https://doi.org/10.20383/102.0673> (Cyr et al., 2022) and is  
357 updated annually.

Deleted: e

Deleted: generally

Deleted: -

Deleted: using the CO2SYS program modified for Python  
(<https://github.com/mvdb7/PyCO2SYS/tree/v1.2.1>, last access: 8  
January 2023; Humphreys et al., 2022)

358 9) **MOCHA:** Kennedy et al. (2023) curated a comprehensive coastal ocean data product called “Multistressor  
359 Observations of Coastal Hypoxia and Acidification (MOCHA)”, encompassing temperature, salinity, DO,  
360 ocean carbonate system variables (DIC, TA, pH,  $p\text{CO}_2$ ,  $f\text{CO}_2$ ), nutrients, and chlorophyll measurements  
361 from the full water column along the U.S. west coast. The synthesis integrates observations from 71  
362 different sources, including high-resolution autonomous sensors, synoptic oceanographic cruises, and  
363 shoreline samples. The MOCHA synthesis spans from the shoreline to well beyond the continental shelf  
364 and incorporates observations from CODAP-NA (see No. 7 above), California Cooperative Oceanic  
365 Fisheries Investigations (CalCOFI), and other large-scale oceanographic cruises to facilitate linking  
366 nearshore, high-resolution observations to broader oceanographic conditions. As of 2025, MOCHA  
367 includes 15.9 million temperature readings, 5.0 million salinity measurements, 3.9 million DO records, and  
368 2.3 million pH measurements, along with 8,368 DIC, 10,144 TA, and 505,000  $p\text{CO}_2/f\text{CO}_2$  measurements,  
369 with limited additional chlorophyll and nutrient observations. To reduce the computational load from high-  
370 resolution sensors, the synthesis is also available as a “daily aggregated” dataset, with all data sources  
371 averaged by day, location, and depth. All data in the MOCHA synthesis product has been quality\_

379 controlled to a “plausible and reasonable” standard, but researchers requiring high-precision coastal data  
380 may need to apply additional QC tests. The data product is available at  
381 <https://www.ncei.noaa.gov/data/oceans/ncei/ocads/metadata/0277984.html> (Kennedy et al., 2023), while  
382 the methods and the product are described in Kennedy et al. (2024).

Deleted: OCADS:

383 **10) ARIOS:** The Acidification in the Rias and the Iberian Continental Shelf (ARIOS) project involved  
384 compiling and analyzing the historical record of ocean carbonate system measurements and associated  
385 variables conducted by the Instituto de Investigaciones Mariñas (IIM-CSIC) in Vigo, Spain. This dataset  
386 comprises 3,343 oceanographic stations and 17,653 discrete samples, combining measurements of pH, TA,  
387 and other physical (pressure, temperature, and salinity) and biogeochemical variables (DO, nitrate,  
388 phosphate, and silicate) off the northwestern Iberian Peninsula from June 1976 to September 2018 (Padin et  
389 al., 2020). The oceanography cruises funded by 24 projects were primarily carried out in the Ría de Vigo  
390 coastal inlet, but also in an area ranging from the Bay of Biscay to the Portuguese coast. Robust seasonal  
391 cycles and long-term trends were calculated along a longitudinal section, gathering data from the coastal  
392 and oceanic zones of the Iberian upwelling system. The data product is available at  
393 <https://doi.org/10.20350/digitalCSIC/12498> (Pérez et al., 2020).

Deleted: o

Deleted: e

Deleted: A synthesis paper is available at <https://doi.org/10.5194/essd-12-2647-2020> (Padin et al., 2020), and the ...

394 **11) Marine Inorganic Carbonate Chemistry in the Northern Gulf of Alaska:** Monacci et al. (2023)  
395 compiled a data product of discrete seawater samples collected each May and September over a 10-year  
396 period from 2008 to 2017 along the long-term hydrographic line in the Gulf of Alaska (GAK Line).  
397 Samples were collected from a sampling rosette on a profiling CTD. Data variables include profiled  
398 seawater temperature, salinity, and DO. Discrete sample variables include DO (i.e., Winkler titrations),  
399 macronutrients (nitrate, nitrite, phosphate, silicic acid), DIC, and TA. This data product is available at  
400 <https://www.ncei.noaa.gov/data/oceans/ncei/ocads/metadata/0277034.html> (Monacci et al., 2023), and the  
401 synthesis paper can be accessed at <https://doi.org/10.5194/essd-16-647-2024> (Monacci et al., 2024).

Deleted: The repeat hydrographic cruises were funded by the Alaska Ocean Observing System (AOOS), the Exxon Valdez Oil Spill Trustee Council (EVOS), Gulf Watch Alaska, and the North Pacific Research Board (NPRB) and were mostly conducted aboard the United States Fish and Wildlife Service (USFWS) R/V Tiglax. All carbonate system variables were analyzed at the Ocean Acidification Research Center (OARC) at the University of Alaska Fairbanks (UAF).

Deleted: OCADS:

402 **12) Coral Reef Carbonate Chemistry Off the Florida Keys:** Palacio-Castro et al. (2023) compiled discrete  
403 seawater samples from 38 permanent stations located along 10 inshore-offshore transects at the Florida  
404 Coral Reef. These samples were collected as part of NOAA's National Coral Reef Monitoring Program  
405 (NCRMP) and the South Florida Ecosystem Restoration Research (SFER) cruises. Sampling efforts  
406 commenced in 2010, with every two months collections initiated in 2015, resulting in a total of 47 sampling  
407 cruises and 1,538 discrete seawater samples. For all samples, a minimum of two of the carbonate system  
408 variables (TA, DIC) were measured, in addition to salinity and temperature. The  $\Omega_{\text{arrg}}$ ,  $p\text{CO}_2$ , and pH were  
409 derived from the measured variables using the R package seacarb (Gattuso et al., 2021a). The time-series  
410 analysis provides insight into the dynamic carbonate conditions spanning the inshore to offshore gradients,  
411 encompassing four distinct regions of the Florida Coral Reef: Biscayne Bay, the Upper Keys, Middle Keys,  
412 and Lower Keys. Data is available at [https://www.ncei.noaa.gov/access/metadata/landing-](https://www.ncei.noaa.gov/access/metadata/landing-page/bin/iso?id=gov.noaa.nodc:NCRMP-CO3-Atlantic)  
413 [page/bin/iso?id=gov.noaa.nodc:NCRMP-CO3-Atlantic](https://www.ncei.noaa.gov/access/metadata/landing-page/bin/iso?id=gov.noaa.nodc:NCRMP-CO3-Atlantic) (Manzello et al., 2018).

Deleted: NCEI:

430 **13) Salish Cruise Data Package and Multi-stressor Data Product:** Alin et al. (2025a) compiled data from 61  
431 individual cruise data sets that sampled marine waters of the southern Salish Sea and northern Washington  
432 coast (United States) from 2008 to 2024. Ongoing seasonal sampling occurred during April, July, and  
433 September for Puget Sound cruises has occurred since 2014 and most frequently during May and October  
434 for Sound-to-sea cruises, which sample from Puget Sound through the Strait of Juan de Fuca to the  
435 northern Washington coast. The Salish cruise data package contains observations from water column  
436 profiles, with CTD sensor measurements of temperature, salinity, and DO; as well as discrete measurements  
437 of DO, nutrients (nitrate, phosphate, silicate, ammonium, nitrite), DIC, and TA. A follow-on data product is  
438 also available, containing only samples with complete records for temperature, salinity, and DO from  
439 sensors, and DO, nutrients, DIC, and TA from discrete measurements, along with the most commonly used  
440 calculated carbonate system variables: pH (total scale),  $f\text{CO}_2$ ,  $p\text{CO}_2$ ,  $\Omega_{\text{arag}}$ , and  $\Omega_{\text{calc}}$  (Alin et al., 2025b). The  
441 data package is available at [https://www.ncei.noaa.gov/access/ocean-carbon-acidification-data-](https://www.ncei.noaa.gov/access/ocean-carbon-acidification-data-system/oceans/SalishCruise_DataPackage.html)  
442 [system/oceans/SalishCruise\\_DataPackage.html](https://www.ncei.noaa.gov/access/ocean-carbon-acidification-data-system/oceans/SalishCruise_DataPackage.html). The multi-stressor data product is available [at](https://www.ncei.noaa.gov/access/ocean-carbon-acidification-data-system/oceans/SalishCruises_DataProduct.html)  
443 [https://www.ncei.noaa.gov/access/ocean-carbon-acidification-data-](https://www.ncei.noaa.gov/access/ocean-carbon-acidification-data-system/oceans/SalishCruises_DataProduct.html)  
444 [system/oceans/SalishCruises\\_DataProduct.html](https://www.ncei.noaa.gov/access/ocean-carbon-acidification-data-system/oceans/SalishCruises_DataProduct.html). Two synthesis papers describing the Salish cruises, as well  
445 as seasonality and extreme ocean acidification conditions observed during the 2008–2018 part of the time-  
446 series, can be found [at](https://essd.copernicus.org/articles/16/837/2024/) <https://essd.copernicus.org/articles/16/837/2024/> (Alin et al., 2024a) and  
447 <https://bg.copernicus.org/articles/21/1639/2024/> (Alin et al., 2024b). A preliminary description of the 2019–  
448 2024 Salish cruises can be found at <https://www.psp.wa.gov/psmarinewatersoverview.php> (Alin et al.,  
449 2025c).

Deleted: OCADS:

Deleted: at:

Deleted: at:

450 **14) Line P Marine Carbonate Chemistry Compilation:** This dataset contains marine carbonate system  
451 measurements collected during 55 Line P cruises from 1990 to 2019 in the subarctic Northeast Pacific. The  
452 dataset contains discrete profiles of DIC, TA, seawater temperature, salinity, DO and nutrients. From a total  
453 of 27 hydrographic time-series stations, only the five major stations where DIC and TA are routinely  
454 sampled were included in this compilation. Among them is the outermost station P26, also known as Ocean  
455 Station Papa (Freeland, 2007). Cruises were conducted approximately three times per year, typically in  
456 February, May/June and August/September. Each vertical profile was individually inspected and contrasted  
457 with the whole pool of data (including historical data) relative to salinity, density, and oxygen to detect and  
458 flag poor quality data following the World Ocean Circulation Experiment (WOCE) quality-control  
459 convention (Jiang et al., 2022a). Additionally, the recommended cruise-specific adjustments from  
460 PACIFICA were applied (Suzuki et al., 2013). The Line P marine carbonate chemistry compilation is  
461 described and analyzed in (Franco et al., 2021a) and is publicly available as a single synthesis product at  
462 <https://www.ncei.noaa.gov/data/oceans/ncei/ocads/metadata/0234342.html> (Franco et al., 2021b). The Line  
463 P carbonate chemistry timeseries is maintained by Fisheries and Oceans Canada and continues to the  
464 present day. Data are available and continuously updated in the Line P repository, which can be publicly  
465 accessed after generating an account at <https://waterproperties.ca>.

Deleted: OCADS:

470 **15) Anthropogenic Carbon in the Arctic Ocean:** This dataset includes anthropogenic carbon estimates in the  
 471 Arctic Ocean based on measurements of transient tracers, such as CFC-12 and SF<sub>6</sub> (Terhaar et al., 2020;  
 472 Tanhua et al., 2009). Using the transient time distribution (TTD) method, anthropogenic carbon estimates  
 473 were estimated at measurement locations across all basins of the Arctic Ocean between 1983 and 2005. In  
 474 addition to these estimates, adjusted estimates of anthropogenic carbon at these locations are provided to  
 475 account for differences in the saturation of transient tracers and anthropogenic carbon in Arctic Ocean  
 476 surface waters that caused anthropogenic carbon estimates to be biased low (Terhaar et al., 2020). It is  
 477 recommended to use the adjusted estimates. This dataset can be accessed at  
 478 <https://doi.org/10.17882/103920> (Terhaar et al., 2024).

479 **Table 1. Ocean carbonate chemistry data products out of cruise data compilations (no gridding or gap-filling).**

No.	Name	Open ocean or Coastal ocean	Surface or Water column	Discrete bottle or Continuous	Highlights	Reference
1	SOCAT	Open ocean + Coastal ocean	Surface	Continuous	The largest collection of <i>in situ</i> surface ocean $f\text{CO}_2$ measurements	Bakker et al. (2016)
2	LDEO Surface $p\text{CO}_2$ Database	Open ocean + Coastal ocean	Surface	Continuous	The LDEO database reports $p\text{CO}_2$ exclusively from equilibrator- $\text{CO}_2$ analyzer systems	Takahashi et al. (2017)
3	GLODAPv2	Open ocean	Water column	Discrete bottle	Adjustments are applied by comparing data in the deep ocean (>2000 m) using a crossover and inversion method as described by Johnson et al. (2001)	Lauvset et al. (2024)
4	Quality Edited Hydrographic Data	Open ocean	Water column	Discrete bottle	Similar to GLODAPv2, with no adjustments	Swift (2022)
5	WOD	Open ocean	Water column	Discrete bottle	Similar to GLODAPv2, with no adjustments	Mishonov et al. (2024)
6	SNAPO- $\text{CO}_2$	Open ocean + Coastal ocean	Water column	Discrete bottle and semi-continuous	A compilation of cruises from multiple French initiatives	Metzl et al. (2024)
7	CODAP-NA	Coastal ocean	Water column	Discrete bottle	Like GLODAPv2, but for the coastal ocean	Jiang et al. (2021)
8	AZMP Carbon	Continental shelf and Slope	Water column	Discrete bottle	A compilation of cruises from the Atlantic Zone Monitoring Program (AZMP) since 2014	Gibb et al. (2023)
9	MOCHA	Coastal ocean	Water column	Discrete bottle + Continuous	U.S. West Coast	Kennedy et al. (2024)
10	ARIOS	Coastal ocean	Water column	Discrete bottle	An OA Database for the Galician Upwelling Ecosystem off the NW Iberian Peninsula from 1976 to 2018	Padin et al., (2020)

Deleted: c

Deleted: w

Deleted: c

Deleted: Open + Coastal

Deleted: carbon

Deleted: observations

Deleted: Open + Coastal

Deleted: .

Deleted: Open + Coastal

Deleted: s

11	Marine Inorganic Carbonate Chemistry in the Northern Gulf of Alaska	Coastal ocean	Water column	Discrete bottle	A synthesis of twenty cruises from 2008 to 2017 on the Gulf of Alaska (GAK) Line	Monacci et al. (2023)
12	Coral Reef Carbonate Chemistry Off the Florida Keys	Coastal / Regional	Water column	Discrete bottle	Temporal trends of DIC, TA, $p\text{CO}_2$ , pH, $\Omega_{\text{arag}}$ in different areas of the Florida Keys	Palacio-Castro et al. (2023)
13	Salish Cruise Data Package and Multi-stressor Data Product	Coastal / Estuarine	Water column	Discrete bottle	A data compilation and multi-stressor (OA, hypoxia, temperature) data product based on cruises from 2002 to 2018 in the southern Salish Sea and Washington coast	Alin et al. (2025a, b)
14	Line P Marine Carbonate Chemistry Compilation	Open ocean	Water column	Discrete bottle	A compilation of fifty-five Line P cruises containing discrete DIC and TA profiles at five stations in the Northeast Pacific Ocean. Sampled approximately three times per year from 1990 to 2019	Franco et al. (2021a, b)
15	Anthropogenic carbon in the Arctic Ocean	Open ocean	Water column	Discrete bottle (adjusted to 2005)	Observation-based estimates of anthropogenic carbon in the Arctic Ocean	Tanhua et al. (2009, 2020)

Deleted: r

Deleted: e

Deleted: w

### 490 3.1.2 Time-series Products (no interpolation or gap-filling):

491 The time-series products described in this section include observations collected at regular time intervals, over a  
 492 sustained period, and at fixed locations. The data often represent changes in a particular oceanographic variable over  
 493 time, such as temperature, salinity, TA and DIC. The list below includes both climate-quality time-series data  
 494 products compiled at selected stations, and data products compiling time-series measurements at multiple locations.  
 495 Additionally, some hydrographic sections are measured frequently enough to constitute a time-series, e.g., Line P in  
 496 the northeast Pacific (Franco et al., 2021b, Freeland, 2007), sections in the northwest Pacific (Ishii et al., 2011a), the  
 497 Observatoire de la Variabilité Interannuelle à DÉcennale (OVIDE) lines (Mercier et al., 2024). Measurements from  
 498 these sections are typically included in cruise data compilations (3.1.1) and are not listed separately here.

Deleted: regularly

Deleted: warrant being called

499 **16) BATS:** The Bermuda Atlantic Time-series Study (BATS) observations and data products extend over forty  
 500 years of observations of DIC and TA and OA indicators, and constitute the longest continuous record of  
 501 warming, salinification, ocean deoxygenation, and OA in the open ocean (Bates and Johnson, 2023). The  
 502 sustained observations at the BATS site began in October 1988, approximately 80 km to the southeast of  
 503 Bermuda (<https://bios.asu.edu/bats>). The program comprises monthly cruises with CTD, water-column  
 504 biogeochemical sampling and rate measurements (e.g., primary and export production) plus additional  
 505 cruises in the spring period and annual transects between the Gulf Stream and Puerto Rico.  $\text{CO}_2$ -carbonate  
 506 chemistry sampling includes full-depth bottle DIC and TA data (including additional surface measurements  
 507 going back to 1983 collected at the Hydrostation S site). Hydrostation S is located ~25 km southeast of

Deleted: to

Deleted: -

Deleted: -

516 Bermuda (<https://bios.asu.edu/research/projects/hydrostation-s>) and began in 1954 with biweekly cruises  
517 each year. Underway  $f\text{CO}_2/p\text{CO}_2$  data collected from the R/V *Atlantic Explorer* that supports the BATS  
518 and Hydrostation S sites constitutes part of the annual data submission to SOCAT. The BATS project page  
519 at the Biological and Chemical Oceanography Data Management Office (BCO-DMO) includes metadata  
520 and data streams (<https://demo.bco-dmo.org/project/2124>). Hydrostation S data and DOIs are also available  
521 at BCO-DMO (<https://www.bco-dmo.org/project/859583>).

522 **17) HOT:** The Hawaii Ocean Time-series (HOT) CO<sub>2</sub> measurement program documents more than 35 years of  
523 inorganic carbon dynamics in the open waters of the central North Pacific. Since October 1988, full ocean  
524 depth profiles of DIC and TA have been analyzed, and direct measurements of pH have been made over  
525 most of this longest-running Pacific Ocean time-series study. The program is based on shipboard  
526 observations and experiments conducted on ~10 expeditions per year to Station ALOHA (22.75°N,  
527 158°W). HOT program background information and details of sampling strategy may be found in Karl and  
528 Lukas (1996) and Karl et al. (2001). Results from the HOT CO<sub>2</sub> measurement program can be found in  
529 Winn et al. (1994, 1998), Dore et al. (2003, 2009, 2014), and Knor et al. (2023, 2025). The HOT project  
530 page, metadata, data streams and data identifiers are listed at <https://www.bco-dmo.org/project/2101>. A  
531 MAPCO<sub>2</sub> system on the Woods Hole Oceanographic Institution Hawaii Ocean Time-series Site mooring  
532 (WHOTS; <https://www.soest.hawaii.edu/whots/>) has provided a near-continuous record of surface  $p\text{CO}_2$   
533 since 2004, and is anchored by the longer high-accuracy HOT ship-based program (see Sutton et al., 2019  
534 and Knor et al., 2023). A surface ocean data product that includes CO<sub>2</sub>SYN-calculated values of  $p\text{CO}_2$ ,  
535 carbonate mineral saturation states and other derived quantities may be found at  
536 <https://hahana.soest.hawaii.edu/hot/hotco2/hotco2.html> and <https://doi.org/10.5281/zenodo.15060930>.

537 **18) ESTOC:** The European Station for Time-series in the Ocean (ESTOC) began carbon dioxide monitoring in  
538 October 1995, providing a 30-year record on DIC, TA, and pH. This dataset represents the longest  
539 continuous monthly record of warming, rising carbon dioxide levels, and acidification in the eastern North  
540 Atlantic (González-Dávila and Santana-Casiano, 2023). ESTOC is located 100 km north of the Canary  
541 Islands archipelago (<https://plocan.eu/en/installations/ocean-observatory>). The program includes a ship-  
542 based observation system, measuring physical, chemical, and biological variables throughout the 3,670-  
543 meter water column. It also features a moored platform for surface meteorological and oceanic observations  
544 as well as subsurface measurements, maintained by the Canary Island Oceanic Platform (PLOCAN,  
545 <https://plocan.eu/en>) and the University of Las Palmas de Gran Canaria  
546 (<https://iocag.ulpgc.es/research/research-units/quima>). Carbonate system measurements include full-depth  
547 bottle sampling for photometric pH, TA, and DIC, conducted monthly from 1995 to 2008, every two  
548 months until 2018, and semiannually in recent years due to limited ship time, timed to coincide with  
549 moored structure maintenance. ESTOC is also visited every two weeks by a volunteer observing ship, ES-  
550 SOOP-CanOA ([https://meta.icos-cp.eu/resources/stations/OS\\_687B](https://meta.icos-cp.eu/resources/stations/OS_687B)), part of the European Research

Deleted: +

Deleted: annum

553 Infrastructure ICOS (<https://www.icos-cp.eu/observations/ocean/stations>), which provides real-time surface  
554 data on carbon dioxide fluxes and OA. The program also includes the CO<sub>2</sub>-ESTOC oceanographic buoy  
555 (<https://meta.icos-cp.eu/labeling/>). The full dataset with DOIs is accessible on Pangaea (González-Dávila  
556 and Santana-Casiano, 2023).

557 **19) Point B Time-series:** The Point B Time-series documents the carbonate chemistry at a coastal site in the  
558 Bay of Villefranche (43.686200N 7.314800E) in Villefranche-sur-mer, France, northwestern Mediterranean  
559 Sea. Since January 2007, seawater is sampled weekly at 1 and 50 m, and analyzed for DIC and TA  
560 (Kapsenberg et al., 2017). Salinity and temperature are extracted from CTD profiles. Variables of the  
561 carbonate system such as pH (total scale) are calculated using the R package seacarb (Gattuso et al.,  
562 2021a). Data are available at Pangaea: <https://doi.org/10.1594/PANGAEA.727120> (Gattuso et al., 2021b).

563 **20) Ny-Ålesund Time-series:** The Ny-Ålesund Time-series documents the carbonate chemistry at a coastal  
564 site of Kongsfjorden, Spitsbergen (78.930660N 11.920030E) during the period 2015–2021. It is the first  
565 high-frequency (1 hour), multi-year (6 years) dataset of salinity, temperature, *p*CO<sub>2</sub>, pH, as well as  
566 calculated DIC and TA in the High-Arctic Ocean (Gattuso et al., 2023a). Data are available at Pangaea:  
567 <https://doi.org/10.1594/PANGAEA.957028> (Gattuso et al., 2023b).

568 **21) SPOTS:** The Synthesis Product for Ocean Time-Series (SPOTS) is a ship-based biogeochemical pilot,  
569 aiming at regularly providing high quality data from fixed time-series stations with consistent format and  
570 semantics (Lange et al., 2024a). The pilot includes data from 12 fixed ship-based time-series programs with  
571 a focus on the Global Ocean Observing System's biogeochemical essential ocean variables. These stations  
572 represent unique marine environments across a variety of spatiotemporal resolutions and ranges, with data  
573 from 1983 to 2021. While implementing the FAIR principles (Wilkinson et al., 2016) and promoting open  
574 data, the metadata of the time-series stations were enhanced to interoperate with the IOC-UNESCO Ocean  
575 Data and Information System (ODIS). Additionally, an extensive quality assessment resulted in enhanced  
576 intra- and inter-station comparability. Data are available at <https://www.bco-dmo.org/dataset/896862>  
577 (Lange et al., 2024b).

578 **22) *p*CO<sub>2</sub> and pH Time-series from 40 Surface Buoys:** Sutton et al. (2019) established a living dataset  
579 comprising 40 individual autonomous moored surface ocean *p*CO<sub>2</sub> time-series established between 2004  
580 and 2013, 17 of which also include autonomous pH measurements. These time-series characterize a wide  
581 range of surface ocean carbonate system conditions, across a variety of environments, including 17 oceanic  
582 and 13 coastal locations, as well as 10 coral reefs. Data are available at  
583 <https://www.ncei.noaa.gov/data/oceans/ncei/ocads/metadata/0173932.html> (Sutton et al., 2018).  
584 Additionally, a dedicated webpage for this project is available at [https://www.ncei.noaa.gov/access/ocean-](https://www.ncei.noaa.gov/access/ocean-carbon-acidification-data-system/oceans/Moorings/ndp097.html)  
585 [carbon-acidification-data-system/oceans/Moorings/ndp097.html](https://www.ncei.noaa.gov/access/ocean-carbon-acidification-data-system/oceans/Moorings/ndp097.html).

Deleted: of

Deleted: -

Deleted: /

Deleted: them

Deleted: OCADS:

Deleted: there is

Deleted: OCADS:

593 Table 2. Time-series based ocean carbonate chemistry data synthesis products.

No.	Name	Open ocean or Coastal ocean	Surface or Water column	Discrete bottle or Continuous	Highlights	Reference
16	BATS	Open ocean	Top 4600 m	CTD profiles, discrete bottle data from hydrocast, rate measurements (primary, export and bacterial production), biomass and other biological measurements, underway measurements	One of the longest continuous records of warming, salinification, ocean deoxygenation, and OA in the open ocean	Bates and Johnson (2020, 2023)
17	HOT	Open ocean	Top 4500 m	Discrete bottle for shipboard measurements; sensor measurements on WHOTS mooring	35+ years of inorganic carbon dynamics in the open waters of the central North Pacific	Dore et al. (2009)
18	ESTOC	Open ocean	Top 3570 m	Discrete bottle for shipboard measurements; sensor measurements on ESTOC mooring	The longest continuous monthly record of warming, rising carbon dioxide levels, and OA in the eastern North Atlantic	González-Davila and Santana-Casiano (2023)
19	Point B Time-series	Coastal ocean	5 and 50 m	CTD profiles, discrete bottle data	Carbonate chemistry at a coastal site of the Bay of Villefranche, France	Kapsenberg et al. (2017)
20	Ny-Ålesund Time-series	Coastal ocean	12 m	CTD, discrete bottle data, sensor measurements at the COSYNA/MOSES-AWIPEV underwater observatory	Carbonate chemistry at a coastal site of Kongsfjorden, Spitsbergen	Gattuso et al. (2023a, b)
21	SPOTS	Open ocean + Coastal ocean	Water column	Discrete	The pilot includes biogeochemical data from 12 fixed ship-based time-series programs	Lange et al. (2024a, b)
22	pCO <sub>2</sub> and pH Time-series from 40 Surface Buoys	Open ocean + Coastal ocean	Surface	Continuous	Based on 40 moored surface pCO <sub>2</sub> time-series, with 17 of them containing pH	Sutton et al. (2019)

Deleted: c

Deleted: w

Deleted: c

Deleted: B

Deleted: B

Deleted: C

Deleted: Open + Coastal

602 **3.1.3 Gridded and Derived Products – Surface Ocean:**

603 Although cruise data compilations are valuable for making data available in a uniform format, they often are  
604 constrained by their sampling strategies and can have significant gaps in space and time. Gridded and derived data  
605 products address this limitation by making some variables available at all grid points on a standardized spatial grid  
606 and at standardized depth levels through processes such as interpolation and gap-filling. This section describes  
607 gridded data products that have been derived from observations through interpolation and other gap-filling  
608 procedures, depicting the surface ocean. Note that this compilation focuses primarily on data products with global  
609 coverage, acknowledging that many regional gap-filled products became available in recent years and shall be  
610 include in future updates.

Deleted: :

611 **23) Takahashi Delta  $fCO_2$  and Flux Climatology:** Following on previous climatologies published by the late  
612 Taro Takahashi in 1997 and 2009, Fay et al. (2024) created a legacy climatology using his methodology  
613 and the updated SOCAT database of observations. This product provides 12 months of delta  $fCO_2$  values  
614 and corresponding fluxes for a reference year of 2010 at  $4^\circ \times 5^\circ$  resolution, and subsequently regridded to  
615  $1^\circ \times 1^\circ$  resolution and near-global coverage. This climatology represents the mean of ocean conditions over  
616 the last four decades and is distinctive relative to many other mechanistic machine learning approaches in  
617 that it interpolates in time and space using only the available  $fCO_2$  data and a surface water advection  
618 scheme rather than using proxy variables for gap-filling. It uses the median of observations to determine a  
619 reference year of 2010 and fluxes are provided using air-sea partial pressure differences and inputs from  
620 the SeaFlux product (Fay et al., 2021). The climatology product is available at  
621 <https://www.ncei.noaa.gov/data/oceans/ncei/ocads/metadata/0282251.html>. The related manuscript is  
622 available at ESSD: <https://doi.org/10.5194/essd-16-2123-2024> (Fay et al., 2024).

Deleted: base

Deleted: sub

Deleted: OCADS:

623 **24) MPI-ULB-SOM-FFN:** Landschützer et al. (2020a) created a uniform  $pCO_2$  climatology combining open  
624 and coastal oceans. It is a monthly gridded global surface ocean  $pCO_2$  data product without adjusting for a  
625 specific reference year. Developed on a higher-resolution  $0.25^\circ \times 0.25^\circ$  global surface-ocean grid, this  
626 product is the result of combining two neural network-based  $pCO_2$  products: the open ocean product  
627 described below (i.e., Landschützer et al., 2016) and the coastal product created by Laruelle et al. (2017).  
628 Consequently, it represents coastal zones better. Data collected between 1998 and 2015 from the SOCAT  
629 database (Version 5) were used to create this data product. The merged climatology product is available at  
630 <https://www.ncei.noaa.gov/data/oceans/ncei/ocads/metadata/0209633.html>. Additionally, a dedicated web  
631 page for this project is available at [https://www.ncei.noaa.gov/access/ocean-carbon-acidification-data-](https://www.ncei.noaa.gov/access/ocean-carbon-acidification-data-system/oceans/MPI-ULB-SOM_FFN_clim.html)  
632 [system/oceans/MPI-ULB-SOM\\_FFN\\_clim.html](https://www.ncei.noaa.gov/access/ocean-carbon-acidification-data-system/oceans/MPI-ULB-SOM_FFN_clim.html).

Deleted: OCADS:

Deleted: there is

Deleted: at OCADS

Deleted: :

633 **25) VLIZ-SOM-FFN:** Landschützer et al. (2016) employed the Self-Organizing-Map Feed-Forward Network  
634 (SOM-FFN) neural network method (Landschützer et al., 2013) to map sea surface  $pCO_2$  from SOCAT  
635 (see No. 1 above) (Bakker et al., 2014) to generate monthly  $pCO_2$  fields on a  $1^\circ \times 1^\circ$  global surface ocean

644 grid, covering the period from 1982 to near present. It is based on the gridded  $p\text{CO}_2$  measurements from  
645 SOCAT and is updated regularly. The creation of the  $p\text{CO}_2$  fields involves a two-step neural network  
646 approach, which has been extensively detailed and validated in previous works by Landschützer et al.  
647 (2013, 2014, 2016). In the initial step, the global ocean is clustered into biogeochemical provinces, and  
648 subsequently, the non-linear relationship between  $\text{CO}_2$  driver variables and gridded data from SOCAT  
649 (Bakker et al., 2016) is reconstructed. Air–sea  $\text{CO}_2$  fluxes are also computed based on the air–sea  $p\text{CO}_2$   
650 difference, utilizing a bulk gas transfer formulation as described by Landschützer et al. (2013, 2014, 2016).  
651 The product is available at <https://www.ncei.noaa.gov/data/oceans/ncei/ocads/metadata/0160558.html>.  
652 Additionally, a dedicated page for this project is available at [https://www.ncei.noaa.gov/access/ocean-](https://www.ncei.noaa.gov/access/ocean-carbon-acidification-data-system/oceans/SPCO2_1982_present_ETH_SOM_FFN.html)  
653 [carbon-acidification-data-system/oceans/SPCO2\\_1982\\_present\\_ETH\\_SOM\\_FFN.html](https://www.ncei.noaa.gov/access/ocean-carbon-acidification-data-system/oceans/SPCO2_1982_present_ETH_SOM_FFN.html).

Deleted: OCADS:

Deleted: there is

Deleted: at OCADS

Deleted: :

654 **26) JMA-MLR:** Iida et al. (2021) developed a monthly data product for inorganic carbonate variables on a  $1^\circ$   
655  $\times 1^\circ$  global surface ocean grid for the period 1993–2018. Variables include DIC, TA,  $p\text{CO}_2$ , air–sea  $\text{CO}_2$   
656 flux, pH, and  $\Omega_{\text{arag}}$ . They leveraged data products such as SOCAT.v2019 (Bakker et al., 2016) and  
657 GLODAPv2.2019 (Olsen et al., 2019), as well as satellite-based variables, including sea-surface dynamic  
658 height (SSDH), mixed layer depth (MLD), and chlorophyll-a. The product is updated annually using the  
659 latest SOCAT and GLODAPv2 data. The data product can be accessed at  
660 [https://www.data.jma.go.jp/kaiyou/english/co2\\_flux/co2\\_flux\\_data\\_en.html](https://www.data.jma.go.jp/kaiyou/english/co2_flux/co2_flux_data_en.html).

Deleted: sea-air

Deleted: :

## 661 **27) OceanSODA-ETHZ:**

662 **(a) OceanSODA-ETHZv1** is a monthly gridded global surface ocean data product for multiple ocean  
663 carbonate system variables, including DIC, TA,  $p\text{CO}_2$ , pH (total scale),  $\Omega_{\text{arag}}$ , and  $\Omega_{\text{calc}}$  (Gregor and Gruber,  
664 2020; Gregor and Gruber, 2021; Gregor and Gruber, 2023; Ma et al., 2023). This dataset is structured on a  
665  $1^\circ \times 1^\circ$  global surface ocean grid with monthly resolution from 1982–2022, facilitating research on OA  
666 over seasonal to decadal scales. The OceanSODA-ETHZ data product was created by extrapolating in time  
667 and space the surface ocean observations of  $f\text{CO}_2$  from SOCATv2022 (Bakker et al., 2016) and TA from  
668 GLODAPv2.2022 using the newly developed Geospatial Random Cluster Ensemble Regression (GRaCER)  
669 method (Gregor, 2021). TA and  $p\text{CO}_2$  were then used to calculate the remaining variables of the marine  
670 carbonate system with the PyCO2SYS software (Humphreys et al., 2022). Phosphate and silicate from  
671 WOA 2018 product was used (Boyer et al., 2018; Garcia et al., 2018a). The OceanSODA-ETHZ data  
672 product is available at <https://www.ncei.noaa.gov/data/oceans/ncei/ocads/metadata/0220059.html>.

Deleted: ere

Deleted: OCADS:

673 **(b) OceanSODA-ETHZv2** is a surface  $f\text{CO}_2$  product with a  $0.25^\circ \times 0.25^\circ$  spatial resolution and an 8-day  
674 temporal resolution, providing estimates starting from 1982 (Gregor et al., 2024a; Gregor et al., 2024b).  
675 The high-resolution outputs are suitable for investigating the shorter- and finer-scale dynamics of surface  
676  $f\text{CO}_2$ . Despite sharing a name with its predecessor, OceanSODA-ETHZv2 does not provide TA estimates  
677 and employs a different methodology, as described in the following steps: 1) The atmospheric trend of  $\text{CO}_2$   
678 is removed by subtracting marine boundary layer  $\text{CO}_2$  concentrations from SOCAT  $f\text{CO}_2$  producing a new

687 target  $\Delta^*CO_2$  to reduce the biases at the start and end of the time-series. 2) An 8-day seasonal climatology  
688 of  $\Delta^*CO_2$  is estimated using Gradient Boosted Decision Trees (GBDT), which is later used as a predictor.  
689 3) The non-seasonal thermal component is removed from  $\Delta^*CO_2$ , resulting in a new target,  $\Delta^*CO_2^{nonT}$ . 4)  
690 The new target is estimated using a feed-forward neural network, with the GBDT as one of the forcing  
691 variables. 5) Steps 4 through to 1 are inverted to arrive at  $fCO_2$ . 6) Air-sea  $CO_2$  fluxes are computed using  
692 ERA5 winds. Data are available at <https://doi.org/10.5281/zenodo.11206365> and are updated annually.

693 **28) LDEO-HPD  $fCO_2$ :** The LDEO Hybrid Physics Data (LDEO-HPD) estimates the temporal evolution of  
694 surface ocean  $fCO_2$  and air-sea  $CO_2$  exchange, utilizing the strengths of observations and global ocean  
695 biogeochemical models (GOBMs) (Gloege et al., 2022). GOBMs are internally consistent, mechanistic  
696 representations of the ocean circulation and carbon cycle, and have long been the standard for making  
697 spatiotemporally resolved estimates of air-sea  $CO_2$  fluxes. However, there is often a bias between the  
698 modelled  $fCO_2$  and available surface ocean measurements (Fay and McKinley 2021). The LDEO-HPD  
699 approach trains an eXtreme Gradient Boosting (XGB) algorithm to learn a non-linear relationship between  
700 model-data  $fCO_2$  mismatch and observed predictor variables: sea surface temperature (SST), sea surface  
701 salinity (SSS), chlorophyll concentration, mixed layer depth). The GOBM  $fCO_2$  is then corrected with the  
702 predicted model-data misfit to estimate real-world  $fCO_2$  for the observation period (Gloege et al., 2022).  
703 This results in reconstructed monthly surface ocean  $fCO_2$  and air-sea  $CO_2$  fluxes on a  $1^\circ \times 1^\circ$  grid in the  
704 open ocean beginning in 1982. Additional information can be found at [oceanarbon.ldeo.columbia.edu](http://oceanarbon.ldeo.columbia.edu).  
705 The data product is available at <https://zenodo.org/records/4760205>.

Deleted: at:

706 **29) LDEO-HPD with Extended Temporal Coverage:** Building on the work of Gloege et al. (2022), the  
707 LDEO-HPD product as mentioned above (No. 28) can be extended back in time to predict  $fCO_2$  for all  
708 available model years. Bennington et al. (2022a) find that the largest component of the GOBM corrections  
709 is climatological. The smaller corrections at other timescales suggest either that these are well captured by  
710 the GOBMs or the data are insufficient. The dominance of climatological corrections supports the  
711 extension of the LDEO-HPD  $fCO_2$  product backwards in time. A climatology of model-observation misfits  
712 for the best-observed period (2000-present) is applied to the GOBMs for 1959-1981, while an  
713 interannually varying correction is used for 1982 onward. (Bennington et al., 2022a). This results in  
714 reconstructed monthly surface ocean  $fCO_2$  and air-sea  $CO_2$  fluxes on a  $1^\circ \times 1^\circ$  grid covering the open  
715 ocean, beginning in 1959. Since 2022, the LDEO-HPD Back in Time product has been included in the  
716 annual release of the Global Carbon Budget (GCB). Additional information can be found at  
717 [oceanarbon.ldeo.columbia.edu](http://oceanarbon.ldeo.columbia.edu). The data product can be accessed via Zenodo at  
718 <https://zenodo.org/records/13891722>.

Deleted: -

719 **30) LDEO  $fCO_2$  - Residual Method:** A frequently used approach for estimating full-coverage  $fCO_2$  is to train  
720 a machine learning algorithm on sparse in situ  $fCO_2$  data and associated physical and biogeochemical  
721 observations. While these associated variables have well-known relationships to  $fCO_2$ , it is often unclear

724 how they mechanistically drive  $f\text{CO}_2$  around the world. The LDEO  $f\text{CO}_2$ -Residual method takes the basic  
725 approach and enhances connections between physical understanding and reconstructed  $f\text{CO}_2$ . The novel  
726 approach used here includes applying pre-processing to the  $f\text{CO}_2$  data to remove the direct effect of  
727 temperature – a relationship well-documented in literature and lab experiments (Takahashi et al., 2002).  
728 This enhances the biogeochemical/physical component of  $f\text{CO}_2$  in the target variable (now  $f\text{CO}_2$ -Residual)  
729 and reduces the complexity that the machine learning must disentangle. The resulting algorithm has  
730 physically understandable connections between input data and the output biogeochemical/physical  
731 component of  $f\text{CO}_2$  (Bennington et al., 2022b). This results in reconstructed monthly surface ocean  $f\text{CO}_2$   
732 and air–sea  $\text{CO}_2$  fluxes on a  $1^\circ \times 1^\circ$  grid covering the open ocean, beginning in 1982 and extended to the  
733 most recent year of available data. Additional information can be found at [oceancarbon.ldeo.columbia.edu](https://oceancarbon.ldeo.columbia.edu).  
734 The data product can be accessed via Zenodo at <https://zenodo.org/records/13941548>.

### 31) CMEMS-LSCE Surface Ocean Carbonate Data Products:

735 (a) **CMEMS-LSCEv1**: Monthly surface ocean  $p\text{CO}_2$  and air–sea  $\text{CO}_2$  fluxes on a  $1^\circ \times 1^\circ$  grid in both the  
736 open ocean and coastal seas from 1985–2019 were reconstructed by Chau et al., (2022). CMEMS-LSCE is  
737 short for Copernicus Marine Environment Monitoring Service - Laboratoire des Sciences du Climat et de  
738 l'Environnement. This product is generated from an ensemble-based reconstruction of  $p\text{CO}_2$  maps trained  
739 with gridded data from SOCATv2020 (Bakker et al., 2016). Sea-surface  $p\text{CO}_2$  values (converted from the  
740 original  $f\text{CO}_2$  values in SOCATv2020) were regressed against a set of predictors with non-linear functions,  
741 i.e., feed-forward neural network (FFNN) models. The predictors include: sea-surface height (SSH), SST,  
742 SSS, MLD, chlorophyll a (Chl-a), atmospheric  $\text{CO}_2$  mole fraction ( $x\text{CO}_2$ ), and geographical coordinates  
743 (longitudes and latitudes). This data product is accessible [at](https://data.ipsl.fr/catalog/srv/eng/catalog.search#/metadata/a2f0891b-763a-49e9-af1b-78ed78b16982)  
744 <https://data.ipsl.fr/catalog/srv/eng/catalog.search#/metadata/a2f0891b-763a-49e9-af1b-78ed78b16982>.  
745

746 (b) **CMEMS-LSCEv2**: CMEMS-LSCEv2 corresponds to the latest version of the CMEMS-LSCE FFNN.  
747 It uses the same ensemble-based reconstruction method for  $p\text{CO}_2$  maps as CMEMS-LSCEv1.  
748 Improvements include downscaling the spatial resolution to  $0.25^\circ \times 0.25^\circ$  and reproducing additional  
749 surface ocean carbonate system variables on a global grid from 1985 onwards (Chau et al., 2024a). The  
750 additional surface ocean carbonate system variables are:  $p\text{CO}_2$ , DIC, TA, pH,  $\Omega_{\text{arag}}$ , and  $\Omega_{\text{calc}}$ . Surface  
751 ocean  $p\text{CO}_2$  is reconstructed based on an ensemble of neural network models mapping gridded observation-  
752 based data provided by SOCATv2022 (Bakker et al., 2016). Surface ocean TA is estimated with a multiple  
753 linear regression approach (Carter et al., 2016, 2017). The remaining carbonate variables are calculated  
754 from  $p\text{CO}_2$  and TA using a MATLAB version of CO2SYS (Lewis and Wallace, 1998; Van Heuven et al.,  
755 2011). The CMEMS-LSCE product is updated yearly for surface ocean  $p\text{CO}_2$ , air–sea fluxes, and the  
756 carbonate system variables. Updates are phased with release of the SOCAT database. For surface ocean  
757  $p\text{CO}_2$  and air–sea fluxes the temporal coverage is extended to the present date with a latency of 1 month  
758 (Chau et al., 2024b). Both the multi-year reconstruction and the near-real time prediction can be accessed

Deleted: at:

760 through the CMEMS portal: <https://doi.org/10.48670/moi-00047>.

761 **32) CarboScope (Jena-MLS):** The Jena Mixed-Layer Scheme (within the CarboScope family of data-based  
762 estimates of carbon-cycle variability) is based on observed sea surface  $p\text{CO}_2$  from SOCAT (see above No.  
763 1) (Bakker et al., 2014). It provides daily global fields of  $p\text{CO}_2$  and air-sea  $\text{CO}_2$  fluxes from 1957 to the  
764 year before present, on a resolution of  $2.5^\circ \times 2^\circ$  degrees. In the original method (Rödenbeck et al., 2013), a  
765 diagnostic model of the carbon balance in the ocean mixed layer is being fitted to the  $p\text{CO}_2$  data, by  
766 adjusting the ocean-interior sources and sinks of carbon of the mixed layer. The multi-decadal trend is  
767 derived from the data-based Ocean Circulation Inverse Model (OCIM) estimate provided by DeVries  
768 (2022b). Since a later extension described in Rödenbeck et al. (2022), the variability in the ocean-interior  
769 sources and sinks is first regressed against variability in SST and wind speed. The regression step is  
770 followed by a correction step with explicit temporal variability, to also represent data variability not yet  
771 represented by the predictors of the regression. The CarboScope product is updated yearly. The results from  
772 current and previous releases can be downloaded from <https://www.bgc-jena.mpg.de/CarboScope/>.

773 **33) UOEx-Watson:** This product is an estimate of the atmosphere-ocean flux of  $\text{CO}_2$  that takes into account  
774 near-surface temperature deviations (Watson et al., 2020). Most estimates use data on surface ocean  $p\text{CO}_2$   
775 without considering corrections due to temperature gradients within the uppermost few millimeters of the  
776 sea surface (“Skin temperature effects”) or small effects due to changes in temperature that occur during  
777 sampling and measurement, especially when the measurement is from a commercial vessel rather than a  
778 research ship. This product takes these effects into account by recalculating  $p\text{CO}_2$  from the SOCAT data  
779 base (v2019) using co-located satellite observations of skin temperature. The result is a substantial increase  
780 in the calculated net global uptake of  $\text{CO}_2$ . In other respects, the methodology for this data product follows  
781 the two-step neural network approach described by Landschützer et al. (2013, 2014). The gridded data set  
782 of sea surface  $f\text{CO}_2$  adjusted to satellite-derived subskin surface temperature, is available at  
783 <https://doi.org/10.1594/PANGAEA.905316>. Ocean-atmosphere fluxes interpolated to monthly and  $1^\circ \times 1^\circ$   
784 spatial resolution is available at <https://www.ncei.noaa.gov/data/oceans/ncei/ocads/metadata/0301544.html>.

785 **34) NIES-ML3:** The National Institute for Environmental Studies (NIES-ML3) product includes monthly  
786 global surface ocean  $f\text{CO}_2$  in 1982–2023 on a  $1^\circ \times 1^\circ$  grid. Using a leave-one-year-out (LOYO) validation  
787 method and three machine learning models, Zeng et al. (2022) found that the time variant trends of ocean  
788  $\text{CO}_2$  could be estimated approximately by a harmonic function fitting of the annual atmospheric  $\text{CO}_2$ . They  
789 removed the estimated trends from the ocean  $\text{CO}_2$  and applied the LOYO to the trend-removed data to  
790 obtain the trend that could not be approximated by the fitting for trend correction. The trend-removed data  
791 by the corrected trends were used to train the models. The gap-filled  $\text{CO}_2$  maps were constructed by adding  
792 the trends to model predictions. The product is available at NIES: <https://doi.org/10.17595/20220311.001>  
793 (Zeng 2022).

Deleted: sea-air

Deleted: OCADS:

Deleted: -

797 **35) CSIR-ML6:** Provides monthly  $1^\circ \times 1^\circ$  estimates of surface  $p\text{CO}_2$  (Gregor et al., 2019a). The approach uses  
798 the conceptual two-step approach of clustering and performing regressions for each cluster as Landschützer  
799 et al. (2016). CSIR-ML6 investigates the efficacy of various machine learning (ML) methods in estimating  
800 surface  $p\text{CO}_2$ , namely, feed-forward neural networks (FFNN), extremely randomized trees (ERT), gradient  
801 boosting machines (GBM), and support vector regression (SVR). It is found that the ensemble of all but the  
802 ERT method resulted in the best estimate, highlighting the fact that various ML methods do not produce the  
803 same outcome, particularly when data is sparse. Further, the variance between ensemble members can  
804 inform us about regions where uncertainty may be large due to methodological differences. Despite this, all  
805 methods achieve roughly the same uncertainty – a barrier, or wall beyond which the community has yet to  
806 overcome. The data are available at <https://www.ncei.noaa.gov/data/oceans/nci/ocads/metadata/0206205.html> (Gregor et al., 2019b). The  
807 product is one of the six ensemble members of the SeaFlux dataset.  
808

Deleted: OCADS:

809 **36) Stepwise-FFNN:** Zhong et al. (2022) constructed a monthly global  $1^\circ \times 1^\circ$  surface ocean  $p\text{CO}_2$  product  
810 from January 1992 to December 2024, by combining the stepwise regression algorithm and a feed-forward  
811 neural network (FFNN) to select predictors of  $p\text{CO}_2$  based on the mean absolute error in each of the 11  
812 biogeochemical provinces defined by the self-organizing map (SOM) method. The methodology for this  
813 data product used regionally optimal predictors to account for differences in  $p\text{CO}_2$  drivers, lowering local  
814 biases relative to a single global predictor set. The developed data product is available [at](http://dx.doi.org/10.12157/IOCAS.20250814.001)  
815 <http://dx.doi.org/10.12157/IOCAS.20250814.001>.

Deleted: at:

816 **37) AOML-ET:** Wanninkhof et al. (2024, 2025) developed a monthly global ocean data product of seawater  
817  $p\text{CO}_2$  and [air-sea](#)  $\text{CO}_2$  fluxes, referred to as AOML-ET, using an extremely randomized trees (ET) machine  
818 learning technique. These maps are created on  $1^\circ \times 1^\circ$  spatial grids, providing global surface ocean  
819 coverages from 1998 to 2023. AOML-ET incorporates several predictor variables, including time, location,  
820 SST, SSS, MLD, and chlorophyll-a. The model was trained using the v2020 and v2023 releases of the  
821 SOCAT data product (No. 1). [Air-sea](#)  $\text{CO}_2$  fluxes were calculated using the [air-sea](#)  $\text{CO}_2$  partial pressure  
822 difference ( $\Delta p\text{CO}_2$ ) and a bulk gas transfer formulation incorporating windspeed. The dataset contains  
823 monthly  $1^\circ \times 1^\circ$  NetCDF files of the AOML-ET outputs, along with the predictor variables. The data  
824 [product is available at https://www.ncei.noaa.gov/data/oceans/nci/ocads/metadata/0298989.html](https://www.ncei.noaa.gov/data/oceans/nci/ocads/metadata/0298989.html)  
825 (Wanninkhof et al., 2024).

Deleted: sea-air

Deleted: Sea-a

Deleted: -

Deleted: are

Deleted: OCADS:

833 **38) ULB-SOM-FFN-Coastalv2.1:** Roobaert et al. (2024) present high-resolution ( $0.25^\circ \times 0.25^\circ$  grid) monthly  
834 maps showing the distribution of sea surface  $p\text{CO}_2$  across the global coastal ocean, spanning from 1982 to  
835 2020. This product (ULB-SOM-FFN-coastalv2.1) builds upon the work by Laruelle et al. (2017),  
836 incorporating a two-step methodology that utilizes Self Organizing Maps (SOM) and Feed Forward  
837 Networks (FFN). This updated product now captures temporal variability, enabling the assessment of  
838 interannual variability and long-term trends in coastal air–sea  $\text{CO}_2$  exchange, unlike the product by Laruelle  
839 et al. (2017), which only offers a climatology for a short period (1998–2015). The enhancements include  
840 additional environmental predictors and an expanded dataset for training and validation, featuring  
841 approximately 18 million direct coastal observations from the SOCAT database, specifically the  
842 SOCATv2022 release (Bakker et al., 2016). The product is available at  
843 <https://www.ncei.noaa.gov/data/oceans/ncei/ocads/metadata/0279118.html> (Roobaert et al., 2023).

Deleted: s

Deleted: -

Deleted: OCADS:

844 **39) RFR-LME:** Sharp et al. (2024a) developed a data product delineating the temporal trends of OA indicators  
845 mapped on a  $0.25^\circ \times 0.25^\circ$  spatial grid, across eleven U.S. Large Marine Ecosystems (LMEs), with  
846 monthly coverage from 1998–2023. These indicators, which include the  $p\text{CO}_2$ , pH,  $\Omega_{\text{arag}}$ , DIC, TA, Revelle  
847 Factors, among others, were derived from SOCATv2023, along with other oceanographic properties, e.g.,  
848 SST, SSS, SSH, and MLD. The methodology combined Gaussian Mixture Models to categorize the data  
849 into environmentally similar subregions, Random Forest Regressions for the spatial and temporal  
850 extrapolation of observational  $f\text{CO}_2$  data, and regressions to estimate TA (Carter et al., 2021) to provide a  
851 second carbonate system constraint. The resulting maps are available at  
852 <https://www.ncei.noaa.gov/data/oceans/ncei/ocads/metadata/0287551.html> (Sharp et al., 2024b), while an  
853 online portal at <https://ecowatch.noaa.gov/thematic/ocean-acidification> presents regionally averaged time-  
854 series for three key indicators:  $p\text{CO}_2$ ,  $\Omega_{\text{arag}}$ , and pH.

Deleted: OCADS:

855 **40) ReCAD-NAACOM- $p\text{CO}_2$ :** Wu et al. (2025) developed a reconstructed  $p\text{CO}_2$  product for the North  
856 American Atlantic Coastal Ocean Margins (NAACOM), spanning from the Gulf of Mexico/Gulf of  
857 America to the Grand Banks, called the Reconstructed Coastal Acidification Database- $p\text{CO}_2$  (ReCAD-  
858 NAACOM- $p\text{CO}_2$ ). This product employed a two-step approach combining random forest regression and  
859 linear regression to generate monthly  $p\text{CO}_2$  data at  $0.25^\circ$  spatial resolution from 1993–2021. The model  
860 was trained using SOCAT v2023 observations as ground-truth values, incorporating various satellite-  
861 derived and reanalysis environmental variables known to influence sea surface  $p\text{CO}_2$ . The ReCAD-  
862 NAACOM- $p\text{CO}_2$  dataset is publicly accessible (<https://doi.org/10.5281/zenodo.11500974>) and will be  
863 updated regularly.

864 **41) Gridded Surface OA Indicators in the Northern Caribbean Sea:** This dataset contains a high-quality  
865 dataset of derived products from over a million observations of surface water partial pressure/fugacity of  
866 carbon dioxide ( $p\text{CO}_{2w}/f\text{CO}_{2w}$ ), for the Caribbean Sea, Gulf of Mexico/Gulf of America and North-West  
867 Atlantic Ocean covering the timespan from 2002-01-01 to 2019-12-30. The derived quantities include TA,

Deleted: -

873 acidity (pH),  $\Omega_{\text{arag}}$  and air-sea  $\text{CO}_2$  flux (Wanninkhof et al., 2020). This data product is available at  
874 <https://www.ncei.noaa.gov/data/oceans/ncei/ocads/metadata/0207749.html> (Wanninkhof et al., 2019)

Deleted: OCADS:

875 **42) OA Data in the Gulf of Mexico/Gulf of America and Wider Caribbean:** The Acidification, Climate, and  
876 Coral Reef Ecosystems Team (ACCRETE) Lab within AOML's Ocean Chemistry and Ecosystems  
877 Division (OCED) developed a data product for tracking OA in the Caribbean and Gulf of Mexico/Gulf of  
878 America from 2014 to 2020 (van Hooidonk, 2022). Utilizing satellite imagery and a data-assimilative  
879 hybrid model, the tool maps key indicators of the water's carbonate system, including  $p\text{CO}_2$ , TA, pH,  $\Omega_{\text{arag}}$ ,  
880 and  $\Omega_{\text{calc}}$ . This innovation builds upon an update to the experimental OA Product Suite (OAPS) developed  
881 by NOAA's Coral Reef Watch. The data product is available at  
882 <https://www.ncei.noaa.gov/data/oceans/ncei/ocads/metadata/0245950.html> (van Hooidonk, 2022).

Deleted: OCADS:

883 **43)  $p\text{CO}_2$  Climatology of the Baltic Sea:** Bittig et al. (2024) used biogeochemical model output to inform the  
884 mapping of sea surface  $p\text{CO}_2$  observations in the Baltic Sea and to build a mean monthly climatology for  
885 the period 2003 to 2021, with spatial resolutions of  $0.10^\circ \times 0.05^\circ$  (approximately 3 nautical miles in both  
886 directions). In a first step, spatial patterns of variability were extracted from 20 years of model surface  
887  $p\text{CO}_2$  data by an EOF analysis. These spatial patterns were then used to map surface  $p\text{CO}_2$  observations  
888 from SOCAT (see above No. 1) (Bakker et al., 2014) onto the Baltic Sea domain. By using an ensemble  
889 approach with varying number of EOF patterns, the spatial scales of the mapping were locally adjusted  
890 based on the observation's data density. Mapped monthly fields of  $p\text{CO}_2$  from 2003-2021 were combined  
891 for the product into a mean monthly climatology and a spatially-resolved linear trend. The climatology  
892 product is available at PANGAEA: <https://doi.org/10.1594/PANGAEA.961119> (Bittig et al., 2023).

Deleted: -

893 **44) INCOIS-ReML:** The Indian National Centre for Ocean Information Services-Regional Machine Learning  
894 model (INCOIS-ReML)  $p\text{CO}_2$  data product offers machine learning based monthly climatological sea  
895 surface  $p\text{CO}_2$  and the corresponding air-sea  $\text{CO}_2$  flux for the Bay of Bengal (Joshi et al., 2024). This data  
896 product integrates publicly available open-ocean observations with data from the Indian Exclusive  
897 Economic Zone. This high-resolution ( $0.083^\circ \times 0.083^\circ$ ) monthly climatological  $p\text{CO}_2$  data product is  
898 available from the INCOIS Portal: <https://las.incois.gov.in>, and from OCADS:  
899 <https://www.ncei.noaa.gov/data/oceans/ncei/ocads/metadata/0307627.html> (Joshi et al., 2025a).

900 **45) INCOIS\_TA:** The Indian National Centre for Ocean Information Services-Total Alkalinity (INCOIS\_TA)  
901 data product offers a machine learning based monthly interannual surface TA from 1993-2020 for the  
902 North Indian Ocean (Joshi et al., 2025b). This data product integrates publicly available open-ocean  
903 observations with data collected during Indian scientific expeditions and from the Indian Exclusive  
904 Economic Zone. This high-resolution ( $0.083^\circ \times 0.083^\circ$ ) long-term monthly TA data product is available  
905 from the INCOIS Portal: <https://las.incois.gov.in>, and from OCADS:  
906 <https://www.ncei.noaa.gov/data/oceans/ncei/ocads/metadata/0307789.html> (Joshi et al., 2025c).

Deleted: -

911 Table 3. Gridded and derived ocean carbonate chemistry data synthesis products in the surface ocean.

No.	Name	Open ocean or Coastal ocean	Spatial resolution	Temporal resolution	Methodology	Highlights	Reference
23	Takahashi Delta /CO <sub>2</sub> and Flux Climatology	Open ocean	1° × 1°	12-month climatology referenced to 2010	Advection Scheme	Does not use proxy variables for extrapolation. Only produced as monthly climatology.	Fay et al. (2024)
24	MPI-ULB-SOM-FFN	Open ocean + Coastal ocean	0.25° × 0.25°	12-Month climatology without a reference year	2-step machine learning: Merged product of the SOM-FFN approach applied to the open ocean (Landschützer et al., 2016) and the coastal ocean (Laruelle et al., 2017)	Monthly gridded pCO <sub>2</sub> without adjusting for a specific reference year, high-resolution coastal ocean coverage	Landschützer et al. (2020a)
25	VLIZ SOM-FFN	Open ocean	1° × 1°	Monthly from January 1982 onwards	2-step machine learning: Self organizing map clustering followed by a feed forward network (SOM-FFN)	Monthly gridded pCO <sub>2</sub> from 1982 through near present	Landschützer et al. (2016)
26	JMA-MLR	Open ocean	1° × 1°	Monthly from January 1990 onwards	Multiple linear regressions	Temporal trends of DIC, TA, pCO <sub>2</sub> , air-sea CO <sub>2</sub> flux, pH, and Ω <sub>arag</sub>	Iida et al. (2021)
27(a)	OceanSODA-ETHZv1	Open ocean	1° × 1°	Monthly from 1982 to 2023	Ensemble of 2-step members: K-means clustering with gradient boosting and SVR regression	Temporal trends of DIC, TA, pCO <sub>2</sub> , pH, Ω <sub>arag</sub> , and Ω <sub>calc</sub>	Gregor and Gruber (2021)
27(b)	OceanSODA-ETHZv2	Open ocean + Coastal ocean	0.25° × 0.25°	8-day from 1982 to 2022	FFNN	Highlighting fine-scale and short-term variability of the ocean carbon sink	Gregor et al. (2024a, b)
28	LDEO-HPD fCO <sub>2</sub>	Open ocean	1° × 1°	Monthly from 1982	XGBoost algorithm	Temporal evolution of surface ocean fCO <sub>2</sub> and air-sea CO <sub>2</sub> exchange	Gloege et al. (2022)

Deleted: c

Deleted: .

Deleted: Open + Coastal

Deleted: Open + Coastal

29	LDEO-HPD with Extended Temporal Coverage	Open ocean	1° × 1°	Monthly from 1959	XGBoost algorithm	Uses model-data misfit climatology to extend estimate back in time to 1959	Bennington et al. (2022a)
30	LDEO/CO <sub>2</sub> - Residual Method	Open ocean	1° × 1°	Monthly from 1982	XGBoost algorithm	Removes the temperature component before ML	Bennington et al. (2022b)
31(a)	CMEMS -LSCEv1	Open ocean + Coastal ocean	1° × 1°	Monthly from 1985 to 2019	FFNN	Seamless reconstruction from coastal to open ocean	Chau et al. (2022)
31(b)	CMEMS -LSCEv2	Open ocean + Coastal ocean	0.25° × 0.25°	Monthly from 1985 to 2025	FFNN	Yearly extension of time-series & monthly reconstruction at low latency	Chau et al. (2024a, b)
32	CarboScope (Jena-MLS)	Open ocean	2.5° × 2°	Daily from 1957	Multi-linear regression against long-term predictors, plus auto-regressive correction	Variability of pCO <sub>2</sub> and air-sea CO <sub>2</sub> fluxes since 1957, sensitivities to SST and wind speed variations	Rödenbeck et al. (2022)
33	UOEx-Watson	Open ocean	1° × 1°	Monthly from January 1992	Two-step neural network approach described by Landschützer et al. (2013, 2014, 2016)	Air-sea fluxes of CO <sub>2</sub> with adjusted skin temperature effect	Watson et al., 2020
34	NIES-ML3	Open ocean	1° × 1°	Monthly from 1982 to 2023	FNN, GBM, RF	The prediction of a ML method was obtained from ten trainings with different seeds. The mean of the three methods was taken as the final prediction.	Zeng (2022), Zeng et al. (2022)
35	CSIR-ML6	Open ocean	1° × 1°	Monthly from 1982 to 2016	Ensemble: FFNN, SVR, ERT, Gradient Boosted Trees	Various ML methods produce different results when data is sparse, but all still achieving roughly the same uncertainty.	Gregor et al. (2019a)

Deleted: Open + Coastal

Deleted: Open + Coastal

Deleted: sea-air

Deleted: .

Deleted: .

36	Stepwise-FFNN	Open ocean	1° × 1°	Monthly from 1992 to 2024	SOM, FFNN, Stepwise regression	ML-based selection of predictors considering regional differences of pCO <sub>2</sub> drivers	Zhong et al. (2022)
37	AOML-ET	Open ocean	1° × 1°	Monthly from 1998 to 2023	Extremely randomized trees (ET) machine learning technique	Monthly global air-sea CO <sub>2</sub> flux maps in modern era	Wanninkhof et al. (2015)
38	ULB-SOM-FFN-Coastalv2.1	Coastal ocean	0.25° × 0.25°	Monthly from 1982 to 2020	2-step machine learning: Self organizing map clustering followed by a feed forward network (SOM-FFN)	Global temporal trends of coastal pCO <sub>2</sub> and air-sea CO <sub>2</sub> fluxes based on SOCATv2022 with data collected from 1982–2020	Roobaert et al. (2024)
39	RFR-LME	Coastal ocean	0.25° × 0.25°	Monthly from 1998 to 2023	Gaussian mixture models and random forest regressions	Temporal trends of OA indicators and estimated uncertainties across 11 U.S. Large Marine Ecosystems (LMEs), with monthly coverage from 1998–2023.	Sharp et al. (2024a)
40	ReCAD-NAACOM-pCO <sub>2</sub>	Coastal ocean	0.25° × 0.25°	Monthly from 1993 to 2021	2-step machine learning: random forest regression followed by linear regression	Sea surface pCO <sub>2</sub> in the North American Atlantic Coastal Ocean Margins (NAACOM)	Wu et al. (2025)
41	Gridded Surface OA Indicators in the Northern Caribbean Sea	Coastal ocean	1° × 1°	Monthly from 2002 to 2019	Gridding of the observations of fCO <sub>2</sub> , SST and SSS was performed by binning and averaging the data in (1° × 1° by month) cells	A 17-year record of fCO <sub>2</sub> , TA, pH, Ω <sub>arag</sub> , and air-sea CO <sub>2</sub> flux in the Caribbean Sea	Wanninkhof et al. (2020)
42	OA data in the Gulf of Mexico/Gulf of America and Wider Caribbean	Regional	0.088° × 0.88°	Monthly from 2014 to 2020	Utilizing satellite imagery and a data-assimilative hybrid model, the tool maps key indicators of the water's carbonate system, including pCO <sub>2</sub> , TA, pH, Ω <sub>arag</sub> , and Ω <sub>calc.</sub>	A new tool to monitor OA over the wider Caribbean and Gulf of Mexico/Gulf of America	van Hooijdonk (2022)

Deleted: sea-air

Deleted: .

Deleted:

Deleted: -sea

Deleted: .

43	<i>p</i> CO <sub>2</sub> Climatology of the Baltic Sea	Regional	0.10° × 0.05°	12-month climatology referenced to 2013; linear trend 2003–2021	Extrapolation using model-based patterns of variability	Does not use proxy variables for extrapolation. Spatial scales adjust locally to data density	Bittig et al. (2024)
44	INCOIS-ReML	Regional	0.083° × 0.083°	Monthly climatology referenced to 2015.	Xtreme Gradient Boosting (XGB) based Machine Learning Model	This data product integrates publicly available open-ocean observations with data from the Indian EEZ region in the Bay of Bengal to provide surface <i>p</i> CO <sub>2</sub> and air–sea CO <sub>2</sub> flux estimates.	Joshi et al. (2024)
45	INCOIS_TA	Regional	0.083° × 0.083°	Monthly from 1993 to 2020	Xtreme Gradient Boosting (XGB) based Machine Learning Model	Integrates publicly available open-ocean observations with data collected during Indian scientific expeditions and from the Indian Exclusive Economic Zone to provide surface TA estimates for the North Indian Ocean.	Joshi et al. (2025b)

Deleted: -

Deleted: .

Deleted: .

926 **3.1.4 Gridded and Derived Products – Interior Ocean:**

927 This section describes gridded data products derived from observations through interpolation and other gap-filling  
928 procedures, depicting the interior ocean.

Deleted: that have been

929 **46) GLODAPv2 Climatology (referenced to 2002):** Lauvset et al. (2016) generated a comprehensive set of  
930 global interior ocean climatologies, mapping key biogeochemical variables on a 1° × 1° grid for 33 depth  
931 levels from the surface to 5500 m. These climatologies cover temperature, salinity, DO, nitrate, phosphate,  
932 silicate, DIC, TA, pH, Ω<sub>arag</sub>, and Ω<sub>calc</sub>. This data product was created based on the quality-controlled and  
933 internally consistent GLODAPv2.2016 (Olsen et al., 2016) using the data-interpolating variational analysis  
934 (DIVA) method (Barth et al., 2014). The conceivably confounding temporal trends in DIC, pH, Ω<sub>arag</sub> and  
935 Ω<sub>calc</sub> due to anthropogenic influence were removed prior to mapping by normalizing their values to a  
936 reference year of 2002 using first-order calculations of anthropogenic carbon accumulation rates. For all  
937 variables, all data from the full 1972–2013 period were used, including data that did not receive full  
938 secondary quality-control. This data product is not updated each year along with the main GLODAPv2 data

Deleted: )

944 product. The mapped data product is available at  
945 <https://www.ncei.noaa.gov/data/oceans/ncei/ocads/metadata/0286118.html> (Lauvset et al., 2023a). It can  
946 also be accessed from the GLODAP website: <https://glodap.info/>. For reference, the original GLODAP  
947 Climatology (Version 1.1) is accessible at  
948 <https://www.ncei.noaa.gov/data/oceans/ncei/ocads/metadata/0001644.html> (Sabine et al., 2004b).

Deleted: OCADS:

Deleted: at:

949 **47) Aragonite Saturation State Climatology:** Jiang et al. (2015a) developed an interior ocean  $\Omega_{\text{arag}}$   
950 climatology (referenced to 2000), on a  $1^\circ \times 1^\circ$  grid at 9 standardized depth levels from the surface down to  
951 4000 m. This was accomplished by integrating data from the first version of GLODAP (Key et al., 2004),  
952 CARINA (Key et al., 2010), and PACIFICA (Suzuki et al., 2013), along with additional recent cruise  
953 datasets up to 2012. Temporal adjustments were made to a reference year of 2000, accounting for an annual  
954 increase of  $f\text{CO}_2$  of  $1.6 \mu\text{atm}$  in the surface mixed layer (SML), with a rate that decreases linearly to zero  
955  $\mu\text{atm yr}^{-1}$  from the bottom of the SML to a depth of 1000 m (Sabine et al., 2008). The data product is  
956 available at <https://www.ncei.noaa.gov/data/oceans/ncei/ocads/metadata/0139360.html> (Jiang et al.,  
957 2015b).

Deleted: Calculations of  $\Omega_{\text{arag}}$  utilized a MATLAB version of the CO2SYS program (Orr et al., 2015), with the dissociation constants for carbonic acid of Lueker et al. [2000], potassium bisulfate ( $\text{KHSO}_4^-$ ) of Dickson [1990], hydrofluoric acid (HF) of Perez and Fraga (1987), and the total borate concentration equations of Lee et al. [2010].

Deleted:  $^{-1}$

Deleted: OCADS:

#### 958 **48) Mapped Observation-Based Oceanic Dissolved Inorganic Carbon (MOBO-DIC):**

959 (a) **MOBO-DIC (Version 2020):** Keppler et al. (2020) produced a global interior ocean DIC monthly  
960 climatology (average climatological values for January through December) on a  $1^\circ \times 1^\circ$  grid at 33  
961 standardized depth levels from the surface to 2000 m. The MOBO-DIC mapping method adapts and  
962 extends the SOM-FFN technique originally introduced by Landschützer et al. (2013). It starts by  
963 categorizing the ocean into clusters with comparable physical and biogeochemical characteristics using  
964 self-organizing maps (SOM). Subsequently, within each SOM-defined cluster, a feed-forward network  
965 (FFN) is employed to estimate and enforce the statistical correlation between the targeted DIC data and the  
966 predictor data available in globally mapped fields. The product uses data from January 2004 to December  
967 2017, and is thus centered around the years 2010/2011. The data product is available at  
968 [https://www.ncei.noaa.gov/access/ocean-carbon-acidification-data-system/oceans/ndp\\_104/ndp104.html](https://www.ncei.noaa.gov/access/ocean-carbon-acidification-data-system/oceans/ndp_104/ndp104.html).

Deleted: OCADS:

969 (b) **MOBO-DIC (Version 2023):** Keppler et al. (2023a) extended the temporal resolution of MOBO-DIC  
970 to resolve monthly fields from January 2004 to December 2019, as opposed to the average climatological  
971 values in Keppler et al. (2020). This data product is on a  $1^\circ \times 1^\circ$  grid at 28 depth levels from the surface to  
972 1500 m. The data product is available at  
973 <https://www.ncei.noaa.gov/data/oceans/ncei/ocads/metadata/0277099.html> (Keppler et al., 2023b).

Deleted: OCADS:

974 **49) Monthly Interior Ocean TA Climatology:** Broullón et al. (2019) developed a monthly global interior  
975 ocean TA climatology using a feed-forward neural network approach. This dataset offers a spatial  
976 resolution of  $1^\circ \times 1^\circ$  in the horizontal, spans 102 depth levels (ranging from 0–5500 m) in the vertical  
977 dimension, and features a temporal resolution that varies from monthly (0–1500 m) to annual (1550–5500

990 m). The development of this climatology was based on the analysis of TA in relation to several key  
991 predictor variables, including temperature, salinity, nutrients (phosphate, nitrate, and silicate), DO, and  
992 sampling position (coordinates and depth), as outlined in Velo et al. (2013). Both TA and these predictor  
993 variables were sourced from GLODAPv2 (version 2016) (Olsen et al., 2016). The global interior ocean TA  
994 climatology was constructed by leveraging the established relationships between TA and the predictor  
995 variables, as well as the monthly climatologies of temperature, salinity, and DO from the WOA 2013  
996 (Locarnini et al., 2013; Zweng et al., 2013; Garcia et al., 2014), and nutrients data that were obtained  
997 through the CANYON-B neural network process, applied to the previously mentioned fields. The data  
998 product is available at <https://www.ncei.noaa.gov/data/oceans/ncei/ocads/metadata/0222470.html> (Broullón  
999 et al., 2020b).

Deleted: OCADS:

1000 **50) Monthly Interior Ocean DIC Climatology:** Broullón et al. (2020a) employed a feed-forward neural  
1001 network approach to create a monthly global interior ocean DIC climatology, centered around the year  
1002 1995. This dataset offers a  $1^\circ \times 1^\circ$  spatial resolution in the horizontal domain, encompassing 102 depth  
1003 levels ranging from 0–5500 m vertically. The temporal resolution varies, ranging from monthly (0–1500 m)  
1004 to annual (1550–5500 m). In contrast to their previous work on TA (Broullón et al., 2019), this analysis  
1005 includes the variable "year" to account for anthropogenic DIC pool changes. It also incorporates data from  
1006 the LDEO  $p\text{CO}_2$  database (Takahashi et al., 2017) alongside GLODAPv2.2019 (Olsen et al., 2019) to  
1007 establish relationships between DIC and its input variables: temperature, salinity, DO, as well as location,  
1008 pressure, and time. The DIC climatology was derived using these relationships, along with monthly  
1009 climatological data for temperature, salinity, and DO from WOA 2013 (Locarnini et al., 2013; Zweng et al.,  
1010 2013; Garcia et al., 2014), as well as phosphate, nitrate, and silicate values computed from the CANYON-B  
1011 neural network fed with the aforementioned fields. The data product is available at  
1012 <https://www.ncei.noaa.gov/data/oceans/ncei/ocads/metadata/0222469.html> (Broullón et al., 2020c).

Deleted: OCADS:

1013 **51) Acidification Metrics in the Ocean Interior:** Fassbender et al. (2023) generated estimates of global  
1014 interior ocean changes to pH,  $[\text{H}^+]$ ,  $\Omega_{\text{arag}}$ ,  $p\text{CO}_2$ , and the Revelle sensitivity factor driven by the  
1015 accumulation of anthropogenic carbon ( $C_{\text{ant}}$ ) from the preindustrial period to 2002, and quantified the  
1016 component of these changes caused by carbonate system nonlinearities. For each OA metric, the dataset  
1017 includes year 2002 values and quasi-preindustrial values, which were estimated by subtracting  $C_{\text{ant}}$  from the  
1018 year 2002 carbonate chemistry information and recomputing each OA metric without considering any  
1019 warming, circulation, or biological changes that may have occurred since the preindustrial era. Data from  
1020 the upper 2000 m of the GLODAPv2 Climatology (No. 46, Lauvset et al., 2016), and from the preformed  
1021 properties product of Carter et al. (2021) were used to make these estimates on the  $1^\circ \times 1^\circ$  GLODAPv2  
1022 Climatology grid for 26 depth levels from the surface to 2000 m. The provided uncertainties were estimated  
1023 using a 1000-iteration Monte Carlo simulation. Calculation details are described in Fassbender et al.  
1024 (2023). Year 2002  $\Omega_{\text{arag}}$  and pH values, and their uncertainties, are reproduced from the GLODAPv2

Deleted: the year

Deleted: o

Deleted: in the carbonate system

Deleted: .2016b mapped data product

Deleted: , described in

Deleted: ,

Deleted: ,

Deleted: .2016b

Deleted: .2016b mapped data product

1036 [Climatology](#) and are provided in this dataset for user convenience with the permission of the original data  
1037 producer. This data product is available at  
1038 <https://www.ncei.noaa.gov/data/oceans/ncei/ocads/metadata/0290073.html> (Fassbender et al., 2024).

Deleted: OCADS:

1039 **52) Ocean Interior Acidification Over the Industrial Era:** Building on the total anthropogenic carbon  
1040 estimates for 1994 from Sabine et al. (2004) and the decadal changes between 1994 and 2014 reconstructed  
1041 by Müller et al. (2023a), Müller and Gruber (2024a) quantified ocean interior acidification over the  
1042 industrial era. To convert the increasing anthropogenic carbon concentrations into acidification estimates,  
1043 their approach relied on time-invariant climatologies of ocean interior DIC, TA, temperature, salinity, and  
1044 other relevant variables to determine the background state of the marine carbonate system. Hence, their  
1045 estimates resolve exclusively the acidification driven by the anthropogenic carbon accumulation. In  
1046 contrast to direct observations of acidification variables, such as those collected at time-series stations, this  
1047 approach does not account for changes in the natural carbon cycle or the displacement of water masses. The  
1048 approach by Müller and Gruber (2024a) is conceptually similar to that of Fassbender et al. (2023), but  
1049 provides temporally resolved estimates, enabling the tracking of both the spatial distribution and temporal  
1050 evolution of ocean interior acidification. The data product is available at  
1051 <https://www.ncei.noaa.gov/data/oceans/ncei/ocads/metadata/0298993.html> (Müller and Gruber, 2024b).

Deleted: OCADS:

### 1052 **53) Decadal changes of anthropogenic CO<sub>2</sub>:**

1053 **(a) Anthropogenic CO<sub>2</sub> from 1994 to 2007:** Gruber et al. (2019a) estimated the decadal time-scale  
1054 changes in the oceanic content of anthropogenic CO<sub>2</sub> ( $\Delta C_{\text{ant}}$ ) between 1994 to 2007. The results were  
1055 derived from the GLODAPv2.2016 product (Olsen et al., 2016), utilizing the eMLR(C\*) methodology  
1056 pioneered by Clement and Gruber (2018). The product is combined with the estimated amount of  $C_{\text{ant}}$  for  
1057 1994 derived by Sabine et al. (2004) from GLODAPv1 to infer  $C_{\text{ant}}$  for 2007. All estimates are geospatially  
1058 distributed on a horizontal grid with a resolution of  $1^\circ \times 1^\circ$ . Two primary files are available: one providing  
1059 the complete three-dimensional distribution of  $\Delta C_{\text{ant}}$ , and the other containing vertically integrated values,  
1060 i.e., the column inventories. This data product is available at  
1061 <https://www.ncei.noaa.gov/data/oceans/ncei/ocads/metadata/0186034.html> (Gruber et al., 2019b).

Deleted: OCADS:

1062 **(b) Decadal Trends in Anthropogenic CO<sub>2</sub> from 1994 to 2014:** Müller et al. (2023a) extended the  
1063 analysis by Gruber et al. (2019a) to reconstruct decadal trends in the oceanic storage of  $\Delta C_{\text{ant}}$  in the global  
1064 ocean interior from mid-year 1994 to mid-year 2004, and further to mid-year 2014. They applied the  
1065 extended multiple linear regression (eMLR) method (Clement and Gruber, 2018) to ship-borne  
1066 observations of DIC and other biogeochemical variables from GLODAPv2.2021 (Lauvset et al., 2021). All  
1067 estimates are provided on a  $1^\circ \times 1^\circ$  horizontal grid. Two principal data files are provided: one featuring the  
1068 comprehensive three-dimensional distribution of  $\Delta C_{\text{ant}}$  for the two time periods, and the other presenting the  
1069 vertically integrated quantities, i.e., the column inventories. The data product is available at

1073 <https://www.ncei.noaa.gov/data/oceans/nci/ocads/metadata/0279447.html> (Müller et al., 2023b).

Deleted: OCADS:

1074 **54) Tracer-based rapid anthropogenic carbon estimation from 1750 to 2500:** Carter et al. (2025) developed  
1075 a method for estimating  $C_{\text{ant}}$  based on a machine learning translation of ocean circulation information  
1076 inferred from transient tracer distributions. They applied it to the gridded GLODAPv2 climatology to  
1077 obtain estimates of the past and projected  $C_{\text{ant}}$  distribution between 1750 and 2500. Projections are made  
1078 using a range of simple assumptions and shared socioeconomic pathway projections. Estimates are  
1079 provided on  $1^\circ \times 1^\circ$  spatial grids at 33 standard depth levels in micromoles  $C_{\text{ant}}$  per kg of seawater. This  
1080 data product is available [at https://doi.org/10.5281/zenodo.15692788](https://doi.org/10.5281/zenodo.15692788).

Deleted: at:

1081 **55) Preformed TA and other biogeochemical properties:** Carter et al. (2020) estimated preformed seawater  
1082 TA, nitrate, silicate, phosphate, and oxygen using empirical seawater property estimation routines (Carter et  
1083 al., 2017) with ocean circulation pathway information from ocean circulation transport matrices (John et  
1084 al., 2020). Preformed properties are estimated property contents that seawater had when it last left contact  
1085 with the atmosphere, and are used as an aid in interpretation of measured ocean property distributions. This  
1086 data product is available [at https://doi.org/10.5281/zenodo.3745002](https://doi.org/10.5281/zenodo.3745002).

Deleted: at:

1087 **56) Monthly Interior Ocean pH Climatology:** Zhong et al. (2025) developed a monthly  $1^\circ \times 1^\circ$  gridded  
1088 global seawater pH (total scale) climatology from 1992 to 2020 at in situ temperature, derived using a  
1089 machine learning algorithm trained on pH observations from GLODAPv2 (Lauvset et al., 2024). The  
1090 product spans from 1992 to 2020 and covers depths from the surface to 2000 m across 41 vertical levels. Its  
1091 development involved a three-step machine-learning approach: (1) regional division using a self-organizing  
1092 map neural network, (2) predictor selection via stepwise regression, which iteratively adds or removes  
1093 variables based on their impact on reconstruction error, and (3) nonlinear regression using feedforward  
1094 neural networks (FFNNs). The developed data product is available [at](http://dx.doi.org/10.12157/IOCAS.20230720.001)  
1095 <http://dx.doi.org/10.12157/IOCAS.20230720.001>.

Deleted: at:

1096 **57) CODAP-NA Climatology:** Jiang et al. (2024) developed a coastal OA indicators climatology on a  $1^\circ \times 1^\circ$   
1097 grid, covering North American ocean margins from the surface to 500 m at 14 standardized depth levels.  
1098 This product includes 10 key oceanographic variables:  $f\text{CO}_2$ , pH,  $[\text{H}^+]_{\text{total}}$ , free hydrogen ion content  
1099 ( $[\text{H}^+]_{\text{free}}$ ), carbonate ion content ( $[\text{CO}_3^{2-}]$ ),  $\Omega_{\text{arag}}$ ,  $\Omega_{\text{calc}}$ , DIC, TA, and Revelle Factor (RF), as well as  
1100 temperature and salinity. The climatology was produced with the WOA gridding technologies of the  
1101 NOAA National Centers for Environmental Information (NCEI), based on the recently released Coastal  
1102 Ocean Data Analysis Product in North America (CODAP-NA) (Jiang et al., 2021), along with  
1103 GLODAPv2.2022 (Lauvset et al., 2022). The relevant variables were adjusted to the year of 2010 before  
1104 the gridding. The first-guess fields for this analysis were calculated using ESPERs (Carter et al., 2021),  
1105 based on the WOA (Version 2018) climatologies for salinity (Zweng et al., 2019), temperature (Locarnini  
1106 et al., 2019) and DO (Garcia et al., 2018b). The data product is available in NetCDF at

1111 <https://www.ncei.noaa.gov/data/oceans/ncei/ocads/metadata/0270962.html> (Jiang et al., 2022b).

1112 Additionally, maps of these indicators are available in jpeg at <https://www.ncei.noaa.gov/access/ocean->

1113 carbon-acidification-data-system/synthesis/nacoastal.html (Jiang et al., 2022b).

Deleted: OCADS:

Deleted: at:

1114 **Table 4. Gridded and derived ocean carbonate chemistry data synthesis products in the subsurface ocean.**

No.	Name	Open ocean or Coastal ocean	Resolution	Temporal resolution	Methodology	Highlights	Reference
46	GLODAPv2 Climatology	Open ocean	1° × 1°	Referenced to 2002	Data Interpolating Variational Analysis (DIVA)	Ocean interior climatology for multiple variables from the surface to the bottom of the ocean (referenced to 2002)	Lauvset et al. (2016)
47	Aragonite Saturation State Climatology	Open ocean	1° × 1°	Referenced to 2000	Data Interpolating Variational Analysis (DIVA)	Ocean interior climatology for $\Omega_{\text{arag}}$ from the surface to 4000 m (referenced to 2000)	Jiang et al. (2015a)
48(a)	MOBO-DIC (Version 2020)	Open ocean	1° × 1°	Monthly climatology referenced to January 2011	Machine learning	Seasonal variability of DIC in the interior ocean from the surface to 2000 m	Keppler et al. (2020)
48(b)	MOBO-DIC (Version 2023)	Open ocean	1° × 1°	Monthly from January 2004 to December 2019	Machine learning	Temporal trends and interannual variability of DIC in the interior ocean from the surface to 1500 m	Keppler et al. (2023a,b)
49	Monthly Interior Ocean TA Climatology	Open ocean	1° × 1°	Monthly climatology	Machine learning	Ocean interior climatology for TA from the surface to the bottom	Broullón et al. (2019, 2020b)
50	Monthly Interior Ocean DIC Climatology	Open ocean	1° × 1°	Monthly from 1957 to 2018	Machine learning	Ocean interior climatology for DIC from the surface to the bottom (referenced to 1995)	Broullón et al. (2020a, c)
51	Acidification Metrics in the Ocean Interior	Open ocean	1° × 1°	2002 and preindustrial	Reproduced from GLODAPv2 Climatology (Lauvset et al., 2016) and the preformed properties of Carter et al., (2021)	Metrics of acidification in the ocean interior (to 2000 m) and the component of those changes caused by carbonate system nonlinearities	Fassbender et al. (2023)

Deleted: c

Deleted: year

Deleted: year

Deleted: .2016b

52	Ocean Interior Acidification over the Industrial Era	Open ocean	1° × 1°	1800-1994, 2004-2014	Conversion of anthropogenic carbon accumulation into acidification rates	Temporal trends in the progression of acidification in the interior ocean are resolved	Müller and Gruber (2024a)
53(a)	Anthropogenic CO <sub>2</sub> from 1994 to 2007	Open ocean	1° × 1°	From 1994 to 2007	eMLR(C*) extended Multiple Linear Regression applied to the tracer C*	The oceanic sink for anthropogenic CO <sub>2</sub> over the period 1994 to 2007	Gruber et al. (2019a)
53(b)	Decadal Trends in Anthropogenic CO <sub>2</sub> from 1994 to 2014	Open ocean	1° × 1°	Decadal from 1994 to 2014	eMLR(C*) extended Multiple Linear Regression applied to the tracer C*	Temporal trends in the accumulation of anthropogenic CO <sub>2</sub> in the interior ocean are resolved	Müller et al. (2023a)
54	Anthropogenic carbon from 1750 to 2500 (TRACE)	Open ocean	1° × 1°	Referenced to 20 years ranging from ~1750 to 2500	Estimated from atmospheric transients and ocean tracer distributions	Estimates over time based on assumptions of steady state ocean circulation and CO <sub>2</sub> exchange	Carter et al. (2025)
55	Preformed TA and other biogeochemical properties	Open ocean	1° × 1°	Not referenced in time	Empirical algorithms with inversions to find source outcrops	Estimates of the properties of seawater at the time of last contact with the atmosphere	Carter et al. (2021)
56	Monthly Interior Ocean pH Climatology	Open ocean	1° × 1	Monthly from January 1992 to December 2020	Machine learning	Temporal variability of pH in the interior ocean from the surface to 2000 m over 3 decades	Zhong et al. (2025)
57	CODAP-NA Climatology	Coastal ocean	1° × 1°	Referenced to 2010	Objective analysis approach of the WOA	The first discrete bottle-based climatology in the North American ocean margins	Jiang et al. (2024)

Deleted: -  
Deleted: to  
Deleted: -

Deleted: and

1121

1122 **3.1.5 Multi-product Analyses:**

1123 This section includes data products that have been generated by community synthesis efforts designed to inform the  
1124 GCB.

1125 **58) SeaFlux:** Harmonization of air-sea CO<sub>2</sub> fluxes from surface pCO<sub>2</sub> data products using a standardized  
1126 approach (Gregor and Fay, 2021). This resource provides an ensemble of six pCO<sub>2</sub> products with air-sea  
1127 CO<sub>2</sub> fluxes computed consistently. The six included products are: CMEMS-LSCEv1, CSIR-ML6, JENA-  
1128 MLS, JMA-MLR, MPI-SOMFFN, and NIES-FNN. First, missing areas of pCO<sub>2</sub> estimates (mostly high-  
1129 latitude and marginal seas) are filled using a linear-regression approach, thus addressing differences in  
1130 spatial coverage between the mapping products. Further, it also accounts for methodological  
1131 inconsistencies in flux calculations. Fluxes are calculated using three wind products (CCMPv2, ERA5, and

1136 JRA55) along with the application of a scaled gas exchange coefficient for each of the wind products.  
1137 Through these steps, SeaFlux presents an **ensemble** product of interpolated global surface ocean  $p\text{CO}_2$  and  
1138 air–sea carbon flux estimates for the years 1990–2019. For more details, refer to Fay et al. (2021).

Deleted: ensemble

1139 **59) RECCAP2:** In the context of the second iteration of the project REgional Carbon Cycle Assessment and  
1140 Processes (RECCAP2), the ocean carbon community compiled, quality-controlled, and harmonized (in the  
1141 sense of providing output on the same regular grid at the same spatial and temporal resolution) 12 GOBMs  
1142 simulations, 11  $p\text{CO}_2$  products, one ocean interior DIC product, and three data assimilation models to  
1143 constrain the ocean carbon sink between 1985 and 2018. The RECCAP2 synthesis effort stands as a distinct  
1144 but complementary resource to the GCB project (Friedlingstein et al., 2025), which primarily focuses on  
1145 anthropogenically perturbed surface  $\text{CO}_2$  fluxes from a global budgeting perspective. The individual  
1146 chapters of RECCAP2 were published in this special issue of *Global Biogeochemical Cycles*:  
1147 [https://agupubs.onlinelibrary.wiley.com/doi/toc/10.1002/\(ISSN\)2169-8961.RECCAP2](https://agupubs.onlinelibrary.wiley.com/doi/toc/10.1002/(ISSN)2169-8961.RECCAP2). The data products  
1148 of this assessment are available on a  $1^\circ \times 1^\circ$  horizontal grid, with monthly resolution for surface ocean  
1149 variables such as air–sea  $\text{CO}_2$  fluxes, and annual resolution for interior ocean variables, such as DIC  
1150 content. The data compilation, which is described in detail in DeVries et al. (2023), is available at  
1151 <https://zenodo.org/records/7990823> (Müller, 2023).

Deleted: at:

1152 **60) Global Carbon Budget:** The GCB collects annually updated estimates of the ocean carbon sink from  
1153 currently nine  $f\text{CO}_2$ -products and ten GOBMs for the period 1959 to the past calendar year  
1154 (<https://globalcarbonbudget.org/gcb-2025>, Friedlingstein et al., 2025, **under review**). In contrast to Earth  
1155 System Models (ESMs), the GOBMs are here forced with atmospheric reanalysis that ingested atmosphere  
1156 and ocean observations and are thus thought to be closer to the observed climate. Gridded fields are  
1157 provided on a  $1^\circ \times 1^\circ$  horizontal grid and monthly resolution. In addition, globally and regionally integrated  
1158 air–sea  $\text{CO}_2$  fluxes from the native model grids are provided. Globally integrated time-series are adjusted  
1159 for full ocean coverage and model bias and drift and are available for each individual  $f\text{CO}_2$ -product and  
1160 GOBM (<https://globalcarbonbudget.org/download/1442/?tmstv=1731323337>). The model data goes well  
1161 beyond surface fluxes and includes data to analyze drivers of carbon fluxes, including several 3D variables.  
1162 The model data request has been updated since RECCAP2 and also provides, for example, monthly interior  
1163 ocean data of DIC, TA, nutrients and DO. The GOBM data request was also updated to have all variables  
1164 available that are needed to serve as a testbed for  $f\text{CO}_2$ -products (e.g., sea surface height). Gridded surface  
1165 data of sea surface fugacity and air–sea  $\text{CO}_2$  flux of all  $f\text{CO}_2$ -products and GOBMs as used in the latest  
1166 release of GCB (2024) are published on Zenodo (<https://zenodo.org/records/14639761>, Hauck et al., 2025).  
1167 All other GOBM output is available via <https://globalcarbonbudgetdata.org/closed-access-requests.html>.

Deleted: 4

1171 **Table 5. Ocean carbonate chemistry data product synthesis and harmonizations.**

No.	Name	Open ocean or Coastal ocean	Surface or Water column	Spatial resolution	Temporal resolution	Methodology	Highlights	Reference
58	SeaFlux	Open ocean + Coastal ocean	Surface only	1° × 1°	Monthly from 1990 to 2022	Consistent flux calculations for 6 pCO <sub>2</sub> products to produce an ensemble estimate	Careful consideration of flux calculation provides a resource and code to the community for independent flux calculations	Gregor and Fay (2021)
59	RECCAP2	Open ocean + Coastal ocean	Surface + Water column	1° × 1° (open) 0.25° × 0.25° (coastal)	Monthly from 1985 to 2018	Harmonized compilation of surface fCO <sub>2</sub> products, model simulations and ocean interior products	Quality-controlled data compilation with a harmonized horizontal grid and temporal resolution	Müller (2023), DeVries et al. (2023), Resplandy et al. (2024)
60	Global Carbon Budget	Open ocean + Coastal ocean	Surface + Water column	1° × 1°	Monthly from 1959 to 2023	Harmonized compilation of surface fCO <sub>2</sub> products, and GOBM simulations	Annually updated and quality-controlled datasets. Availability of monthly 4D ocean model output.	Friedlingstein et al. (2025)

Deleted: c

Deleted: w

Deleted: Open + Coastal

Deleted: Open + Coastal

Deleted: Open + Coastal

Deleted:

1172

1173 **3.1.6 Model-based and Hybrid Products and Analyses:**

1174 Model-based projections of biogeochemical variables are often available from global and regional models, such  
1175 as those in the Seventh Coupled Model Intercomparison Project (CMIP7) (Dunne et al., 2024; Durack et al., 2025).

1176 This section further includes hybrid data products, which adjust model estimates towards observation-based  
1177 constraints.

1178 **61) Decadal Trends in the Ocean Carbon Sink:** The DeVries et al. (2019) analysis examines decadal trends  
1179 in global and regional air–sea CO<sub>2</sub> fluxes from a variety of ocean biogeochemical models that contributed  
1180 to the GCB (see No. 60). Three sets of model simulations were performed. Simulation A uses variable  
1181 climate forcing (e.g., variable wind stress, heat and freshwater fluxes) and observed atmospheric CO<sub>2</sub>  
1182 forcing, Simulation B uses constant (repeated) climate forcing and observed atmospheric CO<sub>2</sub>, and  
1183 simulation C uses both constant climate forcing and constant atmospheric CO<sub>2</sub> concentrations. With these  
1184 simulations, the authors partitioned decadal trends in ocean CO<sub>2</sub> uptake into those driven by climate  
1185 variability and those driven by atmospheric CO<sub>2</sub>. They found that climate variability drove a weakening  
1186 trend of the ocean carbon sink during the 1990s, and a strengthening trend during the first decade of the  
1187 2000s. The magnitude of these trends agreed with those of an OCIM that was trained to replicate tracer data  
1188 from the 1990s and 2000s (DeVries et al., 2017), indicating that the decadal trends may be driven by

1195 variability in ocean circulation. ~~The~~ data from this analysis ~~are~~ accessible at  
1196 <https://doi.org/10.6084/m9.figshare.8091161.v1>.

**Deleted:** This

**Deleted:** is

1197 **62) ECCO-Darwin:** Carroll et al. (2022) used the Estimating the Circulation and Climate of the Ocean-Darwin  
1198 (ECCO-Darwin) global-ocean biogeochemistry state estimate to generate a data-constrained DIC budget  
1199 and investigate how spatiotemporal variability in advection and mixing, air-sea CO<sub>2</sub> flux, and the  
1200 biological pump have modulated the ocean sink for 1995–2018. ECCO-Darwin assimilates ocean  
1201 circulation and physical tracers, including temperature, salinity, and sea ice, derived from the Estimating  
1202 the Circulation and Climate of the Ocean (ECCO) LLC270 global-ocean and sea-ice data synthesis (Zhang  
1203 et al., 2018). Additionally, it assimilates biogeochemical observations encompassing the cycling of carbon,  
1204 nitrogen, phosphorus (PO<sub>4</sub>), iron (Fe), silica (SiO<sub>2</sub>), DO, and TA. This inclusive approach enhances the  
1205 model's fidelity by aligning it with a diverse array of observations. All ECCO-Darwin model output is  
1206 available on the ECCO Data Portal: <https://data.nas.nasa.gov/ecco/>. The model code and platform-  
1207 independent instructions for running ECCO-Darwin simulations can be found ~~at~~  
1208 [https://github.com/MITgcm-contrib/ecco\\_darwin](https://github.com/MITgcm-contrib/ecco_darwin).

**Deleted:** at:

### 1209 **63) Global Surface Ocean Acidification Indicators:**

1210 **(a) Surface pH and Revelle Factor:** Jiang et al. (2019a) produced a high-resolution (1° × 1°) data product  
1211 delineating ~~a~~ regionally varying view of global surface ocean pH, acidity, and Revelle Factor (RF) from  
1212 1770 to 2100 by amalgamating recent observational seawater CO<sub>2</sub> data from the SOCAT database (Version  
1213 6) (Bakker et al., 2016) and temporal trends at individual locations of the global surface ocean from an  
1214 Earth System Model, i.e., GFDL-ESM2M (Dunne et al., 2013). The calculations were conducted under  
1215 historical atmospheric CO<sub>2</sub> levels (pre-2005) and four Representative Concentrations Pathways (post-2005)  
1216 corresponding to the Intergovernmental Panel on Climate Change (IPCC)'s 5th Assessment Report,  
1217 specifically RCP2.6, RCP4.5, RCP6.0, and RCP8.5. Surface ocean TA was calculated from SSS ~~and~~ SST  
1218 using the updated locally interpolated alkalinity regression (LIARv2) method (Carter et al., 2017). Surface  
1219 ocean pH, acidity, and RF were then calculated using a MATLAB version of the CO2SYS program (Orr et  
1220 al., 2015). The data product is available at  
1221 <https://www.ncei.noaa.gov/data/oceans/ncei/ocads/metadata/0206289.html> (Jiang et al., 2019b).

**Deleted:** ,

**Deleted:** OCADS:

1222 **(b) Surface OA Indicators:** Jiang et al. (2023) developed a comprehensive model-data fusion product that  
1223 delineates the trajectory of 10 OA indicators:  $f\text{CO}_2$ , pH,  $[\text{H}^+]_{\text{total}}$ ,  $[\text{H}^+]_{\text{free}}$ ,  $[\text{CO}_3^{2-}]$ ,  $\Omega_{\text{arag}}$ ,  $\Omega_{\text{calc}}$ , DIC, TA, and  
1224 RF, as well as temperature and salinity at all locations of the global surface ocean from 1750 to 2100. This  
1225 product marks a significant breakthrough in OA forecasting by refining temporal trends with data from 14  
1226 ~~ESMs~~ within CMIP6, and by applying bias and drift corrections ~~using~~ three updated observational ocean  
1227 carbonate system data products: SOCAT (Version 2022) (Bakker et al., 2016), GLODAPv2.2022 (Lauvset  
1228 et al., 2022), and CODAP-NA (Jiang et al., 2021). This dataset offers 10-year averages on a 1° × 1° global

**Deleted:** Earth System Models (

**Deleted:** )

**Deleted:** from

1237 surface ocean grid, capturing trends from preindustrial times (1750), through historical conditions (1850–  
1238 2010), and projects future conditions to 2100 across five Shared Socioeconomic Pathways: SSP1-1.9,  
1239 SSP1-2.6, SSP2-4.5, SSP3-7.0, and SSP5-8.5. The gridded data product is available in NetCDF at  
1240 <https://www.ncei.noaa.gov/data/oceans/ncei/ocads/metadata/0259391.html> (Jiang et al., 2022c), and global  
1241 maps of these indicators are available in JPEG at [https://www.ncei.noaa.gov/access/ocean-carbon-](https://www.ncei.noaa.gov/access/ocean-carbon-acidification-data-system/synthesis/surface-oa-indicators.html)  
1242 acidification-data-system/synthesis/surface-oa-indicators.html (Jiang et al., 2022c).

Deleted: ,

Deleted: OCADS:

Deleted: at:

1243 **64) Simulated and Constrained Global and Southern Ocean Carbon Sink:** These two datasets include  
1244 spatially-integrated and annually averaged values for the ocean carbon sink from 1850 to 2100 for different  
1245 scenarios over the 21st century for the global ocean (Terhaar et al., 2022a, 2022b) and the Southern Ocean  
1246 (Terhaar et al., 2021b, 2021c). All results are based on CMIP5 and CMIP6 models. For the global ocean  
1247 carbon sink, values are available for SSP1-2.6, SSP2-4.5, and SSP5-8.5. For the Southern Ocean, values are  
1248 also available for SSP1-2.6, SSP2-4.5, and SSP5-8.5 and additionally for RCP2.6, RCP4.5, and RCP8.5. In  
1249 addition, to the raw simulated values, constrained estimates of the annually averaged ocean carbon sink  
1250 estimates are available. These constrained estimates adjusted the simulated carbon sink estimates for biases  
1251 on the ocean's circulation and surface carbonate chemistry (see Terhaar et al., 2021b, 2022a for details). It  
1252 is recommended to use the constrained estimates. The datasets are available at  
1253 <https://doi.org/10.17882/103934> and <https://doi.org/10.17882/103938>.

Deleted: also

1254 **65) Composite model-based estimate of the ocean carbon sink from 1959 to 2022:** This data product,  
1255 developed by Terhaar (2025), presents an estimate of the global ocean carbon sink by combining forced  
1256 hindcast simulations and simulations made by coupled **ESMs**. Hindcast models manage to adequately  
1257 simulate the short-term variability of the ocean, but struggle to simulate the long-term climate change trend  
1258 (Huguenin et al., 2022; Takano et al., 2023; Hollitzer et al., 2024). **ESMs** cannot simulate the observed  
1259 short-term variability by definition, but accurately simulate long-term trends (Takano et al., 2023; Hollitzer  
1260 et al., 2024). The composite model-based estimate combines the simulated short-term variability from  
1261 hindcast simulations and the long-term trend from **ESMs**. The output is supplied with the associated study  
1262 (<https://bg.copernicus.org/articles/22/1631/2025/>) (Terhaar, 2025).

Deleted: earth system models

Deleted: Earth system models

Deleted: earth system models

1263 **66) pCIBR\_Clim and pCIBR\_Int:** A machine learning (ML) model is employed to correct biases in surface  
1264  $p\text{CO}_2$  simulations generated by the INCOIS-BIO-ROMS model ( $p\text{CO}_2$ model) over the period 1980–2019.  
1265 The ML model is trained using the differences between observed ( $p\text{CO}_2$ obs) and modeled  $p\text{CO}_2$  to estimate  
1266 the spatio-temporal deviations ( $p\text{CO}_2$ obs –  $p\text{CO}_2$ model). These interannually and climatologically varying  
1267 deviations are then added back to the original model output, resulting in two improved data products:  
1268 pCIBR\_Int and pCIBR\_Clim (Ghoshal et al., 2025a). Evaluation against independent datasets, including  
1269 moored observations (BOBOA), the gridded SOCAT product, and other ML-based  $p\text{CO}_2$  products (such as  
1270 CMEMS-LSCEv2 and OceanSODA), demonstrates a significant improvement of approximately  $40\% \pm$   
1271  $3.31\%$  in RMSE compared to the original model. This high-resolution ( $0.083^\circ \times 0.083^\circ$ ), long-term

1279 monthly  $p\text{CO}_2$  data product is available from the INCOIS Portal (<https://las.incois.gov.in>) and from  
 1280 OCADS: <https://www.ncei.noaa.gov/data/oceans/ncei/ocads/metadata/0307788.html> (Ghoshal et al.,  
 1281 2025b).

1282 **67) INCOIS-BIO-ROMS Simulated Surface  $p\text{CO}_2$  and pH for the Indian Ocean:** This data product  
 1283 presents a comprehensive assessment of OA trends across the Indian Ocean and its sub-regions from 1980  
 1284 to 2019, leveraging outputs from a regional, high-resolution coupled ocean-ecosystem model (INCOIS-  
 1285 BIO-ROMS), an offline biogeochemical (BGC) model, and two machine learning-based products  
 1286 (Chakraborty et al., 2024). INCOIS-BIO-ROMS, configured at  $1/12^\circ$  resolution for the Indian Ocean, was  
 1287 developed in accordance with the “RECCAP-2: Ocean Modeling Protocol” for regional oceans. The  
 1288 INCOIS-BIO-ROMS simulated surface  $p\text{CO}_2$  and pH data product is available from the INCOIS Portal  
 1289 (<https://las.incois.gov.in>) and from OCADS:  
 1290 <https://www.ncei.noaa.gov/data/oceans/ncei/ocads/metadata/0307663.html> (Chakraborty et al., 2025).

1291 **68) Ocean Circulation Inverse Model (OCIM):** DeVries (2022b) utilized a two-step procedure to estimate  
 1292 anthropogenic carbon in the ocean interior using an ocean inverse model. First, a steady-state ocean circula-  
 1293 tion inverse model (OCIM) was fit to observations of physical circulation tracers such as temperature, sa-  
 1294 linity, radiocarbon, and CFCs (Holzer et al., 2021). Then, the circulation model was coupled to an abiotic  
 1295 carbon cycle model, spun up to equilibrium in 1780 and then forced by observed atmospheric  $\text{CO}_2$  time  
 1296 history from 1781–2020. Simulations were run with and without historical changes in sea surface tempera-  
 1297 tures. The difference between preindustrial and transient simulations represents the anthropogenic carbon  
 1298 accumulation in the ocean. Results are provided on a regular grid with a nominal resolution of  $2^\circ$  in the hor-  
 1299 izontal with 48 depth levels. The output is available at <https://doi.org/10.6084/m9.figshare.19341974.v2>.

Deleted: Annual gridded anthropogenic carbon estimates from 1780-2020

Formatted: Subscript

Deleted: -

1300 **Table 6. Model based data synthesis products and analyses for ocean carbonate chemistry.**

No.	Name	Open ocean or Coastal ocean	Surface or Water column	Spatial resolution	Temporal resolution	Highlights	Reference
61	Decadal Trends in the Ocean Carbon Sink	Open ocean	Surface	Variable	Decadal	Climate variability drove weakened ocean $\text{CO}_2$ uptake in the 1990s, and strengthened $\text{CO}_2$ uptake in the 2000s	DeVries et al. (2019)
62	ECCO-Darwin	Open ocean + Coastal ocean	Water column	$1/3^\circ \times 1/3^\circ$	3-hourly, daily, and month fields available	Model-data synthesis product based on the Estimating the Circulation and Climate of the Ocean (ECCO) ocean state estimate. Fully-closed, physically-consistent 3-D biogeochemical budgets.	Carroll et al. (2020, 2022, 2024)

Deleted: c

Deleted: w

Deleted: Open + Coastal

Deleted: .

63(a)	Surface pH and Revelle Factor	Open ocean	Surface	1° × 1°	Decadal from 1770 to 2100	A model-observation fusion product for pH, acidity and Revelle Factor, leveraging GFDL-ESM2M and SOCATv6	Jiang et al. (2019a)
63(b)	Surface OA Indicators	Open ocean	Surface	1° × 1°	Decadal from 1750 to 2100	A model-observation fusion product for all major OA indicators, leveraging a consortium of 14 <del>ESMs</del> and 3 observational data products	Jiang et al. (2023)
64	Simulated and Constrained Global and Southern Ocean Carbon Sink	Open ocean	Surface	Spatially integrated	Annual from 1850 to 2100	A constrained estimate of the ocean carbon sink based on the simulated carbon sink from CMIP5 and CMIP6 models and constrained with observations of the ocean physics and carbonate chemistry	Terhaar et al. (2021b, 2022a)
65	Composite model-based estimate of the ocean carbon sink from 1959 to 2022	Open ocean	Surface	Spatially integrated	Annual from 1959 to 2022	A model-based estimate of the ocean carbon sink combining the respective strengths of hindcast simulations and simulations by coupled <del>ESMs</del>	Terhaar (2025)
66	pCIBR_Clim and pCIBR_Int	<del>Open ocean</del> <del>+ Coastal ocean</del>	Surface	0.083° × 0.083°	Monthly	This data product has been developed by employing an innovative hybrid approach, where a machine learning algorithm was used to correct high-resolution (1/12°) coupled ocean-ecosystem model outputs using observational data from SOCAT (1984–2019) and SAS (1991–2019) for the Indian Ocean	Ghoshal et al. (2025a)
67	INCOIS-BIO-ROMS Simulated Surface pCO <sub>2</sub> and pH for the Indian Ocean	<del>Open ocean</del> <del>+ Coastal ocean</del>	Surface	0.083° × 0.083°	Monthly from 1980 to 2019	INCOIS-BIO-ROMS was developed in accordance with the “RECCAP-2: Ocean Modeling Protocol” for regional oceans. By integrating model simulations with available field observations and reconstructed data products, this study advances the current understanding of OA in the Indian Ocean	Chakraborty et al. (2024)

**Deleted:** Earth System Models

**Deleted:** earth system models

**Deleted:** Open + Coastal

**Deleted:** -

**Deleted:** -

**Deleted:** Open + Coastal

68	Ocean Circulation Inverse Model (OCIM)	Open <u>ocean</u>	Surface and <u>Water</u> column	2° × 2° horizontal, 48 vertical layers	Annual from 1780 to 2020	Data-constrained estimate of anthropogenic CO <sub>2</sub> accumulation in the ocean from inverting physical ocean circulation tracers	DeVries (2022b)
----	--	-------------------	---------------------------------	--	--------------------------	--	-----------------

Deleted: w

### 1314 3.2 Overlaps and history

1315 Many of the data products described above exhibit significant overlap in various forms. In some cases, one or more  
 1316 products are used to generate new ones, while in others, the same collection-level cruise datasets underpin multiple  
 1317 products. There are a few foundational data products, such as GLODAPv2 and SOCAT, which are widely utilized to  
 1318 develop other data products, including their respective gridded products (e.g., Lauvset et al., 2016). For instance,  
 1319 SOCAT forms the backbone of nearly all derived products listed in Table 3, serving as a key resource for product  
 1320 development or validation. Some derived products, such as the JMA-MLR (No. 26) and OceanSODA-ETHZv1 (No.  
 1321 27a), incorporate both SOCAT and GLODAPv2 during development. Having overlaps in data and derived products  
 1322 has provided opportunities for data quality-control and intercomparison of different approaches to gap-filling that  
 1323 would not have been available otherwise. Additional overlaps between these data products are provided below:

#### 1324 3.2.1 SOCAT and LDEO:

1325 The quality-control and synthesis of global surface ocean CO<sub>2</sub> data began in 1997 with Dr. Taro Takahashi and his  
 1326 colleagues at LDEO in Palisades, New York. His pioneering work led to the creation of the LDEO Surface pCO<sub>2</sub>  
 1327 Database (No. 2), which focused on high-quality data collected by his team and from various U.S. and international  
 1328 expeditions. Over time, this data set expanded to include contributions from other laboratories, resulting in a highly  
 1329 influential collection of pCO<sub>2</sub> data and several seminal papers on global surface ocean CO<sub>2</sub> variations and air-sea  
 1330 CO<sub>2</sub> fluxes (Takahashi et al., 1997; 2002; 2009). The last update to the LDEO database was in 2019, following Dr.  
 1331 Takahashi's passing, and no further updates are anticipated (Takahashi et al., 2017).

1332 The SOCAT project was developed to address questions around the current and future drivers of CO<sub>2</sub> fluxes raised  
 1333 at the 2007 Surface Ocean CO<sub>2</sub> Variability and Vulnerability (SOCOVV) workshop in Paris, France (Metzl et al.,  
 1334 2007). SOCAT was developed to synthesize all of the publicly available, discoverable, and citable surface CO<sub>2</sub> data.  
 1335 Following the GLODAP model, there was a strong emphasis on an open and transparent secondary quality-control  
 1336 process to ensure the highest data quality. The first data release came in 2011 (Pfeil et al., 2013; Sabine et al., 2013)  
 1337 and included contributions from numerous laboratories, as well as the freely available CO<sub>2</sub> data from the LDEO  
 1338 database. As of 2024, SOCAT contains ~40 million data points, with new observations added annually. All data are  
 1339 rigorously standardized, and recalculated as fCO<sub>2</sub>. SOCAT represents an ongoing global community effort, with  
 1340 participants from all continents contributing data and participating in the quality-control process. Initially new  
 1341 versions were released every other year, however, automation allowed annual public releases since version 4.

Deleted: to

Deleted: but

1345 **3.2.2 GLODAPv2 and Quality Edited Hydrographic Data:**

1346 Starting in the late 1980s, the WOCE, Joint Global Ocean Flux Study (JGOFS), and the NOAA Ocean-Atmosphere  
1347 Exchange Study (OACES) collaborated in a multinational effort to conduct a decadal global hydrographic survey of  
1348 unparalleled quality and quantity. At the conclusion of the survey at the end of the 1990s, GLODAP combined and  
1349 publicly released all of the available hydrographic data with high-quality ocean carbonate system measurements as a  
1350 single database (Key et al., 2004; Sabine et al., 2005). The data were subjected to extensive secondary [quality-](#)  
1351 [control](#) checks where cruise tracks intersected one another, making it the most comprehensive and highest-quality  
1352 ocean inorganic carbon dataset ever generated. A gridded, full-depth global ocean carbon climatology was also  
1353 created and released as part of the project. These data and associated climatology have been extensively used to  
1354 evaluate carbon distributions as well as the accumulation of anthropogenic CO<sub>2</sub> in the ocean. Other regional  
1355 datasets, like the CARINA data synthesis project, an international collaborative effort of the European Union  
1356 CARBOOCEAN program (Key et al., 2010; Tanhua et al., 2010), and PACIFICA, an international synthesis of  
1357 Pacific Ocean data organized through the North Pacific Marine Science Organization (PICES) (Ishii et al., 2011b;  
1358 Suzuki et al., 2013), were combined with GLODAP after its initial release. The GLODAP database is continuing to  
1359 grow with new data collected as part of the Global Ocean Ship-Based Hydrographic Investigations Program (GO-  
1360 SHIP).

1361 For discrete bottle measurements spanning the entire oceanic water column, GLODAPv2 (No. 3) and the Quality  
1362 Edited Hydrographic Data (No. 4) are the primary data products. Most cruise datasets contributing to these two data  
1363 products overlap, but the key difference lies in their approach to data adjustment. The former applies crossover and  
1364 inversion analysis for bias correction, while the latter presents the data without such adjustments. GLODAPv2  
1365 achieves consistency by applying adjustments based on deep-ocean offsets, whereas Quality Edited Hydrographic  
1366 Data provides the data in its original form. While there is substantial overlap between the two, data from a specific  
1367 expedition might differ slightly due to GLODAPv2's secondary [quality-control](#) adjustments. Both GLODAPv2 and  
1368 Quality Edited Hydrographic Data offer global coverage, but several independent regional data products are also  
1369 available, such as SNAPO-CO<sub>2</sub> (No. 6), CODAP-NA (No. 7), AZMP Carbon (No. 8), MOCHA (No. 9), and ARIOS  
1370 (No. 10). Data from these regional products often partially or fully overlap with GLODAPv2 and Quality Edited  
1371 Hydrographic Data.

1372 **a) GLODAPv2 and CODAP-NA:**

1373 All cruise datasets contributing to CODAP-NA were forwarded to the GLODAPv2 [quality-control](#) team in 2022.  
1374 Data from select cruises with deep-water sampling (>1500 m), enabling crossover analysis, were subsequently  
1375 incorporated into the GLODAPv2.2022 data product update (Lauvset et al., 2022).

1376 **b) GLODAPv2 and SPOTS:**

1377 Some time-series data are included in both GLODAPv2 and the Synthesis Product for Ocean Time-Series (SPOTS).

Deleted: quality control

Deleted: quality control

1380 Usually, data present in both products ~~were not~~ measured on dedicated time-series cruises but rather ~~were~~ collected  
1381 as part of a larger cruise passing by a time-series location. As the ~~quality-control~~ of SPOTS is restricted to assigning  
1382 method flags, adjustments that are applied as a result of the QC of GLODAP are not present in SPOTS. Additional  
1383 crossover analyses between SPOTS and GLODAP have revealed ~~good consistency~~ (Lange et al., 2024a).

Deleted: have not been

Deleted: quality control

Deleted: a

### 1384 3.2.3 RECCAP2 and GCB:

1385 RECCAP2 and GCB are not data products themselves, but analyses and syntheses of data-based and model-based  
1386 products. Users should be aware that there is a large degree of overlap between the  $f\text{CO}_2$  products and GOBMs that  
1387 contributed to both RECCAP2 and GCB, and of the resulting datasets. However, the RECCAP2 and GCB analyses  
1388 serve different purposes. GCB is updated annually to the latest complete calendar year and its main purpose is to  
1389 present and estimate the magnitude (and uncertainty) of the ocean  $\text{CO}_2$  sink and the role of  $\text{CO}_2$  and climate drivers  
1390 since 1959 with a focus on the last year, while RECCAP2 presents a deeper analysis of the magnitude, trends, and  
1391 variability of the global and regional ocean  $\text{CO}_2$  sink over the period 1985–2018.

Deleted: -

### 1392 3.2.4 Jiang et al. (2019a) and Jiang et al. (2023):

1393 Both products contain the projection of surface ocean pH,  $[\text{H}^+]_{\text{total}}$ , and buffer capacity from 1750 to 2100. However,  
1394 the former is based on one GFDL model ESM2M, while the latter is based on a consortium of 14 ~~ESMs~~, and  
1395 additional observational data. The latter also contains the projection of seven other OA variables, including  
1396 carbonate ions,  $\Omega_{\text{arag}}$ ,  $\Omega_{\text{calc}}$ ,  $f\text{CO}_2$ , DIC, TA, and  $[\text{H}^+]_{\text{free}}$ .

Deleted: Earth system model

Deleted: and

## 1397 4 Data availability

1398 Access links for all data products mentioned in this paper are provided in their respective paragraphs. Additionally,  
1399 ~~access links~~ **for all products** are available in Table 7 below.

Deleted: their

1407 Table 7. Access links for the compiled ocean carbonate chemistry data products. N/A is short for not applicable.

No.	Name	Data access link	DOI	Reference
1	SOCAT	<a href="https://socat.info/">https://socat.info/</a>	<a href="https://doi.org/10.25921/648f-fv35">https://doi.org/10.25921/648f-fv35</a>	Bakker et al. (2016, 2025)
2	LDEO Surface pCO <sub>2</sub> Database	<a href="https://www.ncei.noaa.gov/data/oceans/ncei/ocads/metadata/0160492.html">https://www.ncei.noaa.gov/data/oceans/ncei/ocads/metadata/0160492.html</a>	<a href="https://doi.org/10.3334/cdiac/otg.ndp088(v2015)">https://doi.org/10.3334/cdiac/otg.ndp088(v2015)</a>	Takahashi et al. (2017)
3	GLODAPv2	<a href="https://glodap.info/">https://glodap.info/</a>	<a href="https://doi.org/10.25921/zyrq-h66">https://doi.org/10.25921/zyrq-h66</a>	Lauvset et al. (2023b, 2024)
4	Quality Edited Hydrographic Data	<a href="https://joa.ucsd.edu/">https://joa.ucsd.edu/</a>	N/A	Swift and Osborne (2022)
5	WOD	<a href="https://www.ncei.noaa.gov/products/world-ocean-database">https://www.ncei.noaa.gov/products/world-ocean-database</a>	<a href="https://doi.org/10.25923/z885-h264">https://doi.org/10.25923/z885-h264</a>	Mishonov et al. (2024)
6	SNAPO-CO <sub>2</sub>	<a href="https://www.ncei.noaa.gov/data/oceans/ncei/ocads/metadata/0285681.html">https://www.ncei.noaa.gov/data/oceans/ncei/ocads/metadata/0285681.html</a>	<a href="https://doi.org/10.17882/95414">https://doi.org/10.17882/95414</a>	Metzl et al. (2023, 2024)
7	CODAP-NA	<a href="https://www.ncei.noaa.gov/data/oceans/ncei/ocads/metadata/0219960.html">https://www.ncei.noaa.gov/data/oceans/ncei/ocads/metadata/0219960.html</a>	<a href="https://doi.org/10.25921/531n-c230">https://doi.org/10.25921/531n-c230</a>	Jiang et al. (2020, 2021)
8	AZMP Carbon	N/A	<a href="https://doi.org/10.20383/102.0673">https://doi.org/10.20383/102.0673</a>	Cyr et al. (2022)
9	MOCHA	<a href="https://www.ncei.noaa.gov/data/oceans/ncei/ocads/metadata/0277984.html">https://www.ncei.noaa.gov/data/oceans/ncei/ocads/metadata/0277984.html</a>	<a href="https://doi.org/10.25921/2vve-fh39">https://doi.org/10.25921/2vve-fh39</a>	Kennedy et al., (2024)
10	ARIOS	<a href="https://digital.csic.es/handle/10261/205135">https://digital.csic.es/handle/10261/205135</a>	<a href="https://doi.org/10.20350/digitalCSIC/12498">https://doi.org/10.20350/digitalCSIC/12498</a>	Pérez et al. (2020)
11	Marine Inorganic Carbonate Chemistry in the Northern Gulf of Alaska	<a href="https://www.ncei.noaa.gov/data/oceans/ncei/ocads/metadata/0277034.html">https://www.ncei.noaa.gov/data/oceans/ncei/ocads/metadata/0277034.html</a>	<a href="https://doi.org/10.25921/x9sg-9b08">https://doi.org/10.25921/x9sg-9b08</a>	Monacci et al. (2023, 2024)
12	Coral Reef Carbonate Chemistry Off the Florida Keys	<a href="https://www.ncei.noaa.gov/access/metadata/landing-page/bin/iso?id=gov.noaa.node:NCRMP-CO3-Atlantic">https://www.ncei.noaa.gov/access/metadata/landing-page/bin/iso?id=gov.noaa.node:NCRMP-CO3-Atlantic</a>	<a href="https://doi.org/10.25921/vfz0-dg77">https://doi.org/10.25921/vfz0-dg77</a>	Manzello et al. (2018)
13	Salish Cruise Data Package and Multi-stressor Data Product	<a href="https://www.ncei.noaa.gov/access/ocean-carbon-acidification-data-system/oceans/SalishCruise_DataPackage.html">https://www.ncei.noaa.gov/access/ocean-carbon-acidification-data-system/oceans/SalishCruise_DataPackage.html</a> , <a href="https://www.ncei.noaa.gov/access/ocean-carbon-acidification-data-system/oceans/SalishCruises_DataProduct.html">https://www.ncei.noaa.gov/access/ocean-carbon-acidification-data-system/oceans/SalishCruises_DataProduct.html</a>	<a href="https://doi.org/10.25921/jgrz-v584">https://doi.org/10.25921/jgrz-v584</a> , <a href="https://doi.org/10.25921/4y18-rw26">https://doi.org/10.25921/4y18-rw26</a>	Alin et al. (2024a, b, 2025a, b, c)
14	Line P Marine Carbonate Chemistry Compilation	<a href="https://www.ncei.noaa.gov/data/oceans/ncei/ocads/metadata/0234342.html">https://www.ncei.noaa.gov/data/oceans/ncei/ocads/metadata/0234342.html</a>	<a href="https://doi.org/10.25921/zrw8-kn24">https://doi.org/10.25921/zrw8-kn24</a>	Franco et al. (2021a, b)
15	Anthropogenic Carbon in the Arctic Ocean	<a href="https://www.seanoe.org/data/00927/103920/">https://www.seanoe.org/data/00927/103920/</a>	<a href="https://doi.org/10.17882/103920">https://doi.org/10.17882/103920</a>	Terhaar et al. (2024)

16	BATS	<a href="https://demo.bco-dmo.org/project/2124">https://demo.bco-dmo.org/project/2124</a>	<a href="https://doi.org/10.26008/1912/bco-dmo.894099.4">https://doi.org/10.26008/1912/bco-dmo.894099.4</a> , <a href="https://doi.org/10.26008/1912/bco-dmo.893182.4">https://doi.org/10.26008/1912/bco-dmo.893182.4</a> , <a href="https://doi.org/10.26008/1912/bco-dmo.926534.4">https://doi.org/10.26008/1912/bco-dmo.926534.4</a> , <a href="https://doi.org/10.26008/1912/bco-dmo.893521.6">https://doi.org/10.26008/1912/bco-dmo.893521.6</a> , <a href="https://doi.org/10.26008/1912/bco-dmo.917255.5">https://doi.org/10.26008/1912/bco-dmo.917255.5</a> , <a href="https://doi.org/10.26008/1912/bco-dmo.939210.7">https://doi.org/10.26008/1912/bco-dmo.939210.7</a> , <a href="https://doi.org/10.26008/1912/bco-dmo.3782.6">https://doi.org/10.26008/1912/bco-dmo.3782.6</a> , <a href="https://doi.org/10.26008/1912/bco-dmo.3918.8">https://doi.org/10.26008/1912/bco-dmo.3918.8</a> , <a href="https://doi.org/10.26008/1912/bco-dmo.881861.5">https://doi.org/10.26008/1912/bco-dmo.881861.5</a>	Bates et al. (2024a, b, c, d, e), Johnson et al. (2024a, b, c), Steinberg and Cope (2024)
17	HOT	<a href="https://www.bco-dmo.org/project/2101">https://www.bco-dmo.org/project/2101</a> , <a href="https://doi.org/10.5281/zenodo.15060930">https://doi.org/10.5281/zenodo.15060930</a>	<a href="https://doi.org/10.1575/1912/bco-dmo.3773.1">https://doi.org/10.1575/1912/bco-dmo.3773.1</a> , <a href="https://doi.org/10.5281/zenodo.15060931">https://doi.org/10.5281/zenodo.15060931</a>	Winn et al. (1994, 1998), Dore et al. (2003, 2009, 2014, 2025), Knor et al. (2023, 2025)
18	ESTOC	N/A	<a href="https://doi.org/10.1594/PANGAEA.959856">https://doi.org/10.1594/PANGAEA.959856</a> , <a href="https://doi.pangaea.de/10.1594/PANGAEA.856590">https://doi.pangaea.de/10.1594/PANGAEA.856590</a> , <a href="https://doi.pangaea.de/10.1594/PANGAEA.856615">https://doi.pangaea.de/10.1594/PANGAEA.856615</a> , <a href="https://doi.pangaea.de/10.1594/PANGAEA.856608">https://doi.pangaea.de/10.1594/PANGAEA.856608</a> , <a href="https://doi.pangaea.de/10.1594/PANGAEA.856616">https://doi.pangaea.de/10.1594/PANGAEA.856616</a> , <a href="https://doi.pangaea.de/10.1594/PANGAEA.856593">https://doi.pangaea.de/10.1594/PANGAEA.856593</a> , <a href="https://doi.pangaea.de/10.1594/PANGAEA.856612">https://doi.pangaea.de/10.1594/PANGAEA.856612</a> , <a href="https://doi.pangaea.de/10.1594/PANGAEA.856614">https://doi.pangaea.de/10.1594/PANGAEA.856614</a> , <a href="https://doi.pangaea.de/10.1594/PANGAEA.856607">https://doi.pangaea.de/10.1594/PANGAEA.856607</a> , <a href="https://doi.pangaea.de/10.1594/PANGAEA.956272">https://doi.pangaea.de/10.1594/PANGAEA.956272</a>	González-Dávila and Santana-Casiano (2023)
19	Point B Time-series	N/A	<a href="https://doi.org/10.1594/PANGAEA.727120">https://doi.org/10.1594/PANGAEA.727120</a>	Gattuso et al. (2021b)
20	Ny-Ålesund Time-series	N/A	<a href="https://doi.org/10.1594/PANGAEA.957028">https://doi.org/10.1594/PANGAEA.957028</a>	Gattuso et al. (2023)
21	SPOTS	<a href="https://www.bco-dmo.org/dataset/896862">https://www.bco-dmo.org/dataset/896862</a>	<a href="https://doi.org/10.26008/1912/bco-dmo.896862.2">https://doi.org/10.26008/1912/bco-dmo.896862.2</a>	Lange et al. (2024a, b)

Deleted: h

Deleted: /

22	$p\text{CO}_2$ and pH Time-series from 40 Surface Buoys	<a href="https://www.ncei.noaa.gov/data/oceans/ncei/ocads/metadata/0173932.html">https://www.ncei.noaa.gov/data/oceans/ncei/ocads/metadata/0173932.html</a>	<a href="https://doi.org/10.7289/v5db8043">https://doi.org/10.7289/v5db8043</a>	Sutton et al. (2018)
23	Takahashi delta $f\text{CO}_2$ and flux climatology	<a href="https://www.ncei.noaa.gov/data/oceans/ncei/ocads/metadata/0282251.html">https://www.ncei.noaa.gov/data/oceans/ncei/ocads/metadata/0282251.html</a>	<a href="https://doi.org/10.25921/295g-sn13">https://doi.org/10.25921/295g-sn13</a>	Fay et al. (2023)
24	MPI-ULB-SOM-FFN	<a href="https://www.ncei.noaa.gov/data/oceans/ncei/ocads/metadata/0209633.html">https://www.ncei.noaa.gov/data/oceans/ncei/ocads/metadata/0209633.html</a>	<a href="https://doi.org/10.25921/qb25-f418">https://doi.org/10.25921/qb25-f418</a>	Landschützer et al. (2020a, b)
25	VLIZ SOM-FFN	<a href="https://www.ncei.noaa.gov/data/oceans/ncei/ocads/metadata/0160558.html">https://www.ncei.noaa.gov/data/oceans/ncei/ocads/metadata/0160558.html</a>	<a href="https://doi.org/10.7289/V5Z899N6">https://doi.org/10.7289/V5Z899N6</a>	Landschützer et al. (2016), Jersild et al. (2017)
26	JMA-MLR	<a href="https://www.data.jma.go.jp/kaiyou/english/co2_flux/co2_flux_data_en.html">https://www.data.jma.go.jp/kaiyou/english/co2_flux/co2_flux_data_en.html</a>	N/A	Iida et al. (2021)
27(a)	OceanSODA-ETHZv1	<a href="https://www.ncei.noaa.gov/data/oceans/ncei/ocads/metadata/0220059.html">https://www.ncei.noaa.gov/data/oceans/ncei/ocads/metadata/0220059.html</a>	<a href="https://doi.org/10.25921/m5wx-ja34">https://doi.org/10.25921/m5wx-ja34</a>	Gregor et al. (2020)
27(b)	OceanSODA-ETHZv2	<a href="https://zenodo.org/records/11206366">https://zenodo.org/records/11206366</a>	<a href="https://doi.org/10.5281/zenodo.11206365">https://doi.org/10.5281/zenodo.11206365</a>	Gregor et al. (2024b)
28	LDEO-HPD $f\text{CO}_2$	<a href="https://zenodo.org/records/4760205">https://zenodo.org/records/4760205</a>	<a href="https://doi.org/10.5281/zenodo.4760205">https://doi.org/10.5281/zenodo.4760205</a>	Gloege et al. (2022)
29	LDEO-HPD with Extended Temporal Coverage	<a href="https://zenodo.org/records/13891722">https://zenodo.org/records/13891722</a>	<a href="https://doi.org/10.5281/zenodo.13891722">https://doi.org/10.5281/zenodo.13891722</a>	Bennington et al. (2022a)
30	LDEO $f\text{CO}_2$ - Residual Method	<a href="https://zenodo.org/records/13941548">https://zenodo.org/records/13941548</a>	<a href="https://doi.org/10.5281/zenodo.13941548">https://doi.org/10.5281/zenodo.13941548</a>	Bennington et al. (2022b)
31(a)	CMEMS-LSCEv1	<a href="https://data.ipsl.fr/catalog/srv/eng/catalog.search#/metadata/a2f0891b-763a-49e9-af1b-78ed78b16982">https://data.ipsl.fr/catalog/srv/eng/catalog.search#/metadata/a2f0891b-763a-49e9-af1b-78ed78b16982</a>	<a href="https://doi.org/10.14768/a2f0891b-763a-49e9-af1b-78ed78b16982">https://doi.org/10.14768/a2f0891b-763a-49e9-af1b-78ed78b16982</a>	Chau et al. (2022)
30(b)	CMEMS-LSCEv2	<a href="https://data.marine.copernicus.eu/product/MULTIOBS_GLO_BIO_CARBON_SURFACE_MYNRT_015_008/services">https://data.marine.copernicus.eu/product/MULTIOBS_GLO_BIO_CARBON_SURFACE_MYNRT_015_008/services</a>	<a href="https://doi.org/10.48670/moi-00047">https://doi.org/10.48670/moi-00047</a>	Chau et al. (2024a, b)
32	CarboScope (Jena-MLS)	<a href="https://www.bgc-jena.mpg.de/CarboScope/?ID=oc">https://www.bgc-jena.mpg.de/CarboScope/?ID=oc</a>	10.17871/CarboScope-oc_v2024E (or analogously for previous and upcoming releases)	Rödenbeck et al. (2022)
33	UOEx-Watson	<a href="https://www.ncei.noaa.gov/data/oceans/ncei/ocads/metadata/0301544.html">https://www.ncei.noaa.gov/data/oceans/ncei/ocads/metadata/0301544.html</a>	<a href="https://doi.org/10.25921/2dp5-xm29">https://doi.org/10.25921/2dp5-xm29</a>	Watson et al. (2025)
34	NIES-ML3	<a href="https://db.eger.nies.go.jp/DL/10.17595/20220311.001.html.en">https://db.eger.nies.go.jp/DL/10.17595/20220311.001.html.en</a>	<a href="https://doi.org/10.17595/202311.001">https://doi.org/10.17595/202311.001</a>	Zeng (2022), Zeng et al. (2022)
35	CSIR-ML6	<a href="https://www.ncei.noaa.gov/data/oceans/ncei/ocads/metadata/0206205.html">https://www.ncei.noaa.gov/data/oceans/ncei/ocads/metadata/0206205.html</a>	<a href="https://doi.org/10.25921/z682-mn47">https://doi.org/10.25921/z682-mn47</a>	Gregor et al. (2019b)

Deleted:

36	Stepwise-FFNN	<a href="https://msdc.qdio.ac.cn/data/metadata-special-detail?id=1955061943609876482">https://msdc.qdio.ac.cn/data/metadata-special-detail?id=1955061943609876482</a>	<a href="http://dx.doi.org/10.12157/IO-CAS.20250814.001">http://dx.doi.org/10.12157/IO-CAS.20250814.001</a>	Zhong et al. (2022)
37	AOML-ET	<a href="https://www.ncei.noaa.gov/data/oceans/ncei/ocads/metadata/0298989.html">https://www.ncei.noaa.gov/data/oceans/ncei/ocads/metadata/0298989.html</a>	<a href="https://doi.org/10.25921/0s8y-q287">https://doi.org/10.25921/0s8y-q287</a>	Wanninkhof et al. (2024, 2025)
38	ULB-SOM-FFN-coastalv2.1	<a href="https://www.ncei.noaa.gov/data/oceans/ncei/ocads/metadata/0279118.html">https://www.ncei.noaa.gov/data/oceans/ncei/ocads/metadata/0279118.html</a>	<a href="https://doi.org/10.25921/4sdep068">https://doi.org/10.25921/4sdep068</a>	Roobaert et al. (2023, 2024)
39	RFR-LME	<a href="https://www.ncei.noaa.gov/data/oceans/ncei/ocads/metadata/0287551.html">https://www.ncei.noaa.gov/data/oceans/ncei/ocads/metadata/0287551.html</a>	<a href="https://doi.org/10.25921/h8vw-e872">https://doi.org/10.25921/h8vw-e872</a>	Sharp et al. (2024a, b)
40	ReCAD-NAACOM-pCO <sub>2</sub>	<a href="https://zenodo.org/records/14038561">https://zenodo.org/records/14038561</a>	<a href="https://doi.org/10.5281/zenodo.1150097">https://doi.org/10.5281/zenodo.1150097</a>	Wu et al. (2025)
41	Gridded Surface OA Indicators and Air-sea CO <sub>2</sub> Fluxes in the Northern Caribbean Sea	<a href="https://www.ncei.noaa.gov/data/oceans/ncei/ocads/metadata/0207749.html">https://www.ncei.noaa.gov/data/oceans/ncei/ocads/metadata/0207749.html</a>	<a href="https://doi.org/10.25921/2swk-9w56">https://doi.org/10.25921/2swk-9w56</a>	Wanninkhof et al. (2019)
42	OA data in the Gulf of Mexico/Gulf of America and Wider Caribbean	<a href="https://www.ncei.noaa.gov/data/oceans/ncei/ocads/metadata/0245950.html">https://www.ncei.noaa.gov/data/oceans/ncei/ocads/metadata/0245950.html</a>	<a href="https://doi.org/10.25921/tt1c-dx53">https://doi.org/10.25921/tt1c-dx53</a>	van Hooidonk (2022)
43	pCO <sub>2</sub> Climatology of the Baltic Sea	N/A	<a href="https://doi.org/10.1594/PAN-GAEA.961119">https://doi.org/10.1594/PAN-GAEA.961119</a>	Bittig et al. (2023)
44	INCOIS-ReML	<a href="https://www.ncei.noaa.gov/data/oceans/ncei/ocads/metadata/0307627.html">https://www.ncei.noaa.gov/data/oceans/ncei/ocads/metadata/0307627.html</a>	<a href="https://doi.org/10.25921/2sjr-pg16">https://doi.org/10.25921/2sjr-pg16</a>	Joshi et al. (2024, 2025a)
45	INCOIS_TA	<a href="https://www.ncei.noaa.gov/data/oceans/ncei/ocads/metadata/0307789.html">https://www.ncei.noaa.gov/data/oceans/ncei/ocads/metadata/0307789.html</a>	<a href="https://doi.org/10.25921/7as7-et15">https://doi.org/10.25921/7as7-et15</a>	Joshi et al. (2025b, c)
46	GLODAPv2 Climatology	<a href="https://www.ncei.noaa.gov/data/oceans/ncei/ocads/metadata/0286118.html">https://www.ncei.noaa.gov/data/oceans/ncei/ocads/metadata/0286118.html</a>	<a href="https://doi.org/10.3334/cdiac/otg.ndp093_glodapv2">https://doi.org/10.3334/cdiac/otg.ndp093_glodapv2</a>	Lauvset et al. (2016, 2023a)
47	Aragonite Saturation State Climatology	<a href="https://www.ncei.noaa.gov/data/oceans/ncei/ocads/metadata/0139360.html">https://www.ncei.noaa.gov/data/oceans/ncei/ocads/metadata/0139360.html</a>	<a href="https://doi.org/10.7289/v5q81b4p">https://doi.org/10.7289/v5q81b4p</a>	Jiang et al. (2015a, b)
48(a)	MOBO-DIC (Version 2020)	<a href="https://www.ncei.noaa.gov/access/ocean-carbon-acidification-data-system/oceans/ndp_104/ndp104.html">https://www.ncei.noaa.gov/access/ocean-carbon-acidification-data-system/oceans/ndp_104/ndp104.html</a>	<a href="https://doi.org/10.25921/yvzj-zx46">https://doi.org/10.25921/yvzj-zx46</a>	Keppler et al. (2020)
48(b)	MOBO-DIC (Version 2023)	<a href="https://www.ncei.noaa.gov/data/oceans/ncei/ocads/metadata/0277099.html">https://www.ncei.noaa.gov/data/oceans/ncei/ocads/metadata/0277099.html</a>	<a href="https://doi.org/10.25921/z31n-3m26">https://doi.org/10.25921/z31n-3m26</a>	Keppler et al. (2023a, b)
49	Monthly Interior Ocean TA Climatology	<a href="https://www.ncei.noaa.gov/data/oceans/ncei/ocads/metadata/0222470.html">https://www.ncei.noaa.gov/data/oceans/ncei/ocads/metadata/0222470.html</a>	<a href="http://doi.org/10.20350/DIGITALCSIC/8564">http://doi.org/10.20350/DIGITALCSIC/8564</a>	Brouillon et al., (2019, 2020b)
50	Monthly Interior Ocean DIC Climatology	<a href="https://www.ncei.noaa.gov/data/oceans/ncei/ocads/metadata/0222469.html">https://www.ncei.noaa.gov/data/oceans/ncei/ocads/metadata/0222469.html</a>	<a href="http://doi.org/10.20350/digitalCSIC/10551">http://doi.org/10.20350/digitalCSIC/10551</a>	Brouillon et al., (2020a, c)

51	Acidification Metrics in the Ocean Interior	<a href="https://www.ncei.noaa.gov/data/oceans/ncei/ocads/metadata/0290073.html">https://www.ncei.noaa.gov/data/oceans/ncei/ocads/metadata/0290073.html</a>	<a href="https://doi.org/10.25921/rdtr-9t74">https://doi.org/10.25921/rdtr-9t74</a>	Fassbender et al. (2023), Fassbender (2024)
52	Ocean Interior Acidification over the Industrial Era	<a href="https://www.ncei.noaa.gov/data/oceans/ncei/ocads/metadata/0298993.html">https://www.ncei.noaa.gov/data/oceans/ncei/ocads/metadata/0298993.html</a>	<a href="https://doi.org/10.25921/tefm-x802">https://doi.org/10.25921/tefm-x802</a>	Müller and Gruber (2024a, b)
53(a)	Anthropogenic CO <sub>2</sub> from 1994 to 2007	<a href="https://www.ncei.noaa.gov/data/oceans/ncei/ocads/metadata/0186034.html">https://www.ncei.noaa.gov/data/oceans/ncei/ocads/metadata/0186034.html</a>	<a href="https://doi.org/10.25921/wdn2-pt10">https://doi.org/10.25921/wdn2-pt10</a>	Gruber et al. (2019a, b)
53(b)	Decadal Trends in Anthropogenic CO <sub>2</sub> From 1994 to 2014	<a href="https://www.ncei.noaa.gov/data/oceans/ncei/ocads/metadata/0279447.html">https://www.ncei.noaa.gov/data/oceans/ncei/ocads/metadata/0279447.html</a>	<a href="https://doi.org/10.25921/ppcf-w020">https://doi.org/10.25921/ppcf-w020</a>	Müller et al. (2023a, b)
54	Anthropogenic carbon from 1750 to 2500 (TRACE)	<a href="https://github.com/BRCScienceProducts/TRACEv1">https://github.com/BRCScienceProducts/TRACEv1</a>	<a href="https://doi.org/10.5281/zenodo.15692788">https://doi.org/10.5281/zenodo.15692788</a>	Carter et al. (2025)
55	Preformed TA and other biogeochemical properties	<a href="https://github.com/BRCScienceProducts/PreformedPropertyEstimates">https://github.com/BRCScienceProducts/PreformedPropertyEstimates</a>	<a href="https://doi.org/10.5281/zenodo.3745002">https://doi.org/10.5281/zenodo.3745002</a>	Carter et al. (2020)
56	Monthly Interior Ocean pH Climatology	<a href="https://doi.org/10.12157/IOCAS.20230720.001">https://doi.org/10.12157/IOCAS.20230720.001</a>	<a href="https://doi.org/10.12157/IOCAS.20230720.001">https://doi.org/10.12157/IOCAS.20230720.001</a>	Zhong et al. (2025)
57	CODAP-NA Climatology	<a href="https://www.ncei.noaa.gov/data/oceans/ncei/ocads/metadata/0270962.html">https://www.ncei.noaa.gov/data/oceans/ncei/ocads/metadata/0270962.html</a>	<a href="https://doi.org/10.25921/g8pb-zy76">https://doi.org/10.25921/g8pb-zy76</a>	Jiang et al. (2022b), Jiang et al. (2024)
58	SeaFlux	<a href="https://zenodo.org/records/8280457">https://zenodo.org/records/8280457</a>	<a href="https://doi.org/10.5281/zenodo.5482547">https://doi.org/10.5281/zenodo.5482547</a>	Gregor & Fay. (2021)
59	RECCAP2	<a href="https://zenodo.org/records/7990823">https://zenodo.org/records/7990823</a>	<a href="https://doi.org/10.5281/zenodo.7990823">https://doi.org/10.5281/zenodo.7990823</a>	Müller (2023)
60	Global Carbon Budget	<a href="https://zenodo.org/records/14639761">https://zenodo.org/records/14639761</a> , <a href="https://globalcarbonbudget.org/download/1442/?tmstv=1731323337">https://globalcarbonbudget.org/download/1442/?tmstv=1731323337</a> , <a href="https://globalcarbonbudgetdata.org/closed-access-requests.html">https://globalcarbonbudgetdata.org/closed-access-requests.html</a>	<a href="https://doi.org/10.5281/zenodo.14639761">https://doi.org/10.5281/zenodo.14639761</a>	Hauck et al. (2025)
61	Decadal Trends in the Ocean Carbon Sink	N/A	<a href="https://doi.org/10.6084/m9.figshare.8091161.v1">https://doi.org/10.6084/m9.figshare.8091161.v1</a>	DeVries et al. (2019)
62	ECCO-Darwin	<a href="https://data.nas.nasa.gov/ecco/">https://data.nas.nasa.gov/ecco/</a>	N/A	Carroll et al. (2020)
63(a)	Surface pH and Revelle Factor	<a href="https://www.ncei.noaa.gov/data/oceans/ncei/ocads/metadata/0206289.html">https://www.ncei.noaa.gov/data/oceans/ncei/ocads/metadata/0206289.html</a>	<a href="https://doi.org/10.25921/kgqr-9h49">https://doi.org/10.25921/kgqr-9h49</a>	Jiang et al. (2019a, b)

63(b)	Surface OA Indicators	<a href="https://www.ncei.noaa.gov/data/oceans/ncei/ocads/metadata/0259391.html">https://www.ncei.noaa.gov/data/oceans/ncei/ocads/metadata/0259391.html</a>	<a href="https://doi.org/10.25921/9ker-bc48">https://doi.org/10.25921/9ker-bc48</a>	Jiang et al. (2022c), Jiang et al. (2023)
64	Simulated and Constrained Global and Southern Ocean Carbon Sink	<a href="https://www.seanoe.org/data/00927/103934/">https://www.seanoe.org/data/00927/103934/</a> , <a href="https://www.seanoe.org/data/00927/103938/">https://www.seanoe.org/data/00927/103938/</a>	<a href="https://doi.org/10.17882/103934">https://doi.org/10.17882/103934</a> , <a href="https://doi.org/10.17882/103938">https://doi.org/10.17882/103938</a>	Terhaar et al. (2021c), Terhaar et al. (2022b)
65	Composite model-based estimate of the ocean carbon sink from 1959 to 2022	<a href="https://bg.copernicus.org/articles/22/1631/2025/">https://bg.copernicus.org/articles/22/1631/2025/</a> (the data is in the annex)	<a href="https://doi.org/10.5194/bg-22-1631-2025">https://doi.org/10.5194/bg-22-1631-2025</a>	Terhaar (2025)
66	pCIBR_Clim and pCIBR_Int	<a href="https://www.ncei.noaa.gov/data/oceans/ncei/ocads/metadata/0307788.html">https://www.ncei.noaa.gov/data/oceans/ncei/ocads/metadata/0307788.html</a>	<a href="https://doi.org/10.25921/r2q9-d197">https://doi.org/10.25921/r2q9-d197</a>	Ghoshal et al. (2025a, b)
67	INCOIS-BIO-ROMS Simulated Surface pCO <sub>2</sub> and pH for the Indian Ocean	<a href="https://www.ncei.noaa.gov/data/oceans/ncei/ocads/metadata/0307663.html">https://www.ncei.noaa.gov/data/oceans/ncei/ocads/metadata/0307663.html</a>	<a href="https://doi.org/10.25921/z2x4-vt48">https://doi.org/10.25921/z2x4-vt48</a>	Chakraborty et al. (2024, 2025)
68	Ocean Circulation Inverse Model (OCIM)	<a href="https://figshare.com/articles/dataset/OCIM2-48L_abiotic_ocean_carbon_cycle_model_output/19341974">https://figshare.com/articles/dataset/OCIM2-48L_abiotic_ocean_carbon_cycle_model_output/19341974</a>	<a href="https://doi.org/10.6084/m9.figshare.19341974.v2">https://doi.org/10.6084/m9.figshare.19341974.v2</a>	DeVries (2022b)

## 1411 5 Summary

1412 The synthesis and gridded data products presented here reflect significant community-based efforts that have  
1413 been made to advance understanding of the ocean's role in global carbon cycling. This synthesis provides an  
1414 overview of key data compilations and gridded data products essential for coastal and global ocean carbonate  
1415 chemistry research. It highlights the key features of each product, serving as a resource for researchers seeking the  
1416 necessary data for their work. The list will be updated periodically to incorporate new data products. The most up-  
1417 to-date list is available at <https://oceanco2.github.io/co2-products/>. New data products ~~can~~ be submitted ~~via~~  
1418 <https://forms.gle/g8hYm37Wg1Uifg8E8>. ~~After submitting a new data product, please send a notification to~~  
1419 ~~[noaa.ocads@noaa.gov](mailto:noaa.ocads@noaa.gov) to ensure the submission is reviewed and added to the webpage.~~

## 1420 Author contributions

1421 L-QJ prepared the initial draft. LG designed and implemented the GitHub webpage and supporting scripts to  
1422 present the most current list of products. AR prepared Figure 1. All authors contributed to the writing of the

Deleted: should

Deleted: through

1425 manuscript. The first 23 authors are listed based on their contributions, while the remaining authors are listed  
1426 alphabetically by their last names.

### 1427 **Competing interests**

1428 One of the (co-)authors, Anton Velo (Instituto de Investigaciones Mariñas, IIM - CSIC, Vigo, Spain), is a  
1429 member of the editorial board of the Earth System Science Data.

Deleted: o

### 1430 **Acknowledgements**

1431 We extend our gratitude to all scientists who collected and measured the original data and those who compiled  
1432 and quality-controlled these data products. We thank Pierre Friedlingstein (University of Exeter, Exeter, UK),  
1433 Bronte Tilbrook (CSIRO Oceans and Atmosphere and Australian Antarctic Program Partnership, University of  
1434 Tasmania, Australia), and Dwight Gledhill (NOAA/OAR Ocean Acidification Program, United States) for their  
1435 valuable insights and discussions, which helped shape the vision of this paper. Additionally, we thank Xiping Hu  
1436 (University of Texas at Austin, United States), Tessa Hill (University of California, Davis, United States), and  
1437 Patrick Duke (University of Victoria, Canada) for recommending numerous data products incorporated into this  
1438 compilation. This is PMEL contribution 5728. This is INCOIS contribution no. 596.

Deleted: quality control

Deleted: \*\*\* (to be added after the paper is accepted)

### 1439 **Financial support**

1440 Funding for L-QJ was from NOAA Ocean Acidification Program (<https://ror.org/02bfn4816>) and NOAA grant  
1441 NA24NESX432C0001 (Cooperative Institute for Satellite Earth System Studies - CISESS) at the Earth System  
1442 Science Interdisciplinary Center, University of Maryland. JDM acknowledges funding by Carbon to Sea through the  
1443 Windward Fund and support from Google for OAEMIP. MT acknowledge funding from the United States National  
1444 Science Foundation (grant no. OCE-2513154) to the Scientific Committee on Oceanic Research (SCOR, United  
1445 States) for the International Ocean Carbon Coordination Project (IOCCP) and from the United Nations Educational,  
1446 Scientific and Cultural Organization (UNESCO) to the Institute of Oceanology of Polish Academy of Sciences for  
1447 the GOOS Biogeochemistry Panel (4500540682). SKL and NL acknowledge funding from OceanICU. OceanICU  
1448 was funded by the European Union under grant agreement no. 101083922. Views and opinions expressed are  
1449 however those of the author(s) only and do not necessarily reflect those of the European Union or European  
1450 Research Executive Agency. Neither the European Union nor the granting authority can be held responsible for  
1451 them. Funding for GLODAPv2 was provided by the EU FP7 project CarboChange (grant agreement 264879) and  
1452 the Research Council of Norway project DECApH (grant agreement 214513), and the 2019-~~2~~2023 updates were  
1453 funded by the EU Horizon 2020 innovation action EuroSea (grant agreement 862626). AJF, SRA, and RAF were  
1454 supported by the NOAA Pacific Marine Environmental Laboratory. GAM was funded by NOAA  
1455 NA24OARX431G0151-T1-01. JPG was supported by the Service d'Observation Rade de Villefranche (SO-Rade),  
1456 the Service d'Observation en Milieu Littoral (SOMLIT/CNRS- INSU), the Coastal Observing System for Northern  
1457 and Arctic Seas (COSYNA), the two Helmholtz large-scale infrastructure projects: ACROSS and MOSES, the

Formatted: Space After: 6 pt, Line spacing: 1.5 lines, No widow/orphan control

Deleted: The authors

Deleted: 2140395

Deleted: -

1464 French Polar Institute (IPEV), and the European Commission, Horizon 2020 Framework Programme (grant nos.  
1465 871153, 951799, 727890 and 869154). Discrete samples reported by JPG were analyzed for CT and AT by the  
1466 Service National d'Analyse des Paramètres Océaniques du CO<sub>2</sub>. AV and FFP were supported by BOCATS2  
1467 (PID2019-104279GB-C21) project funded by MICIU/AEI/10.13039/501100011033, by FICARAM+ (PID2023-  
1468 1489240B-100) and by EuroGO-SHIP project (Horizon Europe #101094690). NM and CLM acknowledge Institut  
1469 National des Sciences de l'Univers du Centre National de la Recherche Scientifique (INSU/CNRS) and  
1470 Observatoire des Science de l'Univers (OSU ECCE-Terra) for supporting the SNAPO-CO<sub>2</sub> facility housed by the  
1471 LOCEAN laboratory in Paris/France. The AZMP Carbon dataset is a contribution to Fisheries and Oceans Canada  
1472 Atlantic Zone Monitoring Program. Funding for the HOT program and WHOTS mooring maintenance were  
1473 provided by the National Science Foundation (grant no. OCE-9617409). CMEMS-LSCE is supported by the  
1474 European Copernicus Marine Environment Monitoring Service (CMEMS, grant no. 83-CMEMSTAC-MOB). The  
1475 work of LGr was supported by the ESA OceanHealth-OA project (contract number 4000137603/22/I-DT), the  
1476 European Space Agency (OceanSODA project, grant no. 4000112091/14/I-LG), the European Commission  
1477 (COMFORT project, grant no. 820989), and the Horizon 2020 (4C project, grant no. 821003). PL received funding  
1478 through the Horizon Europe research and innovation program under grant agreement No. 101137682 (AI4PEX), the  
1479 Horizon2020 program (4C project, grant no. 821003) and through Schmidt Sciences (OBVI InMOS). JH received  
1480 funding from the Initiative and Networking Fund of the Helmholtz Association (Helmholtz Young Investigator  
1481 Group Marine Carbon and Ecosystem Feedbacks in the Earth System [MarESys], Grant VH-NG-1301), and from  
1482 the ERC-2022-STG OceanPeak (Grant 101077209). AK was funded by the NOAA Global Ocean Monitoring and  
1483 Observing program (<https://ror.org/037bamf06>). J.T. was funded by the Swiss National Science Foundation under  
1484 grant # PZ00P2\_209044 (ArcticECO). HCB acknowledges funding by the German Federal Ministry of Education  
1485 and Research under grants no. 03F0877D (C-SCOPE project) and 03F0773A (BONUS INTEGRAL project). TD  
1486 acknowledges support from the US National Science Foundation through Grant # 1948955. RW, LB, AJS, SRA, and  
1487 RAF acknowledge support from the Office of Oceanic and Atmospheric Research of NOAA, U.S. Department of  
1488 Commerce, including resources from the Global Ocean Monitoring and Observing Program and the Ocean  
1489 Acidification Program (Open Funder Registry numbers 100018302 and 100018228, respectively). SRA and RAF  
1490 acknowledge support from the Washington Ocean Acidification Center. [NMM acknowledges support from the](#)  
1491 [Alaska Ocean Observing System \(AOOS\), the Exxon Valdez Oil Spill Trustee Council \(EVOS\), Gulf Watch](#)  
1492 [Alaska, and the North Pacific Research Board \(NPRB\)](#). KC acknowledges the support of the Development of  
1493 Climate Change Advisory Services project, undertaken by the Indian National Centre for Ocean Information  
1494 Services (INCOIS) under the Deep Ocean Mission programme of the Ministry of Earth Sciences (MoES),  
1495 Government of India. LX was supported by the National Key R&D Program of China (2023YFE0113101 and  
1496 2023YFC3108102), the National Natural Science Foundation of China (42176051 and 42376048), and the Taishan  
1497 Scholar Project of Shandong Province (tsqn202306294). [KA-S and DI acknowledge funding from Fisheries and](#)  
1498 [Oceans Canada, including, but not limited to, Aquatic Climate Change Adaptation Service Program. DI and AF](#)  
1499 [acknowledge funding from Canada's Marine Environmental Observation Prediction and Response Network-](#)

Deleted: as

1501 [OxyNet](#).

1502 **References**

1503 Alin, S. R., Newton, J. A., Feely, R. A., Greeley, D., Curry, B., Herndon, J., and Warner, M.: A decade-long cruise  
1504 time series (2008–2018) of physical and biogeochemical conditions in the southern Salish Sea, North America,  
1505 *Earth Syst. Sci. Data*, 16, 837–865, <https://doi.org/10.5194/essd-16-837-2024>, 2024a.

1506 Alin, S. R., Newton, J. A., Feely, R. A., Siedlecki, S., and Greeley, D.: Seasonality and response of ocean  
1507 acidification and hypoxia to major environmental anomalies in the southern Salish Sea, North America (2014–  
1508 2018), *Biogeosciences*, 21, 1639–1673, <https://doi.org/10.5194/bg-21-1639-2024>, 2024b.

1509 Alin, S. R.; Newton, J.; Ikeda, C.; Boyar, A.; Greeley, D.; Herndon, J.; Curry, B.; Kozyr, A.; Feely, R.A.:  
1510 *SalishCruiseDataPackage\_v2025*: An updated compiled data package of sensor profile and discrete physical and  
1511 biogeochemical measurements from 61 individual cruise data sets collected from a variety of ships in the southern  
1512 Salish Sea and northern California Current System (Washington state marine waters) from 2008-02-04 to 2024-10-  
1513 22 (NCEI Accession 0307188). NOAA National Centers for Environmental Information. Dataset.  
1514 <https://doi.org/10.25921/jgrz-v584>, 2025a.

1515 Alin, S.R.; Newton, J.; Feely, R.A.; Ikeda, C.; Boyar, A.; Greeley, D.; Herndon, J.; Kozyr, A.:  
1516 *SalishCruiseMultistressor\_v2025*: An updated multi-stressor data product for marine heatwave, hypoxia, and ocean  
1517 acidification research, including calculated inorganic carbon parameters from the southern Salish Sea and northern  
1518 California Current System from 2008-02-04 to 2024-10-22 (NCEI Accession 0307626). NOAA National Centers for  
1519 Environmental Information. Dataset. <https://doi.org/10.25921/4y18-rw26>, 2025b.

1520 Alin, S. R., Newton, J., Feely, R. A., Boyar, A., and Ikeda, C.: The second half decade of Washington Ocean  
1521 Acidification Center cruises, in PSEMP Marine Waters Workgroup. 2025. Puget Sound marine waters: 2024  
1522 overview. J. Apple, R. Wold, K. Stark, and J. Newton (Eds). Pgs. 24–25, 2025c.

1523 Archer, D., Eby, M., Brovkin, V., Ridgwell, A., Cao, L., Mikolajewicz, U., Caldeira, K., Matsumoto, K., Munhoven,  
1524 G., Montenegro, A., and Tokos, K.: Atmospheric lifetime of fossil fuel carbon dioxide, *Annu. Rev. Earth Planet.*  
1525 *Sci.*, 37(1), 117–134, <https://doi.org/10.1146/annurev.earth.031208.100206>, 2009.

1526 Archer, D.: *The Global Carbon Cycle*, Princeton University Press, JSTOR, <https://doi.org/10.2307/j.ctvcn4hx8>,  
1527 2010.

1528 Bach, L. T., Gill, S. J., Rickaby, R. E., Gore, S., and Renforth, P.: CO<sub>2</sub> removal with enhanced weathering and ocean  
1529 alkalinity enhancement: Potential risks and co-benefits for marine pelagic ecosystems, *Front. clim.*, 1,  
1530 <https://doi.org/10.3389/fclim.2019.00007>, 2019.

1531 Bakker, D. C. E., Pfeil, B., Smith, K., Hankin, S., Olsen, A., Alin, S. R., Cosca, C., Harasawa, S., Kozyr, A., Nojiri,

1532 Y., O'Brien, K. M., Schuster, U., Telszewski, M., Tilbrook, B., Wada, C., Akl, J., Barbero, L., Bates, N. R., Boutin,  
 1533 J., Bozec, Y., Cai, W.-J., Castle, R. D., Chavez, F. P., Chen, L., Chierici, M., Currie, K., de Baar, H. J. W., Evans,  
 1534 W., Feely, R. A., Fransson, A., Gao, Z., Hales, B., Hardman-Mountford, N. J., Hoppema, M., Huang, W.-J., Hunt,  
 1535 C. W., Huss, B., Ichikawa, T., Johannessen, T., Jones, E. M., Jones, S. D., Jutterström, S., Kitidis, V., Körtzinger,  
 1536 A., Landschützer, P., Lauvset, S. K., Lefèvre, N., Manke, A. B., Mathis, J. T., Merlivat, L., Metzl, N., Murata, A.,  
 1537 Newberger, T., Omar, A. M., Ono, T., Park, G.-H., Paterson, K., Pierrot, D., Ríos, A. F., Sabine, C. L., Saito, S.,  
 1538 Salisbury, J., Sarma, V. V. S. S., Schlitzer, R., Sieger, R., Skjelvan, I., Steinhoff, T., Sullivan, K. F., Sun, H., Sutton,  
 1539 A. J., Suzuki, T., Sweeney, C., Takahashi, T., Tjiputra, J., Tsurushima, N., van Heuven, S. M. A. C., Vandemark,  
 1540 D., Vlahos, P., Wallace, D. W. R., Wanninkhof, R., and Watson, A. J.: An update to the Surface Ocean CO<sub>2</sub> Atlas  
 1541 (SOCAT version 2), *Earth Syst. Sci. Data*, 6, 69–90, <https://doi.org/10.5194/essd-6-69-2014>, 2014.

1542 Bakker, D. C. E., Pfeil, B., Landa, C. S., Metzl, N., O'Brien, K. M., Olsen, A., Smith, K., Cosca, C., Harasawa, S.,  
 1543 Jones, S. D., Nakaoka, S., Nojiri, Y., Schuster, U., Steinhoff, T., Sweeney, C., Takahashi, T., Tilbrook, B., Wada,  
 1544 C., Wanninkhof, R., Alin, S. R., Balestrini, C. F., Barbero, L., Bates, N. R., Bianchi, A. A., Bonou, F., Boutin, J.,  
 1545 Bozec, Y., Burger, E. F., Cai, W.-J., Castle, R. D., Chen, L., Chierici, M., Currie, K., Evans, W., Featherstone, C.,  
 1546 Feely, R. A., Fransson, A., Goyet, C., Greenwood, N., Gregor, L., Hankin, S., Hardman-Mountford, N. J., Harlay, J.,  
 1547 Hauck, J., Hoppema, M., Humphreys, M. P., Hunt, C. W., Huss, B., Ibánhez, J. S. P., Johannessen, T., Keeling, R.,  
 1548 Kitidis, V., Körtzinger, A., Kozyr, A., Krasakopoulou, E., Kuwata, A., Landschützer, P., Lauvset, S. K., Lefèvre, N.,  
 1549 Lo Monaco, C., Manke, A., Mathis, J. T., Merlivat, L., Millero, F. J., Monteiro, P. M. S., Munro, D. R., Murata, A.,  
 1550 Newberger, T., Omar, A. M., Ono, T., Paterson, K., Pearce, D., Pierrot, D., Robbins, L. L., Saito, S., Salisbury, J.,  
 1551 Schlitzer, R., Schneider, B., Schweitzer, R., Sieger, R., Skjelvan, I., Sullivan, K. F., Sutherland, S. C., Sutton, A. J.,  
 1552 Tadokoro, K., Telszewski, M., Tuma, M., van Heuven, S. M. A. C., Vandemark, D., Ward, B., Watson, A. J., and  
 1553 Xu, S. (2016). A multi-decade record of high-quality *f*CO<sub>2</sub> data in version 3 of the Surface Ocean CO<sub>2</sub> Atlas  
 1554 (SOCAT), *Earth Syst. Sci. Data*, 8, 383–413, <https://doi.org/10.5194/essd-8-383-2016>.

1555 Bakker, D. C. E.; Alin, S. R.; Aramaki, T.; Barbero, L.; Bates, N. R.; Gkritzalis, T.; Jones, S. D.; Kozyr, A.;  
 1556 Lauvset, S. K.; Macovei, V.; Metzl, N.; Munro, D. R.; Nakaoka, S.-i.; O'Brien, K. M.; Olsen, A.; Pierrot, D.;  
 1557 Steinhoff, T.; Sullivan, K. F.; Sutton, A. J.; Sweeney, C.; Wada, C.; Wanninkhof, R.; Akl, J.; Arbill, L. A.; Azetsu-  
 1558 Scott, K.; Battisti, R.; Beatty, C. M.; Becker, M.; Benoit-Cattin, A.; Berghoff, C. F.; Bittig, H. C.; Bonin, J. A.; Bott,  
 1559 R.; Bozzano, R.; Burger, E. F.; Brunetti, F.; Cantoni, C.; Castelli, G.; Chambers, D. P.; Chierici, M.; Corbo, A.;  
 1560 Cronin, M.; Cross, J. N.; Currie, K. I.; Dentico, C.; Emerson, S. R.; Enochs, I.; Enright, M. P.; Enyo, K.; Ericson,  
 1561 Y.; Evans, W.; Fay, A. R.; Feely, R. A.; Fragiaco, E.; Fransson, A.; Gehrung, M.; Giani, M.; Glockzin, M.;  
 1562 Hamna, S.; Holodkov, N.; Hoppema, M.; Ibánhez, J. S. P.; Kadono, K.; Kamb, L.; Kralj, M.; Kristensin, T. O.;  
 1563 Laudicella, V. A.; Lefèvre, N.; Leseurre, C.; Lo Monaco, C.; Maenner Jones, S. M.; Maenza, R. A.; McAuliffe, A.  
 1564 M.; Mdokwana, B. W.; Monacci, N. M.; Musielewicz, S.; Neill, C.; Newberger, T.; Nojiri, Y.; Ohman, M. D.;  
 1565 Ólafsdóttir, S. R.; Olivier, L.; Omar, A.; Osborne, J.; Pensieri, S.; Petersen, W.; Plueddemann, A. J.; Rehder, G.;  
 1566 Roden, N. P.; Rutgersson, A.; Sallée, J.-B.; Sanders, R.; Sarpe, D.; Schirnik, C.; Schlitzer, R.; Send, U.; Skjelvan, I.;

1567 Sutherland, S., C.; T'Jampens, M.; Tamsitt, V.; Telszewski, M.; Theetaert, H.; Tilbrook, B.; Trull, T.; Tsanwani, M.;  
1568 Van de Velde, S.; Van Heuven, S. M. A. C.; Vecchia, M. H.; Voynova, Y. G.; Weller, R. A.; Williams, N. L.: Surface  
1569 Ocean CO<sub>2</sub> Atlas Database Version 2025 (SOCATv2025) (NCEI Accession 0304549). NOAA National Centers for  
1570 Environmental Information. Dataset. <https://doi.org/10.25921/648f-fv35>, 2025.

1571 Barth, A., Beckers, J.-M., Troupin, C., Alvera-Azcárate, A., and Vandembulcke, L.: DIVAnd-1.0: n-dimensional  
1572 variational data analysis for ocean observations, *Geosci. Model Dev.*, 7, 225-241, [https://doi.org/10.5194/gmd-7-](https://doi.org/10.5194/gmd-7-225-2014)  
1573 225-2014, 2014.

1574 Bates N. R., Johnson R. J.: Acceleration of ocean warming, salinification, deoxygenation, and acidification in the  
1575 surface subtropical North Atlantic Ocean. *Nat. Commun. Earth Environ.* 1, 1–12, 2020.

1576 Bates, N.R., and Johnson, R.J.: Forty years of ocean acidification observations (1983-2023) in the Sargasso Sea at  
1577 the Bermuda Atlantic Time-series Study (BATS) site, *Frontiers in Marine Science*, 10,  
1578 <https://doi.org/10.3389/fmars.2023.1289931>, 2023.

1579 Bates, N., Johnson, R. J., Lomas, M.W., Steinberg, D.K., Lopez, P., Hayden, M., May, R., Derbyshire, L., Lethaby,  
1580 P. J., Smith, D., and Lomas, D.: Determination of carbon, nitrogen, and phosphorus content in sinking particles at  
1581 the Bermuda Atlantic Time-series Study (BATS) site from December 1988 to December 2023 using a Particle  
1582 Interceptor Trap System (PITS). Biological and Chemical Oceanography Data Management Office (BCO-DMO).  
1583 (Version 4) Version Date 2024-11-14 [if applicable, indicate subset used]. doi:10.26008/1912/bco-dmo.894099.4  
1584 [access date], 2024a.

1585 Bates, N., Johnson, R. J., Lethaby, P. J., Smith, D., and Medley, C.: Primary productivity estimates from the  
1586 incubation of seawater collected at the Bermuda Atlantic Time-series Study (BATS) site from December 1988  
1587 through December 2023. Biological and Chemical Oceanography Data Management Office (BCO-DMO). (Version  
1588 4) Version Date 2024-11-14 [if applicable, indicate subset used]. doi:10.26008/1912/bco-dmo.893182.4 [access  
1589 date], 2024b.

1590 Bates, N., Johnson, R. J., Lethaby, P. J., Smith, D., and Medley, C.: HPLC and fluorometric derived phytoplankton  
1591 pigment concentrations from seawater collected on BATS Validation cruises from June 1996 to June 2023.  
1592 Biological and Chemical Oceanography Data Management Office (BCO-DMO). (Version 4) Version Date 2024-09-  
1593 18 [if applicable, indicate subset used]. doi:10.26008/1912/bco-dmo.926534.4 [access date], 2024c.

1594 Bates, N., Johnson, R. J., Lethaby, P. J., Medley, C., and Smith, D.: HPLC and fluorometric derived phytoplankton  
1595 pigment concentrations from seawater collected at the Bermuda Atlantic Time-series Study (BATS) site from  
1596 October 1988 through December 2023. Biological and Chemical Oceanography Data Management Office (BCO-  
1597 DMO). (Version 6) Version Date 2023-09-13 [if applicable, indicate subset used]. doi:10.26008/1912/bco-  
1598 dmo.893521.6 [access date], 2024d.

1599 Bates, N., Johnson, R. J., Smith, D., Lethaby, P. J., Lomas, M.W., and Lomas, D.: Discrete bottle samples collected

1600 during BATS Validation (BVAL) cruises from April 1991 through June 2023. Biological and Chemical  
1601 Oceanography Data Management Office (BCO-DMO). (Version 5) Version Date 2024-10-01 [if applicable, indicate  
1602 subset used]. doi:10.26008/1912/bco-dmo.917255.5 [access date], 2024e.

1603 Bennington, V., Gloege, L., and McKinley, G. A.: Variability in the global ocean carbon sink from 1959 to 2020 by  
1604 correcting models with observations, *Geophys. Res. Lett.*, 49(14), <https://doi.org/10.1029/2022gl098632>, 2022a.

1605 Bennington, V., Galjanic, T., and McKinley, G. A.: Explicit physical knowledge in machine learning for Ocean  
1606 Carbon Flux Reconstruction: The  $p\text{CO}_2$ -residual method. *J. Adv. Model. Earth Syst.*, 14(10),  
1607 <https://doi.org/10.1029/2021ms002960>, 2022b.

1608 Bertin, C., Carroll, D., Menemenlis, D., Dutkiewicz, S., Zhang, H., Matsuoka, A., Tank, S., Manizza, M., Miller, C.  
1609 E., Babin, M., Mangin, A., and Le Fouest, V.: Biogeochemical river runoff drives intense coastal Arctic Ocean  $\text{CO}_2$   
1610 outgassing, *Geophys. Res. Lett.*, 50(8), <https://doi.org/10.1029/2022gl102377>, 2023.

1611 Bittig, H. C., Steinhoff, T., Claustre, H., Fiedler, B., Williams, N. L., Sauzède, R., Körtzinger, A., and Gattuso, J.-P.:  
1612 An alternative to static climatologies: Robust estimation of open ocean  $\text{CO}_2$  variables and nutrient concentrations  
1613 from T, S, and  $\text{O}_2$  data using Bayesian Neural Networks, *Frontiers in Marine Science*, 5,  
1614 <https://doi.org/10.3389/fmars.2018.00328>, 2018.

1615 Bittig, H. C., Jacobs, E., Neumann, T., and Rehder, G.: A regional  $p\text{CO}_2$  climatology of the Baltic Sea, PANGAEA  
1616 [data set], <https://doi.org/10.1594/PANGAEA.961119>, 2023.

1617 Bittig, H.C., Jacobs, E., Neumann, T., and Rehder, G.: A regional  $p\text{CO}_2$  climatology of the Baltic Sea from in situ  
1618  $p\text{CO}_2$  observations and a model-based extrapolation approach, *Earth Syst. Sci. Data*, 16(2), 753–773,  
1619 <https://doi.org/10.5194/essd-16-753-2024>, 2024.

1620 Boyer, T. P., Garcia, H. E., Locarnini, R. A., Zweng, M. M., Mishonov, A. V., Reagan, J. R., Weathers, K. A.,  
1621 Baranova, O. K., Seidov, D., Smolyar, I. V.: World Ocean Atlas 2018, NOAA National Centers for Environmental  
1622 Information, <https://www.ncei.noaa.gov/archive/accession/NCEI-WOA18>, 2018.

1623 Brett, A., Leape, J., Abbott, M., Sakaguchi, H., Cao, L., Chand, K., Golbuu, Y., Martin, T. J., Mayorga, J., and  
1624 Myksovoll, M. S.: Ocean Data Need a sea change to help navigate the Warming World. *Nature*, 582(7811), 181–183,  
1625 <https://doi.org/10.1038/d41586-020-01668-z>, 2020.

1626 Broecker W. S.: Glacial to interglacial changes in ocean chemistry, *Prog. Oceanogr.*, 11(2), 151–97,  
1627 [https://doi.org/10.1016/0079-6611\(82\)90007-6](https://doi.org/10.1016/0079-6611(82)90007-6), 1982.

1628 Broullón, D., Pérez, F. F., Velo, A., Hoppema, M., Olsen, A., Takahashi, T., Key, R. M., Tanhua, T., González-  
1629 Dávila, M., Jeansson, E., Kozyr, A., and van Heuven, S. M. A. C.: A global monthly climatology of total alkalinity:  
1630 a neural network approach, *Earth Syst. Sci. Data*, 11, 1109–1127, <https://doi.org/10.5194/essd-11-1109-2019>, 2019.

Deleted: R

1632 Broullón, D., Pérez, F. F., Velo, A., Hoppema, M., Olsen, A., Takahashi, T., Key, R. M., Tanhua, T., Santana-  
1633 Casiano, J. M., and Kozyr, A.: A global monthly climatology of oceanic total dissolved inorganic carbon: A Neural  
1634 Network approach, *Earth Syst. Sci. Data*, 12(3), 1725–1743, <https://doi.org/10.5194/essd-12-1725-2020>, 2020a.

1635 Broullón, D.; Pérez, F. F.; Velo, A.; Hoppema, M.; Olsen, A.; Takahashi, T.; Key, R. M.; Tanhua, T.; González-  
1636 Dávila, M.; Jeansson, E.; Kozyr, A.; van Heuven, S. M. A. C.: A global monthly climatology of total alkalinity  
1637 (AT): a neural network approach (NCEI Accession 0222470). NOAA National Centers for Environmental  
1638 Information. Dataset. <https://doi.org/10.25921/5p69-y471>, 2020b.

1639 Broullón, D.; Pérez, F. F.; Velo, A.; Hoppema, M.; Olsen, A.; Takahashi, T.; Key, R. M.; Tanhua, T.; Santana-  
1640 Casiano, J. M.; Kozyr, A.: A global monthly climatology of oceanic total dissolved inorganic carbon (DIC): a neural  
1641 network approach (NCEI Accession 0222469). NOAA National Centers for Environmental Information. Dataset.  
1642 <https://doi.org/10.25921/ndgj-jp24>, 2020c.

1643 Cai, W.-J., Hu, X., Huang, W.-J., Murrell, M. C., Lehrter, J. C., Lohrenz, S. E., Chou, W.-C., Zhai, W., Hollibaugh,  
1644 J. T., Wang, Y., Zhao, P., Guo, X., Gundersen, K., Dai, M., and Gong, G.-C.: Acidification of subsurface coastal  
1645 waters enhanced by eutrophication, *Nature Geoscience*, 4(11), 766–770, <https://doi.org/10.1038/ngeo1297>, 2011.

1646 Carroll, D., Menemenlis, D., Adkins, J. F., Bowman, K. W., Brix, H., Dutkiewicz, S., Fenty, I., Gierach, M. M.,  
1647 Hill, C., Jahn, O., Landschützer, P., Lauderdale, J. M., Liu, J., Manizza, M., Naviaux, J. D., Rödenbeck, C., Schimel,  
1648 D. S., Van der Stocken, T., and Zhang, H.: The ECCO-Darwin data-assimilative global ocean biogeochemistry  
1649 model: Estimates of seasonal to multidecadal surface ocean pCO<sub>2</sub> and air-sea CO<sub>2</sub> flux, *J. Adv. Model. Earth Syst.*,  
1650 12(10), <https://doi.org/10.1029/2019ms001888>, 2020.

1651 Carroll, D., Menemenlis, D., Dutkiewicz, S., Lauderdale, J. M., Adkins, J. F., Bowman, K. W., Brix, H., Fenty, I.,  
1652 Gierach, M. M., Hill, C., Jahn, O., Landschützer, P., Manizza, M., Mazloff, M. R., Miller, C. E., Schimel, D. S.,  
1653 Verdy, A., Whitt, D. B., and Zhang, H.: Attribution of space-time variability in global-ocean dissolved inorganic  
1654 Carbon, *Global Biogeochemical Cycles*, 36(3), <https://doi.org/10.1029/2021gb007162>, 2022.

1655 Carroll, D., Menemenlis, D., Zhang, H., Mazloff, M., McKinley, G., Fay, A., Dutkiewicz, S., Lauderdale, J., and  
1656 Fenty, I.: Evaluation of the ECCO-Darwin Ocean Biogeochemistry State Estimate vs. In-situ Observations (ver 1.0),  
1657 Zenodo, <https://doi.org/10.5281/zenodo.10627664>, 2024.

1658 Carter, B. R., Williams, N. L., Gray, A. R., and Feely, R. A.: Locally interpolated alkalinity regression for global  
1659 alkalinity estimation, *Limnology and Oceanography: Methods*, 14(4), 268–277, <https://doi.org/10.1002/lom3.10087>,  
1660 2016.

1661 Carter, B. R., Feely, R. A., Williams, N. L., Dickson, A. G., Fong, M. B., and Takeshita, Y.: Updated methods for  
1662 global locally interpolated estimation of alkalinity, ph, and nitrate, *Limnology and Oceanography: Methods*, 16(2),  
1663 119–131, <https://doi.org/10.1002/lom3.10232>, 2017.

1664 Carter, B. R., Feely, R. A., Lauvset, S. K., Olsen, A., DeVries, T., and Sonnerup, R.: Preformed properties for  
1665 marine organic matter and carbonate mineral cycling quantification. *Global Biogeochemical Cycles*, 35(1).  
1666 <https://doi.org/10.1029/2020gb006623>, 2020.

1667 Carter, B. R., Bittig, H. C., Fassbender, A. J., Sharp, J. D., Takeshita, Y., Xu, Y.-Y., et al.: New and updated global  
1668 empirical seawater property estimation routines, *Limnol. and Oceanogr.: Methods*, 19(12), 785–809,  
1669 <https://doi.org/10.1002/lom3.10461>, 2021.

1670 Carter, B. R., Schwinger, J., Sonnerup, R., Fassbender, A. J., Sharp, J. D., Dias, L. M., and Sandborn, D. E.: Tracer-  
1671 based Rapid Anthropogenic Carbon Estimation (TRACE), *Earth Syst. Sci. Data*, 17, 3073–3088,  
1672 <https://doi.org/10.5194/essd-17-3073-2025>, 2025.

1673 Carter, B.: Anthropogenic carbon distributions from preindustrial to 2500 c.e. estimated using Tracer-based Rapid  
1674 Anthropogenic Carbon Estimation (version 1) [Data set]. Zenodo. <https://doi.org/10.5281/zenodo.15003059>, 2025.

1675 Chakraborty, K., Joshi, A. P., Ghoshal, P. K., Baduru, B., Valsala, V., Sarma, V. V. S. S., Metzl, N., Gehlen, M.,  
1676 Chevallier, F., and Lo Monaco, C.: Indian Ocean acidification and its driving mechanisms over the last four decades  
1677 (1980–2019), *Global Biogeochemical Cycles*, 38(9), <https://doi.org/10.1029/2024gb008139>, 2024.

1678 Chakraborty, K.; Joshi, A. P.; Ghoshal, P. K.; Baduru, B.; Valsala, V.; Sarma, V. V. S. S.; Metzl, N.; Gehlen, M.;  
1679 Chevallier, F.; Lo Monaco, C.: Indian ocean acidification and its driving mechanisms over the last four decades  
1680 from 1980-01-01 to 2019-12-31 (NCEI Accession 0307663). NOAA National Centers for Environmental  
1681 Information. Dataset. <https://doi.org/10.25921/z2x4-vt48>, 2025.

1682 Chau, T.-T.-T., Gehlen, M., and Chevallier, F.: A seamless ensemble-based reconstruction of surface ocean  $p\text{CO}_2$   
1683 and air–sea  $\text{CO}_2$  fluxes over the global coastal and open oceans. *Biogeosciences*, 19(4), 1087–1109,  
1684 <https://doi.org/10.5194/bg-19-1087-2022>, 2022.

1685 Chau, T.-T.-T., Gehlen, M., Metzl, N., and Chevallier, F.: CMEMS-LSCE: a global, 0.25°, monthly reconstruction  
1686 of the surface ocean carbonate system, *Earth Syst. Sci. Data*, 16, 121–160, [https://doi.org/10.5194/essd-16-121-](https://doi.org/10.5194/essd-16-121-2024)  
1687 2024, 2024a.

1688 Chau, T.-T.-T., Chevallier, F. and Gehlen, M.: Global analysis of surface ocean  $\text{CO}_2$  fugacity and air–sea fluxes  
1689 with low latency, *Geophys. Res. Lett.*, <https://doi.org/10.1029/2023GL106670>, 2024b.

1690 Chen, C.-T. A., Lui, H.-K., Hsieh, C.-H., Yanagi, T., Kosugi, N., Ishii, M., and Gong, G.-C.: Deep oceans may  
1691 acidify faster than anticipated due to global warming, *Nat. Clim. Change.*, 7(12), 890–894,  
1692 <https://doi.org/10.1038/s41558-017-0003-y>, 2017.

1693 Clement, D., and Gruber, N.: The EMLR(C\*) method to determine decadal changes in the global ocean storage of  
1694 Anthropogenic  $\text{CO}_2$ . *Global Biogeochemical Cycles*, 32(4), 654–679, <https://doi.org/10.1002/2017gb005819>, 2018.

- 1695 Cooley, S. R., and Doney, S. C.: Anticipating ocean acidification's economic consequences for commercial  
1696 fisheries. *Environmental Research Letters*, 4(2), 024007, <https://doi.org/10.1088/1748-9326/4/2/024007>, 2009.
- 1697 Crisp, D., Dolman, H., Tanhua, T., McKinley, G. A., Hauck, J., Bastos, A., Sitch, S., Eggleston, S., and Aich, V.:  
1698 How well do we understand the land-ocean-atmosphere carbon cycle? *Reviews of Geophysics*, 60(2),  
1699 <https://doi.org/10.1029/2021RG000736>, 2022.
- 1700 Cyr, F., Gibb, O., Azetsu-Scott, K., Chassé, J., Galbraith, P., Maillet, G., Pepin, P., Punshon, S., and Starr, M.:  
1701 Ocean carbonate parameters on the Canadian Atlantic Continental Shelf, Federated Research Data Repository,  
1702 <https://doi.org/10.20383/102.0673>, 2022.
- 1703 Delaigue, L., Sulpis, O., Reichart, G. -J., and Humphreys, M. P.: The changing biological carbon pump of the South  
1704 Atlantic Ocean. *Global Biogeochemical Cycles*, 38(9), <https://doi.org/10.1029/2024gb008202>, 2024.
- 1705 DeVries, T., Holzer, M. and Primeau, F.: Recent increase in oceanic carbon uptake driven by weaker upper-ocean  
1706 overturning, *Nature*, 542, 215–218, <https://doi.org/10.1038/nature21068>, 2017.
- 1707 DeVries, T., Le Quéré, C., Andrews, O., Berthet, S., Hauck, J., Ilyina, T., Landschützer, P., Lenton, A., Lima, I. D.,  
1708 Nowicki, M., Schwinger, J., and Séférian, R.: Decadal trends in the ocean carbon sink, *Proceedings of the National  
1709 Academy of Sciences*, 116(24), 11646–11651, <https://doi.org/10.1073/pnas.1900371116>, 2019.
- 1710 DeVries, T.: The Ocean Carbon Cycle, *Annual Review of Environment and Resources*, 47(1), 317–341,  
1711 <https://doi.org/10.1146/annurev-environ-120920-111307>, 2022a.
- 1712 DeVries, T.: Atmospheric CO<sub>2</sub> and sea surface temperature variability cannot explain recent decadal variability of  
1713 the Ocean CO<sub>2</sub> Sink. *Geophysical Research Letters*, 49(7). <https://doi.org/10.1029/2021gl096018>, 2022b.
- 1714 DeVries, T., Yamamoto, K., Wanninkhof, R., Gruber, N., Hauck, J., Müller, J. D., Bopp, L., Carroll, D., Carter, B.,  
1715 Chau, T., Doney, S. C., Gehlen, M., Gloege, L., Gregor, L., Henson, S., Kim, J. H., Iida, Y., Ilyina, T.,  
1716 Landschützer, P., Le Quéré, C., Munro, D., Nissen, C., Patara, L., Pérez, F. F., Resplandy, L., Rodgers, K. B.,  
1717 Schwinger, J., Séférian, R., Sicardi, V., Terhaar, J., Triñanes, J., Tsujino, H., Watson, A., Yasunaka, S., Zeng, J.  
1718 (2023). Magnitude, trends, and variability of the Global Ocean Carbon Sink from 1985 to 2018. *Global  
1719 Biogeochemical Cycles*, 37(10). <https://doi.org/10.1029/2023gb007780>, 2023.
- 1720 Doney, S. C., Busch, D. S., Cooley, S. R., and Kroeker, K. J.: The impacts of ocean acidification on marine  
1721 ecosystems and reliant human communities, *Annual Review of Environment and Resources*, 45(1), 83–112,  
1722 <https://doi.org/10.1146/annurev-environ-012320-083019>, 2020.
- 1723 Dore, J. E., Lukas, R., Sadler, D. W., and Karl, D. M.: Climate-driven changes to the atmospheric CO<sub>2</sub> sink in the  
1724 subtropical North Pacific Ocean, *Nature*, 424, 754–757, <https://doi.org/10.1038/nature01885>, 2003.

**Deleted:** Dickson, A. G.: Standard potential of the reaction:  $\text{AgCl(s)} + 1/2 \text{H}_2\text{(g)} = \text{Ag(s)} + \text{HCl(aq)}$ , and the standard acidity constant of the ion  $\text{HSO}_4^-$  in synthetic seawater from 273.15 to 318.15K, *Journal of Chemical Thermodynamics*, 22(2), 113–127, [https://doi.org/10.1016/0021-9614\(90\)90074-Z](https://doi.org/10.1016/0021-9614(90)90074-Z), 1990. ¶

1730 Dore, J. E., Lukas, R., Sadler, D. W., Church, M. J., and Karl, D. M.: Physical and biogeochemical modulation of  
1731 ocean acidification in the central North Pacific, *Proc. Natl. Acad. Sci.*, 106, 12235-12240,  
1732 <https://doi.org/10.1073/pnas.0906044106>, 2009.

1733 Dore, J. E., Church, M. J., Karl, D. M., Sadler, D. W., and Letelier, R. M.: Paired windward and leeward  
1734 biogeochemical time series reveal consistent surface ocean CO<sub>2</sub> trends across the Hawaiian Ridge, *Geophys. Res.*  
1735 *Let.*, 41, 6459-6467, <https://doi.org/10.1002/2014GL060725>, 2014.

1736 Dore, J.E., White, A.E., and Karl, D.M.: Hawaii Ocean Time-series (HOT) Carbon Dioxide (Version 1) [Data set].  
1737 Zenodo. <https://doi.org/10.5281/zenodo.15060931>, 2025.

1738 Dunne, John P., John, J. G., Shevliakova, E., Stouffer, R. J., Krasting, J. P., Malyshev, S. L., Milly, P. C., Sentman,  
1739 L. T., Aderofo, A. J., Cooke, W., Dunne, K. A., Griffies, S. M., Hallberg, R. W., Harrison, M. J., Levy, H.,  
1740 Wittenberg, A. T., Phillips, P. J., and Zadeh, N.: GFDL's ESM2 global coupled climate-carbon earth system  
1741 models. part II: Carbon system formulation and baseline simulation characteristics, *Journal of Climate*, 26(7), 2247–  
1742 2267, <https://doi.org/10.1175/jcli-d-12-00150.1>, 2013.

1743 Dunne, J. P., Hewitt, H. T., Arblaster, J., Bonou, F., Boucher, O., Cavazos, T., Durack, P. J., Hassler, B., Juckes, M.,  
1744 Miyakawa, T., Mizielinski, M., Naik, V., Nicholls, Z., O'Rourke, E., Pincus, R., Sanderson, B. M., Simpson, I. R.,  
1745 and Taylor, K. E.: An Evolving Coupled Model Intercomparison Project Phase 7 (CMIP7) and Fast Track in  
1746 Support of Future Climate Assessment, <https://doi.org/10.5194/egusphere-2024-3874>, 2024.

1747 Durack, P. J., Taylor, K. E., Gleckler, P. J., Meehl, G. A., Lawrence, B. N., Covey, C., Stouffer, R. J., Levvasseur,  
1748 G., Ben-Nasser, A., Denvil, S., Stockhouse, M., Gregory, J. M., Juckes, M., Ames, S. K., Antonio, F., Bader, D. C.,  
1749 Dunne, J. P., Ellis, D., Eyring, V., Fiore, S. L., Joussaume, S., Kershaw, P., Lamarque, J.-F., Lautenschlager, M.,  
1750 Lee, J., Mauzey, C. F., Mizielinski, M., Nassisi, P., Nuzzo, A., O'Rourke, E., Painter, J., Potter, G. L., Rodriguez,  
1751 S., Williams, D. N.: The Coupled Model Intercomparison Project (CMIP): Reviewing Project History, Evolution,  
1752 Infrastructure and Implementation, <https://doi.org/10.5194/egusphere-2024-3729>, 2025.

1753 Edmond, J. M.: High precision determination of titration alkalinity and total carbon dioxide content of sea water by  
1754 potentiometric titration, *Deep Sea Research and Oceanographic Abstracts*, 17(4), 737–750,  
1755 [https://doi.org/10.1016/0011-7471\(70\)90038-0](https://doi.org/10.1016/0011-7471(70)90038-0), 1970.

1756 Fassbender, A. J., Carter, B. R., Sharp, J. D., Huang, Y., Arroyo, M. C., and Frenzel, H.: Amplified subsurface  
1757 signals of ocean acidification, *Global Biogeochemical Cycles*, 37, e2023GB007843,  
1758 <https://doi.org/10.1029/2023GB007843>, 2023.

1759 Fassbender, A. J.: Near-global, upper 2000 m estimates of preindustrial and year 2002 ocean pH, aragonite  
1760 saturation state, carbon dioxide partial pressure, hydrogen ion concentration, and Revelle factor values, and their  
1761 total changes caused by anthropogenic carbon accumulation in addition to the component of the changes induced by

1762 carbonate system nonlinearities (NCEI Accession 0290073). NOAA National Centers for Environmental  
1763 Information. Dataset. <https://doi.org/10.25921/rdtr-9t74>, 2024.

1764 Fay, A. R., Gregor, L., Landschützer, P., McKinley, G. A., Gruber, N., Gehlen, M., Iida, Y., Laruelle, G. G.,  
1765 Rödenbeck, C., Roobaert, A., and Zeng, J.: SeaFlux: harmonization of air–sea CO<sub>2</sub> fluxes from surface pCO<sub>2</sub> data  
1766 products using a standardized approach, *Earth Sys. Sci. Data*, 13(10), 4693–4710, [https://doi.org/10.5194/essd-13-](https://doi.org/10.5194/essd-13-4693-2021)  
1767 4693-2021, 2021.

1768 Fay, A. R., and McKinley, G. A.: Observed regional fluxes to constrain modelled estimates of the Ocean Carbon  
1769 Sink, *Geophysical Res. Lett.*, 48(20), <https://doi.org/10.1029/2021gl095325>, 2021.

1770 Fay, A. R., Munro, D. R., McKinley, G. A., Pierrot, D., Sutherland, S. C., Sweeney, C., and Wanninkhof, R.:  
1771 Updated climatological mean  $\Delta$ /CO<sub>2</sub> and net sea–air CO<sub>2</sub> flux over the global open ocean regions, *Earth Syst. Sci.*  
1772 *Data*, 16, 2123–2139, <https://doi.org/10.5194/essd-16-2123-2024>, 2024.

1773 Feely, R. A., Jiang, L.-Q., Wanninkhof, R., Carter, B. R., Alin, S. A., Bednaršek, N., and Cosca, C. E.: Acidification  
1774 of the global surface ocean: What we have learned from observations, *Oceanography*, 36, 120-129,  
1775 <https://doi.org/10.5670/oceanog.2023.222>, 2023.

1776 Fennel, K., Mattern, J. P., Doney, S. C., Bopp, L., Moore, A. M., Wang, B., and Yu, L.: Ocean biogeochemical  
1777 modelling, *Nat. Rev. Methods Primers*, 2, 76, <https://doi.org/10.1038/s43586-022-00154-2>, 2022.

1778 Franco, A. C., Ianson, D., Ross, T., Hamme, R. C., Monahan, A. H., Christian, J. R., Davelaar, M., Johnson, W. K.,  
1779 Miller, L. A., Robert, M., and Tortell, P. D.: Anthropogenic and climatic contributions to observed carbon system  
1780 trends in the northeast Pacific. *Global Biogeochemical Cycles*, 35(7). <https://doi.org/10.1029/2020GB006829>,  
1781 2021a.

1782 Franco, A. C., Ianson, D., Ross, T., Hamme, R. C., Monahan, A. H., Christian, J. R., Davelaar, M., Johnson, W. K.,  
1783 Miller, L. A., Robert, M., and Tortell, P. D.: A compilation of inorganic carbon system and other hydrographic and  
1784 chemical discrete profile measurements obtained during the fifty five Line P cruises in the Northeast Pacific Ocean  
1785 over the period from 1990 to 2019 (NCEI Accession 0234342). NOAA National Centers for Environmental  
1786 Information. Dataset. <https://doi.org/10.25921/zrw8-kn24>, 2021b.

1787 Freeland, H.: A short history of Ocean Station Papa and Line P. *Progress in Oceanography*, 75(2), 120–125,  
1788 <https://doi.org/10.1016/j.pocan.2007.08.005>, 2007.

1789 [Friedlingstein, P., O'Sullivan, M., Jones, M. W., Andrew, R. M., Bakker, D. C. E., Hauck, J., Landschützer, P., Le](#)  
1790 [Quéré, C., Li, H., Luijckx, I. T., Peters, G. P., Peters, W., Pongratz, J., Schwingshackl, C., Sitch, S., Canadell, J. G.,](#)  
1791 [Ciais, P., Aas, K., Alin, S. R., Anthoni, P., Barbero, L., Bates, N. R., Bellouin, N., Benoit-Cattin, A., Berghoff, C.](#)  
1792 [F., Bernardello, R., Bopp, L., Brasika, I. B. M., Chamberlain, M. A., Chandra, N., Chevallier, F., Chini, L. P.,](#)

1793 [Collier, N. O., Colligan, T. H., Cronin, M., Djeutchouang, L., Dou, X., Enright, M. P., Enyo, K., Erb, M., Evans,](#)  
1794 [W., Feely, R. A., Feng, L., Ford, D. J., Foster, A., Fransner, F., Gasser, T., Gehlen, M., Gkritzalis, T., Goncalves De](#)  
1795 [Souza, J., Grassi, G., Gregor, L., Gruber, N., Guenet, B., Gürses, Ö., Harrington, K., Harris, I., Heinke, J., Hurtt, G.](#)  
1796 [C., Iida, Y., Ilyina, T., Ito, A., Jacobson, A. R., Jain, A. K., Jarniková, T., Jersild, A., Jiang, F., Jones, S. D., Kato,](#)  
1797 [E., Keeling, R. F., Klein Goldewijk, K., Knauer, J., Kong, Y., Korsbakken, J. I., Koven, C., Kunimitsu, T., Lan, X.,](#)  
1798 [Liu, J., Liu, Z., Liu, Z., Lo Monaco, C., Ma, L., Marland, G., McGuire, P. C., McKinley, G. A., Melton, J., Monacci,](#)  
1799 [N., Monier, E., Morgan, E. J., Munro, D. R., Müller, J. D., Nakaoka, S.-I., Navagam, L. R., Niwa, Y., Nutzelt, T.,](#)  
1800 [Olsen, A., Omar, A. M., Pan, N., Pandey, S., Pierrot, D., Qin, Z., Regnier, P. A. G., Rehder, G., Resplandy, L.,](#)  
1801 [Roobaert, A., Rosan, T. M., Rödenbeck, C., Schwinger, J., Skjelvan, I., Smallman, T. L., Spada, V., Sreeush, M. G.,](#)  
1802 [Sun, Q., Sutton, A. J., Sweeney, C., Swingedouw, D., Séférian, R., Takao, S., Tatebe, H., Tian, H., Tian, X.,](#)  
1803 [Tilbrook, B., Tsujino, H., Tubiello, F., van Ooijen, E., van der Werf, G., van de Velde, S. J., Walker, A.,](#)  
1804 [Wanninkhof, R., Yang, X., Yuan, W., Yue, X., and Zeng, J.: Global Carbon Budget 2025, Earth Syst. Sci. Data](#)  
1805 [Discuss. \[preprint\], <https://doi.org/10.5194/essd-2025-659>, in review, 2025.](#)

1806 Garcia, H. E., Locarnini, R. A., Boyer, T. P., Antonov, J. I., Baranova, O. K., Zweng, M. M., Reagan, J. R., and  
1807 Johnson, D. R.: World Ocean Atlas 2013, Volume 3: Dissolved Oxygen, Apparent Oxygen Utilization, and Oxygen  
1808 Saturation, edited by: Levitus, S. and Mishonov, A., Technical Ed., NOAA Atlas NES- DIS 75, 27 pp., 2014.

1809 Garcia, H. E., Weathers, K., Paver, C. R., Smolyar, I., Boyer, T. P., Locarnini, R. A., Zweng, M. M., Mishonov, A.  
1810 V., Baranova, O. K., Seidov, D., and Reagan, J. R.: World Ocean Atlas 2018, Volume 4: Dissolved Inorganic  
1811 Nutrients (phosphate, nitrate and nitrate+nitrite, silicate), A. Mishonov Technical Ed., NOAA Atlas NESDIS 84,  
1812 35pp, 2018a.

1813 Garcia H. E., Weathers, K. W., Paver, C. R., Smolyar, I.V., Boyer, T. P., Locarnini, R. A., Zweng, M. M.,  
1814 Mishonov, A. V., Baranova, O.K., and Reagan, J. R.: World Ocean Atlas 2018, Volume 3: Dissolved Oxygen,  
1815 Apparent Oxygen Utilization, and Oxygen Saturation, Mishonov, A., Technical Editor, NOAA Atlas NESDIS 83,  
1816 2018b.

1817 Garcia H. E., Boyer, T. P., Locarnini, R. A., Reagan, J. R., Mishonov, A. V., Baranova, O. K., Paver, C. R., Wang,  
1818 Z., Bouchard, C. N., Cross, S. L., Seidov, D., and Dukhovskoy, D.: World Ocean Database 2023: User's Manual.  
1819 A.V. Mishonov, Technical Ed., NOAA Atlas NESDIS 98, pp 129. <https://doi.org/10.25923/j8gq-eee82>, 2024.

1820 Gattuso, J.-P., and Hansson, L.: Ocean acidification, Oxford University Press, pp. 326, 2011.

1821 Gattuso, J.-P., Epitalon, J.-M., Lavigne, H., and Orr, J.: seacarb: Seawater Carbonate Chemistry, R Package  
1822 (Version 3.2.16), <https://CRAN.R-project.org/package=seacarb>, 2021a.

1823 Gattuso, J.-P., Alliouane, S., Mousseau, L.: Seawater carbonate chemistry in the Bay of Villefranche, Point B  
1824 (France), January 2007 - June 2023 [dataset], PANGAEA, <https://doi.org/10.1594/PANGAEA.727120>, 2021b.

**Deleted:** Friedlingstein, P., O'Sullivan, M., Jones, M. W., Andrew, R. M., Hauck, J., Landschützer, P., Le Quééré, C., Li, H., Luijckx, I. T., Olsen, A., Peters, G. P., Peters, W., Pongratz, J., Schwingshackl, C., Sitch, S., Canadell, J. G., Ciais, P., Jackson, R. B., Alin, S. R., Armeth, A., Arora, V., Bates, N. R., Becker, M., Bellouin, N., Berghoff, C. F., Bittig, H. C., Bopp, L., Cadule, P., Campbell, K., Chamberlain, M. A., Chandra, N., Chevallier, F., Chini, L. P., Colligan, T., Decayeux, J., Djeutchouang, L. M., Dou, X., Duran Rojas, C., Enyo, K., Evans, W., Fay, A. R., Feely, R. A., Ford, D. J., Foster, A., Gasser, T., Gehlen, M., Gkritzalis, T., Grassi, G., Gregor, L., Gruber, N., Gürses, Ö., Harris, I., Hefner, M., Heinke, J., Hurtt, G. C., Iida, Y., Ilyina, T., Jacobson, A. R., Jain, A. K., Jarniková, T., Jersild, A., Jiang, F., Jin, Z., Kato, E., Keeling, R. F., Klein Goldewijk, K., Knauer, J., Korsbakken, J. I., Lan, X., Lauvset, S. K., Lefèvre, N., Liu, Z., Liu, J., Ma, L., Maksyutov, S., Marland, G., Mayot, N., McGuire, P. C., Metzl, N., Monacci, N. M., Morgan, E. J., Nakaoka, S.-I., Neill, C., Niwa, Y., Nützel, T., Olivier, L., Ono, T., Palmer, P. I., Pierrot, D., Qin, Z., Resplandy, L., Roobaert, A., Rosan, T. M., Rödenbeck, C., Schwinger, J., Smallman, T. L., Smith, S. M., Sospedra-Alfonso, R., Steinhoff, T., Sun, Q., Sutton, A. J., Séférian, R., Takao, S., Tatebe, H., Tian, H., Tilbrook, B., Torres, O., Tourigny, E., Tsujino, H., Tubiello, F., van der Werf, G., Wanninkhof, R., Wang, X., Yang, D., Yang, X., Yu, Z., Yuan, W., Yue, X., Zaehle, S., Zeng, N., and Zeng, J.: Global Carbon Budget 2024. Earth Syst. Sci. Data, 17, 965–1039, <https://doi.org/10.5194/essd-17-965-2025>, 2025

1851 Gattuso, J.-P., Alliouane, S., and Fischer, P.: High-frequency, year-round time series of the carbonate chemistry in a  
1852 high-Arctic fjord (Svalbard), *Earth Syst. Sci. Data*, 15, 2809–2825, <https://doi.org/10.5194/essd-15-2809-2023>,  
1853 2023a.

1854 Gattuso, J.-P., Alliouane, S., and Fischer, P.: High-frequency, year-round time series of the carbonate chemistry in a  
1855 high-Arctic fjord (Svalbard) [dataset], PANGAEA, <https://doi.org/10.1594/PANGAEA.957028>, 2023b.

1856 Ghoshal, P. K., Joshi, A. P., and Chakraborty, K.: An improved long-term high-resolution surface  $p\text{CO}_2$  data  
1857 product for the Indian Ocean using machine learning, *Scientific Data*, 12(1), [https://doi.org/10.1038/s41597-025-](https://doi.org/10.1038/s41597-025-04914-z)  
1858 [04914-z](https://doi.org/10.1038/s41597-025-04914-z), 2025a.

1859 Ghoshal, P. K.; Joshi, A. P.; Chakraborty, K.: An improved long-term high-resolution surface  $p\text{CO}_2$  data product for  
1860 the Indian Ocean using machine learning from 1980-01-01 to 2020-12-31 (NCEI Accession 0307788). NOAA  
1861 National Centers for Environmental Information. Dataset. <https://doi.org/10.25921/r2q9-d197>, 2025b.

1862 Gibb, O., Cyr, F., Azetsu-Scott, K., Chassé, J., Childs, D., Gabriel, C.-E., Galbraith, P. S., Maillet, G., Pepin, P.,  
1863 Punshon, S., and Starr, M.: Spatiotemporal variability in pH and carbonate parameters on the Canadian Atlantic  
1864 continental shelf between 2014 and 2022, *Earth Syst. Sci. Data*, 15, 4127–4162, [https://doi.org/10.5194/essd-15-](https://doi.org/10.5194/essd-15-4127-2023)  
1865 [4127-2023](https://doi.org/10.5194/essd-15-4127-2023), 2023.

1866 Gloege, L., Yan, M., Zheng, T., and McKinley, G. A.: Improved quantification of ocean carbon uptake by using  
1867 machine learning to merge global models and  $p\text{CO}_2$  data, *Journal of Advances in Modeling Earth Systems*, 14(2),  
1868 <https://doi.org/10.1029/2021ms002620>, 2022.

1869 González-Dávila, M. and Santana-Casiano J. M.: Long-term trends of pH and inorganic carbon in the Eastern North  
1870 Atlantic: the ESTOC site, *Front. Mar. Sci.*, 10, 1236214, <https://doi.org/10.3389/fmars.2023.1236214>, 2023.

1871 Gregor, L.: luke-gregor/OceanSODA-ETHZ: code, Zenodo, <https://doi.org/10.5281/zenodo.4455354>, 2021.

1872 Gregor, L. and Fay, A.: SeaFlux: harmonised sea-air  $\text{CO}_2$  fluxes from surface  $p\text{CO}_2$  data products using a  
1873 standardised approach [Data set], Zenodo, <https://doi.org/10.5281/zenodo.5482547>, 2021.

1874 Gregor, L., Lebehot, A. D., Kok, S., and Monteiro, P. M. S.: A comparative assessment of the uncertainties of  
1875 Global Surface Ocean  $\text{CO}_2$  Estimates using a machine-learning ensemble (CSIR-ML6 version 2019a) – have we hit  
1876 the wall? *Geoscientific Model Development*, 12(12), 5113–5136, <https://doi.org/10.5194/gmd-12-5113-2019>, 2019a.

1877 Gregor, L., Lebehot, A. D., Kok, S., Monteiro, P. M. S.: Global surface-ocean partial pressure of carbon dioxide  
1878 ( $p\text{CO}_2$ ) estimates from a machine learning ensemble: CSIR-ML6 v2019a (NCEI Accession 0206205), NOAA  
1879 National Centers for Environmental Information, Dataset, <https://doi.org/10.25921/z682-mn47>, 2019b.

1880 Gregor, L., and Gruber, N.: OceanSODA-ETHZ: A global gridded dataset of the surface ocean carbonate system for

1881 seasonal to decadal studies of ocean acidification (v2023) (NCEI Accession 0220059), NOAA National Centers for  
1882 Environmental Information, Dataset, <https://doi.org/10.25921/m5wx-ja34>, 2020.

1883 Gregor, L., and Gruber, N.: Oceansoda-ETHZ: A global gridded data set of the surface ocean carbonate system for  
1884 seasonal to decadal studies of ocean acidification, *Earth System Science Data*, 13(2), 777–808,  
1885 <https://doi.org/10.5194/essd-13-777-2021>, 2021.

1886 Gregor, L., and Gruber, N.: OceanSODA-ETHZ: A global gridded dataset of the surface ocean carbonate system for  
1887 seasonal to decadal studies of ocean acidification (v2023) (NCEI accession 0220059) [Dataset], NOAA National  
1888 Centers for Environmental Information, <https://doi.org/10.25921/m5wx-ja34>, 2023.

1889 Gregor, L., Shutler, J., and Gruber, N.: High-resolution variability of the Ocean Carbon Sink, *Global  
1890 Biogeochemical Cycles*, 38(8), <https://doi.org/10.1029/2024gb008127>, 2024a.

1891 Gregor, L., Shutler, J., and Gruber, N.: OceanSODA-ETHZ-v2: Surface ocean sea-air CO<sub>2</sub> fluxes from 1982 to 2022  
1892 (8-day by 0.25° x 0.25°) (v2.2024r01), [Data set], Zenodo, <https://zenodo.org/records/11206366>, 2024b.

1893 Gruber, N., Clement, D., Carter, B. R., Feely, R. A., van Heuven, S., Hoppema, M., Ishii, M., Key, R. M., Kozyr,  
1894 A., Lauvset, S. K., Lo Monaco, C., Mathis, J. T., Murata, A., Olsen, A., Perez, F. F., Sabine, C. L., Tanhua, T., and  
1895 Wanninkhof, R.: The oceanic sink for anthropogenic CO<sub>2</sub> from 1994 to 2007, *Science*, 363(6432), 1193–1199,  
1896 <https://doi.org/10.1126/science.aau5153>, 2019a.

1897 Gruber, N., Clement, D., Carter, B. R., Feely, R. A., van Heuven, S., Hoppema, M., Ishii, M., Key, R. M., Kozyr,  
1898 A., Lauvset, S. K., Lo Monaco, C., Mathis, J. T., Murata, A., Olsen, A., Perez, F. F., Sabine, C. L., Tanhua, T., and  
1899 Wanninkhof, R.: The oceanic sink for anthropogenic CO<sub>2</sub> from 1994 to 2007 - the data (NCEI Accession 0186034),  
1900 NOAA National Centers for Environmental Information, Dataset, <https://doi.org/10.25921/wdn2-pt10>, 2019b.

1901 Gruber, N., Bakker, D. C. E., DeVries, T., Gregor, L., Hauck, J., Landschützer, P., McKinley, G. A., and Müller, J.  
1902 D.: Trends and variability in the ocean carbon sink, *Nature Reviews Earth and Environment*, 4(2), 119–134,  
1903 <https://doi.org/10.1038/s43017-022-00381-x>, 2023.

1904 Hauck, J., Mayot, N., Landschützer, P., and Jersild, A.: Global Carbon Budget 2024, surface ocean fugacity of CO<sub>2</sub>  
1905 (*f*CO<sub>2</sub>) and air–sea CO<sub>2</sub> flux of individual global ocean biogeochemical models and surface ocean *f*CO<sub>2</sub>-based data-  
1906 products, Zenodo. <https://doi.org/10.5281/zenodo.14639761>, 2025.

1907 Hollitzer, H. A. L., Patara, L., Terhaar, J., and Oschlies, A.: Competing effects of wind and buoyancy forcing on  
1908 ocean oxygen trends in recent decades. *Nat Commun* 15, 9264. <https://doi.org/10.1038/s41467-024-53557-y>, 2024.

1909 Huguenin, M. F., Holmes, R. M., and England, M. H.: Drivers and distribution of global ocean heat uptake over the  
1910 last half century. *Nat Commun* 13, 4921. <https://doi.org/10.1038/s41467-022-32540-5>, 2022.

1911 Humphreys, M. P., Lewis, E. R., Sharp, J. D., and Pierrot, D.: PyCO2SYS v1.8: Marine carbonate system  
1912 calculations in Python, *Geoscientific Model Development*, 15(1), 15–43, <https://doi.org/10.5194/gmd-15-15-2022>,  
1913 2022.

1914 Iida, Y., Takatani, Y., Kojima, A., and Ishii, M.: Global trends of ocean CO<sub>2</sub> sink and ocean acidification: An  
1915 observation-based reconstruction of surface ocean inorganic carbon variables, *Journal of Oceanography*, 77(2), 323–  
1916 358, <https://doi.org/10.1007/s10872-020-00571-5>, 2021.

1917 IPCC: Climate Change 2023: Synthesis Report, Contribution of Working Groups I, II and III to the Sixth  
1918 Assessment Report of the Intergovernmental Panel on Climate Change [Core Writing Team, H. Lee and J. Romero  
1919 (eds.)], IPCC, Geneva, Switzerland, pp. 35-115, <https://doi.org/10.59327/IPCC/AR6-9789291691647>, 2023.

1920 Ishii, M., Kosugi, N., Sasano, D., Saito, S., Midorikawa, T., & Inoue, H. Y.: Ocean acidification off the south coast  
1921 of Japan: A result from time series observations of CO<sub>2</sub> Parameters from 1994 to 2008. *Journal of Geophysical*  
1922 *Research*, 116(C6), <https://doi.org/10.1029/2010jc006831>, 2011a.

1923 Ishii, M., Suzuki, T., and Key, R.: Pacific Ocean Interior Carbon Data Synthesis, PACIFICA, in Progress, PICES  
1924 Press, 19(1), 20-23, [https://www.pices.int/publications/pices\\_press/volume19/v19\\_n1/pp\\_20-23\\_PACIFICA\\_f.pdf](https://www.pices.int/publications/pices_press/volume19/v19_n1/pp_20-23_PACIFICA_f.pdf),  
1925 2011b.

1926 Jersild, A., Landschützer, P., Gruber, N., Bakker, D. C. E.: An observation-based global monthly gridded sea surface  
1927 pCO<sub>2</sub> and air–sea CO<sub>2</sub> flux product from 1982 onward and its monthly climatology (NCEI Accession 0160558),  
1928 NOAA National Centers for Environmental Information, Dataset, <https://doi.org/10.7289/v5z899n6>, 2017.

1929 Jiang, L.-Q., Feely, R. A., Carter, B. R., Greeley, D. J., Gledhill, D. K., and Arzayus, K. M.: Climatological  
1930 distribution of aragonite saturation state in the global oceans, *Global Biogeochemical Cycles*, 29(10), 1656–1673,  
1931 <https://doi.org/10.1002/2015GB005198>, 2015a.

1932 Jiang, L.-Q., Feely, R. A.: Aragonite saturation state gridded to 1x1 degree latitude and longitude at depth levels of 0,  
1933 50, 100, 200, 500, 1000, 2000, 3000, and 4000 meters in the global oceans (NCEI Accession 0139360), NOAA  
1934 National Centers for Environmental Information, Dataset, <https://doi.org/10.7289/v5q81b4p>, 2015b.

1935 Jiang, L.-Q., Carter, B. R., Feely, R. A., Lauvset, S., and Olsen, A.: Surface ocean pH and buffer capacity: Past,  
1936 present and future, *Scientific Reports*, 9(1), 18624, <https://doi.org/10.1038/s41598-019-55039-4>, 2019a.

1937 Jiang, L.-Q., Carter, B. R., Feely, R. A., Lauvset, S., and Olsen, A.: Global surface ocean pH, acidity, and Revelle  
1938 Factor on a 1x1 degree global grid from 1770 to 2100 (NCEI Accession 0206289), NOAA National Centers for  
1939 Environmental Information, Dataset, <https://doi.org/10.25921/kgqr-9h49>, 2019b.

1940 Jiang, L.-Q., Feely, R. A., Wanninkhof, R., Greeley, D., Barbero, L., Alin, S., Carter, B. R., Pierrot, D.,  
1941 Featherstone, C., Hooper, J., Melrose, C., Monacchi, N., Sharp, J. D., Shellito, S., Xu, Y.-Y., Kozyr, A., Byrne, R. H.,

1942 Cai, W.-J., Cross, J., Johnson, G. C., Hales, B., Langdon, C., Mathis, J., Salisbury, J., and Townsend, D. W.: Coastal  
1943 Ocean Data Analysis Product in North America (CODAP-NA, Version 2021) (NCEI Accession 0219960), NOAA  
1944 National Centers for Environmental Information, Dataset. <https://doi.org/10.25921/531n-c230>, 2020.

1945 Jiang, L.-Q., Feely, R. A., Wanninkhof, R., Greeley, D., Barbero, L., Alin, S., Carter, B. R., Pierrot, D.,  
1946 Featherstone, C., Hooper, J., Melrose, C., Monacci, N., Sharp, J. D., Shellito, S., Xu, Y.-Y., Kozyr, A., Byrne, R. H.,  
1947 Cai, W.-J., Cross, J., Johnson, G. C., Hales, B., Langdon, C., Mathis, J., Salisbury, J., and Townsend, D. W.: Coastal  
1948 Ocean Data Analysis Product in North America (CODAP-NA) – an internally consistent data product for discrete  
1949 inorganic carbon, oxygen, and nutrients on the North American ocean margins, *Earth Syst. Sci. Data*, 13, 2777–  
1950 2799, <https://doi.org/10.5194/essd-13-2777-2021>, 2021.

1951 Jiang, L.-Q., Pierrot, D., Wanninkhof, R., Feely, R. A., Tilbrook, B., Alin, S., Barbero, L., Byrne, R. H., Carter, B.  
1952 R., Dickson, A. G., Gattuso, J.-P., Greeley, D., Hoppema, M., Humphreys, M. P., Karstensen, J., Lange, N.,  
1953 Lauvset, S. K., Lewis, E. R., Olsen, A., Perez, F. F., Sabine, C., Sharp, J. D., Tanhua, T., Trull, T. W., Velo, A.,  
1954 Allegra, A. J., Barker, P., Burger, E., Cai, W.-J., Chen, C.-T. A., Cross, J., Garcia, H., Hernandez-Ayon, J. M., Hu,  
1955 X., Kozyr, A., Langdon, C., Lee, K., Salisbury, J., Wang, Z. A., and Xue, L.: Best practice data standards for  
1956 discrete chemical oceanographic observations. *Frontiers in Marine Science*, 8,  
1957 <https://doi.org/10.3389/fmars.2021.705638>, 2022a.

1958 Jiang, L.-Q., Boyer, T. P., Paver, C. R., Yoo, H., Reagan, J. R., Alin, S. R., Barbero, L., Carter, B. R., Feely, R. A.,  
1959 and Wanninkhof, R.: Climatological distribution of ocean acidification indicators from surface to 500 meters water  
1960 depth on the North American ocean margins from 2003-12-06 to 2018-11-22 (NCEI Accession 0270962), NOAA  
1961 National Centers for Environmental Information, Dataset, <https://doi.org/10.25921/g8pb-zy76>, 2022b.

1962 Jiang, L., Dunne, J., Carter, B. R., Tjiputra, J. F., Terhaar, J., Sharp, J. D., Olsen, A., Alin, S., Bakker, D. C., Feely,  
1963 R. A., Gattuso, J., Hogan, P., Ilyina, T., Lange, N., Lauvset, S. K., Lewis, E. R., Lovato, T., Palmieri, J., Santana-  
1964 Falcón, Y., Schwinger, J., Séférian, R., Strand, G., Swart, N., Tanhua, T., Tsujino, H., Wanninkhof, R., Watanabe,  
1965 M., Yamamoto, A., and Ziehn, T.: Global surface ocean acidification indicators from 1750 to 2100 (NCEI  
1966 Accession 0259391), NOAA National Centers for Environmental Information, Dataset,  
1967 <https://doi.org/10.25921/9ker-bc48>, 2022c.

1968 Jiang, L., Dunne, J., Carter, B. R., Tjiputra, J. F., Terhaar, J., Sharp, J. D., Olsen, A., Alin, S., Bakker, D. C., Feely,  
1969 R. A., Gattuso, J., Hogan, P., Ilyina, T., Lange, N., Lauvset, S. K., Lewis, E. R., Lovato, T., Palmieri, J., Santana-  
1970 Falcón, Y., Schwinger, J., Séférian, R., Strand, G., Swart, N., Tanhua, T., Tsujino, H., Wanninkhof, R., Watanabe,  
1971 M., Yamamoto, A., and Ziehn, T.: Global surface ocean acidification indicators from 1750 to 2100, *Journal of*  
1972 *Advances in Modeling Earth Systems*, 15(3), <https://doi.org/10.1029/2022ms003563>, 2023.

1973 Jiang, L.-Q., Boyer, T. P., Paver, C. R., Yoo, H., Reagan, J. R., Alin, S. R., Barbero, L., Carter, B. R., Feely, R. A.,  
1974 and Wanninkhof, R.: Climatological distribution of ocean acidification variables along the North American ocean

1975 margins, *Earth System Science Data*, 16(7), 3383–3390, <https://doi.org/10.5194/essd-16-3383-2024>, 2024.

1976 John, S. G., Liang, H., Weber, T., DeVries, T., Primeau, F., Moore, K., Holzer, M., Mahowald, N., Gardner, W.,  
1977 Mishonov, A., Richardson, M. J., Faugere, Y., & Taburet, G.: Awesome OCIM: A simple, flexible, and powerful  
1978 tool for modeling elemental cycling in the oceans. *Chemical Geology*, 533, 119403.  
1979 <https://doi.org/10.1016/j.chemgeo.2019.119403>, 2020.

1980 Johnson, G. C., Robbins, P. E., and Hufford, G. E. (2001). Systematic adjustments of hydrographic sections for  
1981 internal consistency. *Journal of Atmospheric and Oceanic Technology*, 18(7), 1234–1244, 2001.

1982 Joshi, A. P., Ghoshal, P. K., Chakraborty, K., and Sarma, V. V. S. S.: Sea-surface  $p\text{CO}_2$  maps for the Bay of Bengal  
1983 based on Advanced Machine Learning Algorithms, *Scientific Data*, 11(1), [https://doi.org/10.1038/s41597-024-](https://doi.org/10.1038/s41597-024-03236-w)  
1984 [03236-w](https://doi.org/10.1038/s41597-024-03236-w), 2024.

1985 Joshi, A. P.; Ghoshal, P. K.; Chakraborty, K.; Sarma, V. V. S. S.: Sea-surface  $p\text{CO}_2$  maps for the Bay of  
1986 Bengal based on advanced machine learning algorithms from 2015-01-01 to 2015-12-31 (NCEI Accession  
1987 0307627). NOAA National Centers for Environmental Information. Dataset. <https://doi.org/10.25921/2sjr-pg16>,  
1988 2025a.

1989 Joshi, A. P., Ghoshal, P. K., Chakraborty, K., Roy, R., Jayaram, C., Sridevi, B., and Sarma, V. V. S. S.: Long-term  
1990 changes of surface total alkalinity and its driving mechanisms in the north Indian Ocean. *Global Biogeochemical*  
1991 *Cycles*, 39, e2024GB008344, <https://doi.org/10.1029/2024GB008344>, 2025b.

1992 Joshi, A. P.; Ghoshal, P. K.; Chakraborty, K.; Roy, R.; Jayaram, C.; Sridevi, B.; Sarma, V. V. S. S.: Long-term  
1993 changes of surface total alkalinity and its driving mechanisms in the Northern Indian Ocean from 1993-01-01 to  
1994 2020-12-31 (NCEI Accession 0307789). NOAA National Centers for Environmental Information. Dataset.  
1995 <https://doi.org/10.25921/7as7-et15>, 2025c.

1996 Kapsenberg, L., Alliouane, S., Gazeau, F., Mousseau, L., and Gattuso, J.-P.: Coastal ocean acidification and  
1997 increasing total alkalinity in the northwestern Mediterranean Sea, *Ocean Sci.*, 13, 411–426,  
1998 <https://doi.org/10.5194/os-13-411-2017>, 2017.

1999 Karl, D. M., and Lukas, R.: The Hawaii Ocean Time-series (HOT) program: Background, rationale and field  
2000 implementation, *Deep Sea Research Part II*, 43(2–3), 129–156, [https://doi.org/10.1016/0967-0645\(96\)00005-7](https://doi.org/10.1016/0967-0645(96)00005-7),  
2001 1996.

2002 Karl, D., Dore, J., Lukas, R., Michaels, A., Bates, N., and Knap, A.: Building the long-term picture: The U.S.  
2003 JGOFS Time-series programs. *Oceanography*, 14(4), 6–17, <https://doi.org/10.5670/oceanog.2001.02>, 2001.

2004 Kennedy, E. G., Zulian, M., Hamilton, S. L., Hill, T. M., Delgado, M., Fish, C. R., Gaylord, B., Kroeker, K. J.,  
2005 Palmer, H. M., Ricart, A. M., Sanford, E., Spalding, A. K., Ward, M., Carrasco, G., Elliott, M., Grisby, G. V.,

2006 Harris, E., Jahncke, J., Rocheleau, C. N., Westerink, S., and Wilmot, M. I.: Multistressor Observations of Coastal  
2007 Hypoxia and Acidification (MOCHA) Synthesis (NCEI Accession 0277984), NOAA National Centers for  
2008 Environmental Information, Dataset, <https://doi.org/10.25921/2vve-fh39>, 2023.

2009 Kennedy, E. G., Zulian, M., Hamilton, S. L., Hill, T. M., Delgado, M., Fish, C. R., Gaylord, B., Kroeker, K. J.,  
2010 Palmer, H. M., Ricart, A. M., Sanford, E., Spalding, A. K., Ward, M., Carrasco, G., Elliott, M., Grisby, G. V.,  
2011 Harris, E., Jahncke, J., Rocheleau, C. N., Westerink, S., and Wilmot, M. I.: A high-resolution synthesis dataset for  
2012 multistressor analyses along the US West Coast, *Earth Syst. Sci. Data*, 16, 219–243, <https://doi.org/10.5194/essd->  
2013 16-219-2024, 2024.

2014 Keppler, L., Landschützer, P., Gruber, N., Lauvset, S. K., and Stemmler, I.: Seasonal carbon dynamics in the near-  
2015 global ocean, *Global Biogeochemical Cycles*, 34(12), e2020GB006571, <https://doi.org/10.1029/2020GB006571>,  
2016 2020.

2017 Keppler, L., Landschützer, P., Lauvset, S. K., and Gruber, N.: Recent trends and variability in the oceanic storage of  
2018 dissolved inorganic carbon, *Global Biogeochemical Cycles*, 37(5), <https://doi.org/10.1029/2022gb007677>, 2023a.

2019 Keppler, L.; Landschützer, P.; Lauvset, S. K.; and Gruber, N.: Mapped Observation-Based Oceanic Dissolved  
2020 Inorganic Carbon Monthly fields from 2004 through 2019 (MOBO-DIC2004-2019) (NCEI Accession 0277099).  
2021 NOAA National Centers for Environmental Information. Dataset. <https://doi.org/10.25921/z31n-3m26>, 2023b.

2022 Key, R. M., Kozyr, A., Sabine, C. L., Lee, K., Wanninkhof, R., Bullister, J. L., Feely, R. A., Millero, F. J., Mordy,  
2023 C., and Peng, T. -H.: A global ocean carbon climatology: Results from Global Data Analysis Project (GLODAP),  
2024 *Global Biogeochemical Cycles*, 18(4), <https://doi.org/10.1029/2004gb002247>, 2004.

2025 Key, R. M., Tanhua, T., Olsen, A., Hoppema, M., Jutterström, S., Schirnick, C., van Heuven, S., Kozyr, A., Lin, X.,  
2026 Velo, A., Wallace, D. W. R., and Mintrop, L.: The CARINA data synthesis project: introduction and overview,  
2027 *Earth Syst. Sci. Data*, 2, 105–121, <https://doi.org/10.5194/essd-2-105-2010>, 2010.

2028 Key, R. M., Olsen, A., van Heuven, S., Lauvset, S. K., Velo, A., Lin, X., Schirnick, C., Kozyr, A., Tanhua, T.,  
2029 Hoppema, M., Jutterström, S., Steinfeldt, R., Jeansson, E., Ishi, M., Perez, F. F., and Suzuki, T.: Global Ocean Data  
2030 Analysis Project, Version 2 (GLODAPv2), ORNL/CDIAC-162, ND-P093, Ocean Carbon and Acidification Data  
2031 System, National Centers for Environmental Information, Silver Spring, Maryland,  
2032 [https://www.ncei.noaa.gov/access/ocean-carbon-acidification-data-system/oceans/GLODAPv2/NDP\\_093.pdf](https://www.ncei.noaa.gov/access/ocean-carbon-acidification-data-system/oceans/GLODAPv2/NDP_093.pdf), 2015.

2033 Kheshgi, H. S.: Sequestering atmospheric carbon dioxide by increasing ocean alkalinity, *Energy*, 20(9), 915–922,  
2034 [https://doi.org/10.1016/0360-5442\(95\)00035-f](https://doi.org/10.1016/0360-5442(95)00035-f), 1995.

2035 Knor, L. A. C. M., Sabine, C. L., Sutton, A. J., White, A. E., Potemra, J., and Weller, R. A.: Quantifying net  
2036 community production and calcification at Station ALOHA near Hawai'i: Insights and limitations from a dual tracer

2037 carbon budget approach, *Global Biogeochemical Cycles*, 37, e2022GB007672,  
2038 <https://doi.org/10.1029/2022GB007672>, 2023.

2039 Knor, L. A. C. M., Sabine, C. L., Dore, J. E., White, A. E., and Potemra, J.: Drivers and variability of intensified  
2040 subsurface ocean acidification trends at Station ALOHA, *Journal of Geophysical Research: Oceans*, 130,  
2041 e2024JC022251, <https://doi.org/10.1029/2024JC022251>, 2025.

2042 Kwiatkowski, L., Torres, O., Bopp, L., Aumont, O., Chamberlain, M., Christian, J. R., Dunne, J. P., Gehlen, M.,  
2043 Ilyina, T., John, J. G., Lenton, A., Li, H., Lovenduski, N. S., Orr, J. C., Palmieri, J., Santana-Falcón, Y., Schwinger,  
2044 J., Séférian, R., Stock, C. A., Tagliabue, A., Takano, Y., Tjiputra, J., Toyama, K., Tsujino, H., Watanabe, M.,  
2045 Yamamoto, A., Yool, A., and Ziehn, T.: Twenty-first century ocean warming, acidification, deoxygenation, and  
2046 upper-ocean nutrient and primary production decline from CMIP6 model projections, *Biogeosciences*, 17, 3439–  
2047 3470, <https://doi.org/10.5194/bg-17-3439-2020>, 2020.

2048 Landschützer, P., Gruber, N., Bakker, D. C. E., Schuster, U., Nakaoka, S., Payne, M. R., Sasse, T., and Zeng, J.: A  
2049 neural network-based estimate of the seasonal to inter-annual variability of the Atlantic Ocean carbon sink,  
2050 *Biogeosciences*, 10, 7793–7815, <https://doi.org/10.5194/bg-10-7793-2013>, 2013.

2051 Landschützer, P., Gruber, N., Bakker, D. C. E., and Schuster, U.: Recent variability of the Global Ocean Carbon  
2052 Sink, *Global Biogeochemical Cycles*, 28(9), 927–949, <https://doi.org/10.1002/2014gb004853>, 2014.

2053 Landschützer, P., Gruber, N., and Bakker, D. C. E.: Decadal variations and trends of the Global Ocean Carbon Sink,  
2054 *Global Biogeochemical Cycles*, 30(10), 1396–1417. <https://doi.org/10.1002/2015gb005359>, 2016.

2055 Landschützer, P., Laruelle, G. G., Roobaert, A., and Regnier, P.: A uniform  $p\text{CO}_2$  climatology combining open and  
2056 coastal oceans, *Earth Syst. Sci. Data*, 12, 2537–2553, <https://doi.org/10.5194/essd-12-2537-2020>, 2020a.

2057 Landschützer, P., Laruelle, G. G., Roobaert, A., and Regnier, P.: A combined global ocean  $p\text{CO}_2$  climatology  
2058 combining open ocean and coastal areas (NCEI Accession 0209633), NOAA National Centers for Environmental  
2059 Information, Dataset, <https://doi.org/10.25921/qb25-f418>, 2020b.

2060 Lange, N., Tanhua, T., Pfeil, B., Bange, H. W., Lauvset, S. K., Grégoire, M., Bakker, D. C., Jones, S. D., Fiedler, B.,  
2061 O'Brien, K. M., and Körtzinger, A.: A status assessment of selected data synthesis products for ocean  
2062 biogeochemistry, *Frontiers in Marine Science*, 10, <https://doi.org/10.3389/fmars.2023.1078908>, 2023.

2063 Lange, N., Fiedler, B., Álvarez, M., Benoit-Cattin, A., Benway, H., Buttigieg, P. L., Coppola, L., Currie, K., Flecha,  
2064 S., Gerlach, D. S., Honda, M., Huertas, I. E., Lauvset, S. K., Muller-Karger, F., Körtzinger, A., O'Brien, K. M.,  
2065 Ólafsdóttir, S. R., Pacheco, F. C., Rueda-Roa, D., Skjelvan, I., Wakita, M., White, A., and Tanhua, T.: Synthesis  
2066 product for ocean time series (spots) – a ship-based biogeochemical pilot, *Earth System Science Data*, 16(4), 1901–  
2067 1931, <https://doi.org/10.5194/essd-16-1901-2024>, 2024a.

2068 Lange, N., Fiedler, B., Álvarez, M., Benoit-Cattin, A., Benway, H., Buttigieg, P. L., Coppola, L., Currie, K. I.,  
2069 Flecha, S., Gerlach, D. S., Honda, M. C., Huertas, E. I., Kinkade, D., Muller-Karger, F., Lauvset, S. K., Körtzinger,  
2070 A., O'Brien, K. M., Ólafsdóttir, S., Pacheco, F. C., Rueda-Roa, D., Skjelvan, I., Wakita, M., White, A. E., Tanhua,  
2071 T.: Synthesis Product for Ocean Time Series (SPOTS), Biological and Chemical Oceanography Data Management  
2072 Office (BCO-DMO), (Version 2) Version Date 2024-02-22, <https://doi.org/10.26008/1912/bco-dmo.896862.2>,  
2073 2024b.

2074 Laruelle, G. G., Landschützer, P., Gruber, N., Tison, J.-L., Delille, B., and Regnier, P.: Global high-resolution  
2075 monthly  $p\text{CO}_2$  climatology for the coastal ocean derived from neural network interpolation, *Biogeosciences*, 14,  
2076 4545–4561, <https://doi.org/10.5194/bg-14-4545-2017>, 2017.

2077 Lauvset, S. K., and Tanhua, T.: A toolbox for secondary quality control on ocean chemistry and Hydrographic Data,  
2078 *Limnology and Oceanography: Methods*, 13(11), 601–608, <https://doi.org/10.1002/lom3.10050>, 2015.

2079 Lauvset, S. K., Key, R. M., Olsen, A., van Heuven, S., Velo, A., Lin, X., Schirnack, C., Kozyr, A., Tanhua, T.,  
2080 Hoppema, M., Jutterström, S., Steinfeldt, R., Jeansson, E., Ishii, M., Perez, F. F., Suzuki, T., and Watelet, S.: A new  
2081 global interior ocean mapped climatology: The  $1^\circ \times 1^\circ$  GLODAP version 2, *Earth System Science Data*, 8(2), 325–  
2082 340, <https://doi.org/10.5194/essd-8-325-2016>, 2016.

2083 Lauvset, S. K., Lange, N., Tanhua, T., Bittig, H. C., Olsen, A., Kozyr, A., Álvarez, M., Becker, S., Brown, P. J.,  
2084 Carter, B. R., Cotrim da Cunha, L., Feely, R. A., van Heuven, S., Hoppema, M., Ishii, M., Jeansson, E., Jutterström,  
2085 S., Jones, S. D., Karlsen, M. K., Lo Monaco, C., Michaelis, P., Murata, A., Pérez, F. F., Pfeil, B., Schirnack, C.,  
2086 Steinfeldt, R., Suzuki, T., Tilbrook, B., Velo, A., Wanninkhof, R., Woosley, R. J., and Key, R. M.: An updated  
2087 version of the global interior ocean biogeochemical data product, GLODAPv2.2021, *Earth Syst. Sci. Data*, 13,  
2088 5565–5589, <https://doi.org/10.5194/essd-13-5565-2021>, 2021.

2089 Lauvset, S. K., Lange, N., Tanhua, T., Bittig, H. C., Olsen, A., Kozyr, A., Alin, S., Álvarez, M., Azetsu-Scott, K.,  
2090 Barbero, L., Becker, S., Brown, P. J., Carter, B. R., da Cunha, L. C., Feely, R. A., Hoppema, M., Humphreys, M. P.,  
2091 Ishii, M., Jeansson, E., Jiang, L.-Q., Jones, S. D., Lo Monaco, C., Murata, A., Müller, J. D., Pérez, F. F., Pfeil, B.,  
2092 Schirnack, C., Steinfeldt, R., Suzuki, T., Tilbrook, B., Ulfso, A., Velo, A., Woosley, R. J., and Key, R. M.:  
2093 GLODAPv2.2022: the latest version of the global interior ocean biogeochemical data product, *Earth Syst. Sci. Data*,  
2094 14, 5543–5572, <https://doi.org/10.5194/essd-14-5543-2022>, 2022.

2095 Lauvset, S. K., Key, R. M., Olsen, A., van Heuven, S. M. A. C., Velo, A., Lin, X., Schirnack, C., Kozyr, A., Tanhua,  
2096 T., Hoppema, M., Jutterström, S., Steinfeldt, R., Jeansson, E., Ishii, M., Pérez, F. F., Suzuki, T., Watelet, S.: A new  
2097 global interior ocean mapped climatology: the  $1^\circ \times 1^\circ$  GLODAP version 2 from 1972-01-01 to 2013-12-31 (NCEI  
2098 Accession 0286118), NOAA National Centers for Environmental Information, Dataset,  
2099 [https://doi.org/10.3334/cdiac/otg.ndp093\\_glodapv2](https://doi.org/10.3334/cdiac/otg.ndp093_glodapv2), 2023a.

2100 Lauvset, S. K., Lange, N., Tanhua, T., Bittig, H. C., Olsen, A., Kozyr, A., Álvarez, M., Azetsu-Scott, K., Becker, S.,

2101 Brown, P. J., Carter, B. R., Cotrim da Cunha, L., Feely, R. A., Hoppema, M., Humphreys, M. P., Ishii, M., Jeansson,  
2102 E., Jones, S. D., Lo Monaco, C. Murata, A., Müller, J. D., Pérez, F. F., Schirmick, C., Steinfeldt, R., Suzuki, T.,  
2103 Tilbrook, B., Ulfsbo, A., Velo, A., Woosley, R. J., Key, R. M.: Global Ocean Data Analysis Project version 2.2023  
2104 (GLODAPv2.2023) (NCEI Accession 0283442), NOAA National Centers for Environmental Information, Dataset,  
2105 <https://doi.org/10.25921/zyrq-ht66>, 2023b.

2106 Lauvset, S. K., Lange, N., Tanhua, T., Bittig, H. C., Olsen, A., Kozyr, A., Álvarez, M., Azetsu-Scott, K., Brown, P.  
2107 J., Carter, B. R., Cotrim da Cunha, L., Hoppema, M., Humphreys, M. P., Ishii, M., Jeansson, E., Murata, A., Müller,  
2108 J. D., Pérez, F. F., Schirmick, C., Steinfeldt, R., Suzuki, T., Ulfsbo, A., Velo, A., Woosley, R. J., and Key, R. M.:  
2109 The annual update GLODAPv2.2023: the global interior ocean biogeochemical data product, *Earth Syst. Sci. Data*,  
2110 16, 2047–2072, <https://doi.org/10.5194/essd-16-2047-2024>, 2024.

2111 Lee, K., Tong, L. T., Millero, F. J., Sabine, C. L., Dickson, A. G., Goyet, C., Park, G., Wanninkhof, R., Feely, R. A.,  
2112 and Key, R. M.: Global relationships of total alkalinity with salinity and temperature in surface waters of the world's  
2113 oceans, *Geophysical Research Letters*, 33(19), <https://doi.org/10.1029/2006gl027207>, 2006.

2114 Lewis, E., and Wallace, D. W. R.: Program Developed for CO<sub>2</sub> System Calculations, ORNL/CDIAC-105, Carbon  
2115 Dioxide Information Analysis Center, Oak Ridge National Laboratory, Oak Ridge, TN, 1998.

2116 Locarnini, R. A., Mishonov, A. V., Antonov, J. I., Boyer, T. P., Garcia, H. E., Baranova, O. K., Zweng, M. M.,  
2117 Paver, C. R., Reagan, J. R., Johnson, D. R., Hamilton, M., and Seidov, D.: World Ocean Atlas 2013, Volume 1:  
2118 Temperature, edited by: Levitus, S. and Mishonov, A., NOAA Atlas NESDIS 73, 40 pp., 2013.

2119 Locarnini, R. A., Mishonov, A. V., Baranova, O. K., Boyer, T. P., Zweng, M. M., Garcia, H. E., Reagan, J. R.,  
2120 Seidov, D., Weathers, K. W., Paver, C. R., Smolyar, I. V.: World Ocean Atlas 2018, Volume 1: Temperature,  
2121 Mishonov, A. [Technical Editor], NOAA Atlas NESDIS 81, 2019.

2122 Ma, D., Gregor, L., and Gruber, N. (2023). Four decades of trends and drivers of global surface ocean acidification,  
2123 *Global Biogeochemical Cycles*, 37(7), <https://doi.org/10.1029/2023gb007765>, 2023.

2124 Manzello, D. P., Enochs, I. C., Hendee, J. C.: National Coral Reef Monitoring Program: Carbonate chemistry data  
2125 collected in the Atlantic Ocean, NOAA National Centers for Environmental Information, Dataset,  
2126 <https://doi.org/10.25921/vfz0-dg77>, 2018.

2127 Mercier, H., Desbruyères, D., Lherminier, P., Velo, A., Carracedo, L., Fontela, M., & Pérez, F. F.: New insights into  
2128 the eastern subpolar North Atlantic Meridional overturning circulation from OVIDE. *Ocean Science*, 20(3), 779–  
2129 797, <https://doi.org/10.5194/os-20-779-2024>, 2024.

2130 Metz, N., Tilbrook, B., Bakker, D., le Quéré, C., Doney, S., Feely, R., Hood, M., and Dargaville, R.: Surface Ocean  
2131 CO<sub>2</sub> variability and Vulnerability Workshop, Paris, France, 11–14 April 2007. *Eos, Transactions American*

**Deleted:** Lee, K., Kim, T.-W., Byrne, R. H., Millero, F. J., Feely, R. A., and Liu, Y.-M.: The universal ratio of boron to chlorinity for the North Pacific and North Atlantic oceans, *Geochimica et Cosmochimica Acta*, 74(6), 1801–1811, <https://doi.org/10.1016/j.gca.2009.12.027>, 2010. ¶

**Deleted:** Lueker, T. J., Dickson, A. G., and Keeling, C. D.: Ocean *p*CO<sub>2</sub> calculated from dissolved inorganic carbon, alkalinity, and equations for K<sub>1</sub> and K<sub>2</sub>: Validation based on laboratory measurements of CO<sub>2</sub> in gas and seawater at equilibrium, *Marine Chemistry*, 70(1–3), 105–119, [https://doi.org/10.1016/s0304-4203\(00\)00022-0](https://doi.org/10.1016/s0304-4203(00)00022-0), 2000. ¶

2143 Geophysical Union, 88(28), 287–287, <https://doi.org/10.1029/2007co280005>, 2007.

2144 Metz, Nicolas; Fin, Jonathan; Lo Monaco, Claire; Mignon, Claude; Alliouane, Samir; Antoine, David; Bourdin,  
2145 Guillaume; Boutin, Jacqueline; Bozec, Yann; Conan, Pascal; Coppola, Laurent; Diaz, Frédéric; Douville, Eric;  
2146 Durrieu de Madron, Xavier; Gattuso, Jean-Pierre; Gazeau, Frédéric; Golbol, Melek; Lansard, Bruno; Lefèvre,  
2147 Dominique; Lefèvre, Nathalie; Lombard, Fabien; Louanchi, Ferial; Merlivat, Liliane; Olivier, Léa; Petrenko, Anne;  
2148 Petton, Sébastien; Pujo-Pay, Mireille; Rabouille, Christophe; Reverdin, Gilles; Ridame, Céline; Tribollet, Aline;  
2149 Vellucci, Vincenzo; Wagener, Thibaut; Wimart-Rousseau, Cathy (2023). A synthesis of ocean total alkalinity and  
2150 dissolved inorganic carbon measurements in the Global Ocean and Mediterranean Sea from 1993 to 2022: the  
2151 SNAPO-CO2-v1 dataset (NCEI Accession 0285681). NOAA National Centers for Environmental Information.  
2152 Unpublished Dataset. <https://www.ncei.noaa.gov/archive/accession/0285681>, 2023.

2153 Metz, N., Fin, J., Lo Monaco, C., Mignon, C., Alliouane, S., Antoine, D., Bourdin, G., Boutin, J., Bozec, Y.,  
2154 Conan, P., Coppola, L., Diaz, F., Douville, E., Durrieu de Madron, X., Gattuso, J.-P., Gazeau, F., Golbol, M.,  
2155 Lansard, B., Lefèvre, D., Lefèvre, N., Lombard, F., Louanchi, F., Merlivat, L., Olivier, L., Petrenko, A., Petton, S.,  
2156 Pujo-Pay, M., Rabouille, C., Reverdin, G., Ridame, C., Tribollet, A., Vellucci, V., Wagener, T., and Wimart-  
2157 Rousseau, C.: A synthesis of ocean total alkalinity and dissolved inorganic carbon measurements from 1993 to  
2158 2022: the SNAPO-CO2-v1 dataset, *Earth Syst. Sci. Data*, 16, 89–120, <https://doi.org/10.5194/essd-16-89-2024>,  
2159 2024.

2160 Mishonov, A. V., Boyer, T. P., Baranova, O. K., Bouchard, C. N., Cross, S. L., Garcia H. E., Locarnini, R. A., Paver,  
2161 C. R., Wang, Z., Seidov, D., Grodsky, A. I., Beauchamp, J. G.: *World Ocean Database 2023*, C. Bouchard, Technical  
2162 Ed., NOAA Atlas NESDIS 97, 206 pp., <https://doi.org/10.25923/z885-h264>, 2024.

2163 Monacci, N. M., Cross, J. N., Danielson, S. L., Evans, W., Hopcroft, R. R., Mathis, J. T., Mordy, C. W., Naber, D.  
2164 D., Shake, K. L., Trahanovsky, K., Wang, H., Weingartner, T. J., Whitedge, T. E.: Marine carbonate system  
2165 discrete profile data from the Gulf of Alaska (GAK) Seward Line cruises between 2008 and 2017 (NCEI Accession  
2166 0277034). NOAA National Centers for Environmental Information. Dataset. <https://doi.org/10.25921/x9sg-9b08>,  
2167 2023.

2168 Monacci, N. M., Cross, J. N., Evans, W., Mathis, J. T., and Wang, H.: A decade of marine inorganic carbon  
2169 chemistry observations in the northern Gulf of Alaska – insights into an environment in transition, *Earth Syst. Sci.*  
2170 *Data*, 16, 647–665, <https://doi.org/10.5194/essd-16-647-2024>, 2024.

2171 Müller, J. D.: RECCAP2-ocean data collection, <https://doi.org/10.5281/zenodo.7990823>, 2023.

2172 Müller, J. D., Gruber, N., Carter, B., Feely, R., Ishii, M., Lange, N., Lauvset, S. K., Murata, A., Olsen, A., Pérez, F.  
2173 F., Sabine, C., Tanhua, T., Wanninkhof, R., and Zhu, D.: Decadal trends in the oceanic storage of anthropogenic  
2174 carbon from 1994 to 2014, *AGU Advances*, 4(4), <https://doi.org/10.1029/2023av000875>, 2023a.

2175 Müller, J. D.; Gruber, N.; Carter, B. R.; Feely, R. A.; Ishii, M.; Lange, N.; Lauvset, S. K.; Murata, A.; Olsen, A.;  
2176 Pérez, F. F.; Sabine, C. L.; Tanhua, T.; Wanninkhof, R.; Zhu, D.: Decadal Trends in the Oceanic Storage of  
2177 Anthropogenic Carbon from 1994 to 2014 (NCEI Accession 0279447). NOAA National Centers for Environmental  
2178 Information. Dataset. <https://doi.org/10.25921/ppcf-w020>, 2023b.

2179 Müller, J. D., and Gruber, N.: Progression of ocean interior acidification over the industrial era, *Science Advances*,  
2180 10(48), <https://doi.org/10.1126/sciadv.ado3103>, 2024a.

2181 Müller, J. D.; and Gruber, N.: Progression of Ocean Interior Acidification over the Industrial Era from 1800-07-01  
2182 to 2014-06-30 (NCEI Accession 0298993). NOAA National Centers for Environmental Information. Dataset.  
2183 <https://doi.org/10.25921/tefm-x802>, 2024b.

2184 Olsen, A., Key, R. M., van Heuven, S., Lauvset, S. K., Velo, A., Lin, X., Schirnick, C., Kozyr, A., Tanhua, T.,  
2185 Hoppema, M., Jutterström, S., Steinfeldt, R., Jeansson, E., Ishii, M., Pérez, F. F., and Suzuki, T.: The Global Ocean  
2186 Data Analysis Project version 2 (GLODAPv2) – an internally consistent data product for the world ocean, *Earth  
2187 Syst. Sci. Data*, 8, 297–323, <https://doi.org/10.5194/essd-8-297-2016>, 2016.

2188 Olsen, A., Lange, N., Key, R. M., Tanhua, T., Álvarez, M., Becker, S., Bittig, H. C., Carter, B. R., Cotrim da Cunha,  
2189 L., Feely, R. A., van Heuven, S., Hoppema, M., Ishii, M., Jeansson, E., Jones, S. D., Jutterström, S., Karlsen, M. K.,  
2190 Kozyr, A., Lauvset, S. K., Lo Monaco, C., Murata, A., Pérez, F. F., Pfeil, B., Schirnick, C., Steinfeldt, R., Suzuki,  
2191 T., Telszewski, M., Tilbrook, B., Velo, A., and Wanninkhof, R.: GLODAPv2.2019 – an update of GLODAPv2,  
2192 *Earth Syst. Sci. Data*, 11, 1437–1461, <https://doi.org/10.5194/essd-11-1437-2019>, 2019.

2193 Olsen, A., Lange, N., Key, R. M., Tanhua, T., Bittig, H. C., Kozyr, A., Álvarez, M., Azetsu-Scott, K., Becker, S.,  
2194 Brown, P. J., Carter, B. R., Cotrim da Cunha, L., Feely, R. A., van Heuven, S., Hoppema, M., Ishii, M., Jeansson,  
2195 E., Jutterström, S., Landa, C. S., Lauvset, S. K., Michaelis, P., Murata, A., Pérez, F. F., Pfeil, B., Schirnick, C.,  
2196 Steinfeldt, R., Suzuki, T., Tilbrook, B., Velo, A., Wanninkhof, R., and Woosley, R. J.: An updated version of the  
2197 global interior ocean biogeochemical data product, GLODAPv2.2020, *Earth Syst. Sci. Data*, 12, 3653–3678,  
2198 <https://doi.org/10.5194/essd-12-3653-2020>, 2020.

2199 Orr, J. C., Fabry, V. J., Aumont, O., Bopp, L., Doney, S. C., Feely, R. A., Gnanadesikan, A., Gruber, N., Ishida, A.,  
2200 Joos, F., Key, R. M., Lindsay, K., Maier-Reimer, E., Matear, R., Monfray, P., Mouchet, A., Najjar, R. G., Plattner,  
2201 G.-K., Rodgers, K. B., Sabine, C. L., Sarmiento, J. L., Schlitzer, R., Slater, R. D., Totterdell, I. J., Weirig, M.-F.,  
2202 Yamanaka, Y., and Yool, A.: Anthropogenic ocean acidification over the twenty-first century and its impact on  
2203 calcifying organisms, *Nature*, 437(7059), 681–686, <https://doi.org/10.1038/nature04095>, 2005.

2204 Orr, J. C., Epitalon, J.-M., and Gattuso, J.-P.: Comparison of ten packages that compute ocean carbonate chemistry,  
2205 *Biogeosciences*, 12, 1483–1510, <https://doi.org/10.5194/bg-12-1483-2015>, 2015.

2206 Orr, J. C., Epitalon, J.-M., Dickson, A. G., and Gattuso, J.-P.: Routine uncertainty propagation for the Marine

- 2207 Carbon Dioxide System, *Marine Chemistry*, 207, 84–107. <https://doi.org/10.1016/j.marchem.2018.10.006>, 2018.
- 2208 Oschlies, A., Bach, L. T., Fennel, K., Gattuso, J.-P., and Mengis, N.: Perspectives and challenges of marine carbon  
2209 dioxide removal, *Frontiers in Climate*, 6, <https://doi.org/10.3389/fclim.2024.1506181>, 2025.
- 2210 Padin, X. A., Velo, A., & Pérez, F. F.: Arios: A database for ocean acidification assessment in the Iberian Upwelling  
2211 System (1976–2018), *Earth System Science Data*, 12(4), 2647–2663, <https://doi.org/10.5194/essd-12-2647-2020>,  
2212 2020.
- 2213 Palacio-Castro, A. M., Enochs, I. C., Besemer, N., Boyd, A., Jankulak, M., Kolodziej, G., Hirsh, H. K., Webb, A. E.,  
2214 Towle, E. K., Kelble, C., Smith, I., and Manzello, D. P.: Coral Reef carbonate chemistry reveals interannual,  
2215 seasonal, and spatial impacts on ocean acidification off Florida, *Global Biogeochemical Cycles*, 37(12),  
2216 <https://doi.org/10.1029/2023gb007789>, 2023.
- 2217 Pérez, F. F., Fontela, M., García-Ibáñez, M. I., Mercier, H., Velo, A., Lherminier, P., Zunino, P., de la Paz, M.,  
2218 Alonso-Pérez, F., Guallart, E. F., & Padin, X. A.: Meridional overturning circulation conveys fast acidification to  
2219 the deep Atlantic Ocean. *Nature*, 554(7693), 515–518. <https://doi.org/10.1038/nature25493>, 2018.
- 2220 Pérez, F. F., Velo, A., Padin, X. A., Doval, M. D., and Prego, R.: ARIOS Database: An Acidification Ocean  
2221 Database for the Galician Upwelling Ecosystem, Instituto de Investigaciones Marinas, Consejo Superior de  
2222 Investigaciones Científicas (CSIC), <https://doi.org/10.20350/digitalCSIC/12498>, 2020.
- 2223 Pérez, F. F., Olafsson, J., Ólafsdóttir, S. R., Fontela, M., & Takahashi, T.: Contrasting drivers and trends of ocean  
2224 acidification in the Subarctic Atlantic. *Scientific Reports*, 11(1). <https://doi.org/10.1038/s41598-021-93324-3>, 2021.
- 2225 Pfeil, B., Olsen, A., Bakker, D. C. E., Hankin, S., Koyuk, H., Kozyr, A., Malczyk, J., Manke, A., Metzl, N., Sabine,  
2226 C. L., Akl, J., Alin, S. R., Bates, N., Bellerby, R. G. J., Borges, A., Boutin, J., Brown, P. J., Cai, W.-J., Chavez, F.  
2227 P., Chen, A., Cosca, C., Fassbender, A. J., Feely, R. A., González-Dávila, M., Goyet, C., Hales, B., Hardman-  
2228 Mountford, N., Heinze, C., Hood, M., Hoppema, M., Hunt, C. W., Hydes, D., Ishii, M., Johannessen, T., Jones, S.  
2229 D., Key, R. M., Körtzinger, A., Landschützer, P., Lauvset, S. K., Lefèvre, N., Lenton, A., Lourantou, A., Merlivat,  
2230 L., Midorikawa, T., Mintrop, L., Miyazaki, C., Murata, A., Nakadate, A., Nakano, Y., Nakaoka, S., Nojiri, Y.,  
2231 Omar, A. M., Padin, X. A., Park, G.-H., Paterson, K., Perez, F. F., Pierrot, D., Poisson, A., Ríos, A. F., Santana-  
2232 Casiano, J. M., Salisbury, J., Sarma, V. V. S. S., Schlitzer, R., Schneider, B., Schuster, U., Sieger, R., Skjelvan, I.,  
2233 Steinhoff, T., Suzuki, T., Takahashi, T., Tedesco, K., Telszewski, M., Thomas, H., Tilbrook, B., Tjiputra, J.,  
2234 Vandemark, D., Veness, T., Wanninkhof, R., Watson, A. J., Weiss, R., Wong, C. S., and Yoshikawa-Inoue, H.: A  
2235 uniform, quality controlled Surface Ocean CO<sub>2</sub> Atlas (SOCAT), *Earth Syst. Sci. Data*, 5, 125–143,  
2236 <https://doi.org/10.5194/essd-5-125-2013>, 2013.
- 2237 Qi, D., Chen, L., Chen, B., Gao, Z., Zhong, W., Feely, R. A., Anderson, L. G., Sun, H., Chen, J., Chen, M., Zhan,  
2238 L., Zhang, Y., & Cai, W.-J.: Increase in acidifying water in the Western Arctic ocean. *Nature Climate Change*, 7(3),

**Deleted:** Perez, F. F., and Fraga, F.: Association constant of fluoride and hydrogen ions in seawater. *Marine Chemistry*, 21(2), 161–168, [https://doi.org/10.1016/0304-4203\(87\)90036-3](https://doi.org/10.1016/0304-4203(87)90036-3), 1987. 

**Deleted:** o

**Deleted:** e

2244 195–199. <https://doi.org/10.1038/nclimate3228>, 2017.

2245 Qi, D., Ouyang, Z., Chen, L., Wu, Y., Lei, R., Chen, B., Feely, R. A., Anderson, L. G., Zhong, W., Lin, H.,  
2246 Polukhin, A., Zhang, Y., Zhang, Y., Bi, H., Lin, X., Luo, Y., Zhuang, Y., He, J., Chen, J. and Cai, W.-J.: Climate  
2247 change drives rapid decadal acidification in the Arctic Ocean from 1994 to 2020, *Science*, 377, 1544–1550,  
2248 doi:10.1126/science.abo0383, 2022.

2249 Resplandy, L., Hogikyan, A., Müller, J. D., Najjar, R. G., Bange, H. W., Bianchi, D., Weber, T., Cai, W. -J., Doney,  
2250 S. C., Fennel, K., Gehlen, M., Hauck, J., Lacroix, F., Landschützer, P., Le Quéré, C., Roobaert, A., Schwinger, J.,  
2251 Berthet, S., Bopp, L., Chau, T. T. T., Dai, M., Gruber, N., Ilyina, T., Kock, A., Manizza, M., Lachkar, Z., Laruelle,  
2252 G. G., Liao, E., Lima, I. D., Nissen, C., Rödenbeck, C., Séférian, R., Toyama, K., Tsujino, H., and Regnier, P.: A  
2253 synthesis of global coastal Ocean Greenhouse Gas Fluxes, *Global Biogeochemical Cycles*, 38(1),  
2254 <https://doi.org/10.1029/2023gb007803>, 2024.

2255 Revelle, R., and Suess, H. E.: Carbon dioxide exchange between atmosphere and ocean and the question of an  
2256 increase of atmospheric CO<sub>2</sub> during the past decades. *Tellus*, 9(1), 18–27, [https://doi.org/10.1111/j.2153-](https://doi.org/10.1111/j.2153-3490.1957.tb01849.x)  
2257 [3490.1957.tb01849.x](https://doi.org/10.1111/j.2153-3490.1957.tb01849.x), 1957.

2258 Rödenbeck, C., Keeling, R. F., Bakker, D. C., Metzl, N., Olsen, A., Sabine, C., and Heimann, M.: Global surface-  
2259 ocean pCO<sub>2</sub> and sea-air CO<sub>2</sub> flux variability from an observation-driven ocean mixed-layer scheme, *Ocean Science*,  
2260 9(2), 193–216, <https://doi.org/10.5194/os-9-193-2013>, 2013.

2261 Rödenbeck, Christian, DeVries, T., Hauck, J., Le Quéré, C., & Keeling, R. F.: Data-based estimates of interannual  
2262 sea-air CO<sub>2</sub> flux variations 1957-2020 and their relation to environmental drivers, *Biogeosciences*, 19(10), 2627–  
2263 2652, <https://doi.org/10.5194/bg-19-2627-2022>, 2022.

2264 Roobaert, A., Regnier, P., Landschützer, P., Laruelle, G. G.: A novel sea surface partial pressure of carbon dioxide  
2265 (pCO<sub>2</sub>) data product for the global coastal ocean resolving trends over the 1982-2020 period (NCEI Accession  
2266 0279118), NOAA National Centers for Environmental Information, Dataset, <https://doi.org/10.25921/4sde-p068>,  
2267 2023.

2268 Roobaert, A., Regnier, P., Landschützer, P., and Laruelle, G. G.: A novel sea surface pCO<sub>2</sub>-product for the global  
2269 coastal ocean resolving trends over 1982–2020, *Earth System Science Data*, 16(1), 421–441,  
2270 <https://doi.org/10.5194/essd-16-421-2024>, 2024.

2271 Sabine, C. L., Feely, R. A., Gruber, N., Key, R. M., Lee, K., Bullister, J. L., Wanninkhof, R., Wong, C. S., Wallace,  
2272 D. W., Tilbrook, B., Millero, F. J., Peng, T.-H., Kozyr, A., Ono, T., and Rios, A. F.: The oceanic sink for  
2273 anthropogenic CO<sub>2</sub>, *Science*, 305(5682), 367–371, <https://doi.org/10.1126/science.1097403>, 2004a.

2274 Sabine, C. L., Feely, R. A., Key, R. M., Wanninkhof, R., Millero, F. J., Kozyr, A.: GLobal Ocean Data Analysis

2275 Project (GLODAP) version 1.1 (NCEI Accession 0001644). NOAA National Centers for Environmental  
2276 Information. Dataset. <https://doi.org/10.25921/pkjs-5w29>, 2004b.

2277 Sabine, C. L., Key, R. M., Kozyr, A., Feely, R. A., Wanninkhof, R., Millero, F. J., Peng, T.-H., Bullister, J. L., and  
2278 Lee, K.: Global Ocean Data Analysis Project (GLODAP): Results and data. ORNL/CDIAC-145, NDP-083, Carbon  
2279 Dioxide Information Analysis Center, Oak Ridge National Laboratory, U.S. Department of Energy, Oak Ridge, TN,  
2280 110 pp. plus 6 Appendices, 2005.

2281 Sabine, C. L., Feely, R. A., Millero, F. J., Dickson, A. G., Langdon, C., Mecking, S., and Greeley, D.: Decadal  
2282 changes in Pacific Carbon, *Journal of Geophysical Research: Oceans*, 113(C7),  
2283 <https://doi.org/10.1029/2007jc004577>, 2008.

2284 Sabine, C. L., Hankin, S., Koyuk, H., Bakker, D. C. E., Pfeil, B., Olsen, A., Metzl, N., Kozyr, A., Fassbender, A.,  
2285 Manke, A., Malczyk, J., Akl, J., Alin, S. R., Bellerby, R. G. J., Borges, A., Boutin, J., Brown, P. J., Cai, W.-J.,  
2286 Chavez, F. P., Chen, A., Cosca, C., Feely, R. A., González-Dávila, M., Goyet, C., Hardman-Mountford, N., Heinze,  
2287 C., Hoppema, M., Hunt, C. W., Hydes, D., Ishii, M., Johannessen, T., Key, R. M., Körtzinger, A., Landschützer, P.,  
2288 Lauvset, S. K., Lefèvre, N., Lenton, A., Lourantou, A., Merlivat, L., Midorikawa, T., Mintrop, L., Miyazaki, C.,  
2289 Murata, A., Nakadate, A., Nakano, Y., Nakaoka, S., Nojiri, Y., Omar, A. M., Padin, X. A., Park, G.-H., Paterson, K.,  
2290 Perez, F. F., Pierrot, D., Poisson, A., Ríos, A. F., Salisbury, J., Santana-Casiano, J. M., Sarma, V. V. S. S., Schlitzer,  
2291 R., Schneider, B., Schuster, U., Sieger, R., Skjelvan, I., Steinhoff, T., Suzuki, T., Takahashi, T., Tedesco, K.,  
2292 Telszewski, M., Thomas, H., Tilbrook, B., Vandemark, D., Veness, T., Watson, A. J., Weiss, R., Wong, C. S., and  
2293 Yoshikawa-Inoue, H.: Surface Ocean CO<sub>2</sub> Atlas (SOCAT) gridded data products, *Earth Syst. Sci. Data*, 5, 145–153,  
2294 <https://doi.org/10.5194/essd-5-145-2013>, 2013.

2295 Sarma, V. V. S. S., Krishna, M. S., Paul, Y. S., and Murty, V. S. N.: Observed changes in ocean acidity and carbon  
2296 dioxide exchange in the coastal bay of Bengal—A link to air pollution, *Tellus B: Chemical and Physical  
2297 Meteorology*, 67(1), 24638, <https://doi.org/10.3402/tellusb.v67.24638>, 2015.

2298 Schimel, D. S., and Carroll, D.: Carbon cycle–climate feedbacks in the post-paris world, *Annual Review of Earth  
2299 and Planetary Sciences*, 52(1), <https://doi.org/10.1146/annurev-earth-031621-081700>, 2024.

2300 Schoderer, M., Bittig, H., Klein, B., Hägele, R., Steinhoff, T., Castro-Morales, K., Cotrim da Cunha, L., Hornidge,  
2301 A., and Körtzinger, A.: From individual observations to global assessments: Tracing the Marine Carbon Knowledge  
2302 Value Chain, *Ocean and Society*, 2, <https://doi.org/10.17645/oas.8891>, 2024.

2303 Sharp, J. D., Pierrot, D., Humphreys, M. P., Epitalon, J.-M., Orr, J. C., Lewis, E. R., Wallace, D. W. R.: CO<sub>2</sub>SYsv3  
2304 for MATLAB (Version v3.2.1), Zenodo, <http://doi.org/10.5281/zenodo.3950562>, 2023.

2305 Sharp, J. D., Jiang, L.-Q., Carter, B. R., Lavin, P. D., Yoo, H., and Cross, S. L.: A mapped dataset of surface ocean  
2306 acidification indicators in large marine ecosystems of the United States, *Sci. Data*, 11, 715,

2307 <https://doi.org/10.1038/s41597-024-03530-7>, 2024a.

2308 Sharp, J. D., Jiang, L-Q., Carter, B. R., Lavin, P. D., Yoo, H., Cross, S. L. RFR-LME Ocean Acidification Indicators  
2309 from 1998 to 2023 (NCEI Accession 0287551). NOAA National Centers for Environmental Information. Dataset.  
2310 <https://doi.org/10.25921/h8vw-e872>, 2024b.

2311 Sridevi, B., and Sarma, V. V. S. S.: Role of river discharge and warming on ocean acidification and pco2 levels in  
2312 the Bay of Bengal, *Tellus B: Chemical and Physical Meteorology*, 73 (1), 1–20,  
2313 <https://doi.org/10.1080/16000889.2021.1971924>, 2021.

2314 Sutton, A. J., Feely, R. A., Maenner-Jones, S., Musielwicz, S., Osborne, J., Dietrich, C., Monacci, N., Cross, J.,  
2315 Bott, R., Kozyr, A.: Autonomous seawater partial pressure of carbon dioxide (pCO<sub>2</sub>) and pH time series from 40  
2316 surface buoys between 2004 and 2017 (NCEI Accession 0173932), NOAA National Centers for Environmental  
2317 Information, Dataset, <https://doi.org/10.7289/v5db8043>, 2018.

2318 Sutton, A. J., Feely, R. A., Maenner-Jones, S., Musielwicz, S., Osborne, J., Dietrich, C., Monacci, N., Cross, J.,  
2319 Bott, R., Kozyr, A., Andersson, A. J., Bates, N. R., Cai, W.-J., Cronin, M. F., De Carlo, E. H., Hales, B., Howden, S.  
2320 D., Lee, C. M., Manzello, D. P., McPhaden, M. J., Meléndez, M., Mickett, J. B., Newton, J. A., Noakes, S. E., Noh,  
2321 J. H., Olafsdottir, S. R., Salisbury, J. E., Send, U., Trull, T. W., Vandemark, D. C., and Weller, R. A.: Autonomous  
2322 seawater pCO<sub>2</sub> and pH time series from 40 surface buoys and the emergence of anthropogenic trends, *Earth Syst.*  
2323 *Sci. Data*, 11, 421–439, <https://doi.org/10.5194/essd-11-421-2019>, 2019.

2324 Suzuki, T., Ishii, M., Aoyama, M., Christian, J. R., Enyo, K., Kawano, T., Key, R. M., Kosugi, N., Kozyr, A.,  
2325 Miller, L. A., Murata, A., Nakano, T., Ono, T., Saino, T., Sasaki, K., Sasano, D., Takatani, Y., Wakita, M., Sabine,  
2326 C. L. The Pacific Ocean Interior Carbon (PACIFICA) Database (NCEI Accession 0110865). NOAA National  
2327 Centers for Environmental Information. Dataset. <https://doi.org/10.25921/n9nn-8324>, 2013.

2328 Swift, J. (2022), Quality Edited Hydrographic Data, [https://joa.ucsd.edu/Data\\_homepage](https://joa.ucsd.edu/Data_homepage) (Last accessed: 2025-02-  
2329 08).

2330 Takahashi, T., Feely, R. A., Weiss, R. F., Wanninkhof, R. H., Chipman, D. W., Sutherland, S. C., and Takahashi, T.  
2331 T.: Global Air–sea Flux of CO<sub>2</sub>: An estimate based on measurements of sea–air pCO<sub>2</sub> difference, *Proceedings of the*  
2332 *National Academy of Sciences*, 94(16), 8292–8299, <https://doi.org/10.1073/pnas.94.16.8292>, 1997.

2333 Takahashi, T., Sutherland, S. C., Sweeney, C., Poisson, A., Metzl, N., Tilbrook, B., Bates, N., Wanninkhof, R.,  
2334 Feely, R. A., Sabine, C., Olafsson, J., and Nojiri, Y.: Global sea–air CO<sub>2</sub> flux based on climatological surface ocean  
2335 pCO<sub>2</sub>, and seasonal biological and temperature effects, *Deep Sea Research Part II: Topical Studies in*  
2336 *Oceanography*, 49(9–10), 1601–1622, [https://doi.org/10.1016/s0967-0645\(02\)00003-6](https://doi.org/10.1016/s0967-0645(02)00003-6), 2002.

2337 Takahashi, T., Sutherland, S. C., Wanninkhof, R., Sweeney, C., Feely, R. A., Chipman, D. W., Hales, B., Friederich,

2338 G., Chavez, F., Sabine, C., Watson, A., Bakker, D. C. E., Schuster, U., Metzl, N., Yoshikawa-Inoue, H., Ishii, M.,  
 2339 Midorikawa, T., Nojiri, Y., Körtzinger, A., Steinhoff, T., and de Baar, H. J. W.: Climatological mean and decadal  
 2340 change in Surface Ocean  $p\text{CO}_2$ , and net sea–air  $\text{CO}_2$  flux over the Global Oceans, Deep Sea Research Part II:  
 2341 Topical Studies in Oceanography, 56(8–10), 554–577, <https://doi.org/10.1016/j.dsr2.2008.12.009>, 2009.

2342 Takahashi, T., Sutherland, S. C., Kozyr, A.: LDEO Database (Version 2019): Global Ocean Surface Water Partial  
 2343 Pressure of  $\text{CO}_2$  Database: Measurements Performed During 1957-2019 (NCEI Accession 0160492), NOAA  
 2344 National Centers for Environmental Information, Dataset, [https://doi.org/10.3334/cdiac/otg.ndp088\(v2015\)](https://doi.org/10.3334/cdiac/otg.ndp088(v2015)), 2017.

2345 Takano, Y., Ilyina, T., Tjiputra, J., Eddebbar, Y. A., Berthet, S., Bopp, L., Buitenhuis, E., Butenschön, M., Christian,  
 2346 J. R., Dunne, J. P., Gröger, M., Hayashida, H., Hieronymus, J., Koenig, T., Krasting, J. P., Long, M. C., Lovato, T.,  
 2347 Nakano, H., Palmieri, J., Schwinger, J., Séférian, R., Suntharalingam, P., Tatebe, H., Tsujino, H., Urakawa, S.,  
 2348 Watanabe, M., and Yool, A.: Simulations of ocean deoxygenation in the historical era: insights from forced and  
 2349 coupled models. *Front. Mar. Sci.* 10:1139917. doi: 10.3389/fmars.2023.1139917, 2023.

2350 Tanhua, T., Jones, E. P., Jeansson, E., Jutterström, S., Smethie, W. M., Wallace, D. W., and Anderson, L. G.:  
 2351 Ventilation of the Arctic Ocean: Mean ages and inventories of Anthropogenic  $\text{CO}_2$  and CFC-11, *Journal of*  
 2352 *Geophysical Research: Oceans*, 114(C1), <https://doi.org/10.1029/2008jc004868>, 2009.

2353 Tanhua, T., van Heuven, S., Key, R. M., Velo, A., Olsen, A., and Schirnack, C.: Quality control procedures and  
 2354 methods of the CARINA database, *Earth Syst. Sci. Data*, 2, 35-49, <https://doi.org/10.5194/essd-2-35-2010>, 2010.

2355 Tanhua, T., Olsen, A., Hoppema, M., Jutterström, S., Schirnack, C., van Heuven, S. M. A. C., Velo, A., Lin, X.,  
 2356 Kozyr, A., Álvarez, M., Bakker, D. C. E., Brown, P. J., Falck, E., Jeansson, E., Lo Monaco, C., Ólafsson, J., Pérez,  
 2357 F. F., Pierrot, D., Ríos, A. F., Sabine, C. L., Schuster, U., Steinfeldt, R., Stendardo, I., Anderson, L. G., Bates, N.,  
 2358 Bellerby, R. G. J., Blindheim, J., Bullister, J. L., Gruber, N., Ishii, M., Johannessen, T., Jones, E. P., Köhler, J.,  
 2359 Körtzinger, A., Metzl, N., Murata, A., Musielewicz, S., Omar, A. M., Olsson, K. A., de la Paz, M., Pfeil, B., Rey, F.,  
 2360 Rhein, M., Skjelvan, I., Tilbrook, B., Wanninkhof, R., Mintrop, L. J., Wallace, D. W. R., Key, R. M.: The CARbon  
 2361 dioxide IN the Atlantic Ocean (CARINA) Database V1.1 2010 (NCEI Accession 0113899). NOAA National  
 2362 Centers for Environmental Information. Dataset. <https://doi.org/10.3334/cdiac/otg.ndp091>, 2013.

2363 Tans, P., and Keeling, R.: Trends in atmospheric carbon dioxide, NOAA Global Monitoring Laboratory (Boulder,  
 2364 Colorado, USA) and Scripps Institution of Oceanography (LaJolla, California, USA),  
 2365 <https://gml.noaa.gov/ccgg/trends/> and <https://scrippsco2.ucsd.edu/>, 2025.

2366 Terhaar, J.: Composite model-based estimate of the ocean carbon sink from 1959 to 2022, *Biogeosciences*, 22,  
 2367 1631–1649, <https://doi.org/10.5194/bg-22-1631-2025>, 2025.

2368 Terhaar, J., Orr, J. C., Ethé, C., Regnier, P., and Bopp, L.: Simulated Arctic Ocean response to doubling of riverine  
 2369 carbon and nutrient delivery, *Global Biogeochemical Cycles*, 33, 1048–1070,

2370 <https://doi.org/10.1029/2019GB006200>, 2019.

2371 Terhaar, J., Tanhua, T., Stöven, T., Orr, J. C., and Bopp, L.: Evaluation of data-based estimates of anthropogenic  
2372 carbon in the Arctic Ocean, *Journal of Geophysical Research: Oceans*, 125(6),  
2373 <https://doi.org/10.1029/2020jc016124>, 2020.

2374 Terhaar, J., Torres, O., Bourgeois, T., and Kwiatkowski, L.: Arctic Ocean acidification over the 21st century co-  
2375 driven by anthropogenic carbon increases and freshening in the CMIP6 model ensemble, *Biogeosciences*, 18, 2221–  
2376 2240, <https://doi.org/10.5194/bg-18-2221-2021>, 2021a.

2377 Terhaar, Jens, Frölicher, T. L., & Joos, F.: Southern Ocean anthropogenic carbon sink constrained by sea surface  
2378 salinity, *Science Advances*, 7(18), <https://doi.org/10.1126/sciadv.abd5964>, 2021b.

2379 Terhaar, J., Frölicher, T. L., Joos, F.: Simulated and constrained Southern Ocean carbon sink from 1850 to 2100  
2380 based on CMIP5 and CMIP6 models. *SEANOE*. <https://doi.org/10.17882/103938>, 2021c.

2381 Terhaar, J., Frölicher, T. L., and Joos, F.: Observation-constrained estimates of the Global Ocean Carbon Sink from  
2382 earth system models, *Biogeosciences*, 19(18), 4431–4457, <https://doi.org/10.5194/bg-19-4431-2022>, 2022a.

2383 Terhaar, J., Frölicher, T. L., and Joos, F.: Simulated and constrained ocean carbon sink from 1850 to 2100 based on  
2384 CMIP6 models. *SEANOE*. <https://doi.org/10.17882/103934>, 2022b.

2385 Terhaar, J., Frölicher, T. L., and Joos, F.: Ocean acidification in emission-driven temperature stabilization scenarios:  
2386 The role of TCRE and non-CO<sub>2</sub> greenhouse gases, *Environmental Research Letters*, 18(2), 02403,  
2387 <https://doi.org/10.1088/1748-9326/acf91>, 2023.

2388 Terhaar, J., Tanhua, T., Stöven, T., Orr, J. C., Bopp, L.: Observation-based anthropogenic carbon estimates in the  
2389 Arctic Ocean. *SEANOE*. <https://doi.org/10.17882/103920>, 2024.

2390 van Heuven, S., Pierrot, D., Rae, J. W. B., Lewis, E., Wallace, D. W. R.: MATLAB Program Developed for CO<sub>2</sub>  
2391 System Calculations, ORNL/CDIAC-105b, Carbon Dioxide Information Analysis Center, Oak Ridge National  
2392 Laboratory, Oak Ridge, TN, USA, 2011.

2393 van Hooidek, R.: Modeled ocean acidification data in the Gulf of Mexico and wider Caribbean using satellites and  
2394 climate model data for the Ocean Acidification Products for the Gulf of Mexico and East Coast project from 2014-  
2395 01-01 to 2020-12-31 (NCEI Accession 0245950), NOAA National Centers for Environmental Information, Dataset,  
2396 <https://doi.org/10.25921/tt1c-dx53>, 2022.

2397 Velo, A., Pérez, F. F., Tanhua, T., Gilcoto, M., Ríos, A. F., and Key, R. M.: Total alkalinity estimation using MLR  
2398 and neural network techniques, *J. Mar. Syst.*, 111–112, 11–18, <https://doi.org/10.1016/j.jmarsys.2012.09.002>, 2013.

2399 Wanninkhof, R., Pierrot, D., Sullivan, K., Barbero, L., and Triñanes, J.: Gridded surface water fugacity of CO<sub>2</sub>

2400 observations, and calculated pH, aragonite saturation state and air–sea CO<sub>2</sub> fluxes in the northern Caribbean Sea  
2401 from 2002 through 2019 (NCEI Accession 0207749), NOAA National Centers for Environmental Information,  
2402 Dataset, <https://doi.org/10.25921/2swk-9w56>, 2019.

2403 Wanninkhof, R., Pierrot, D., Sullivan, K., Barbero, L., and Triñanes, J.: A 17-year dataset of surface water fugacity  
2404 of CO<sub>2</sub> along with calculated pH, aragonite saturation state and air–sea CO<sub>2</sub> fluxes in the northern Caribbean Sea,  
2405 *Earth Syst. Sci. Data*, 12, 1489–1509, <https://doi.org/10.5194/essd-12-1489-2020>, 2020.

2406 Wanninkhof, R., Triñanes, J., Pierrot, D., Munro, D. R., Sweeney, C., and Fay, A. R.: AOML\_ET: Partial pressure  
2407 of CO<sub>2</sub> (*p*CO<sub>2</sub>) and air–sea CO<sub>2</sub> fluxes for the global ocean, along with the predictor variables from 1998-01-01 to  
2408 2023-12-30, using an Extra Trees (extremely randomized trees) machine learning (NCEI Accession 0298989),  
2409 NOAA National Centers for Environmental Information, Dataset, <https://doi.org/10.25921/0s8y-q287>, 2024.

2410 Wanninkhof, R., Triñanes, J., Pierrot, D., Munro, D. R., Sweeney, C., and Fay, A. R.: Trends in sea-air CO<sub>2</sub> fluxes  
2411 and sensitivities to atmospheric forcing using an extremely randomized trees machine learning approach, *Global*  
2412 *Biogeochemical Cycles*, 39, <https://doi.org/10.1029/2024GB008315>, 2025.

2413 Watson, A. J., Schuster, U., Shutler, J. D., Holding, T., Ashton, I. G., Landschützer, P., Woolf, D., and Goddijn-  
2414 Murphy, L.: Revised estimates of ocean-atmosphere CO<sub>2</sub> flux are consistent with ocean carbon inventory, *Nature*  
2415 *Communications*, 11(1), 1–6, <https://doi.org/10.1038/s41467-020-18203-3>, 2020.

2416 Watson, A. J., Schuster, U., Shutler, J. D., Holding, T., Ashton, I. G., Landschützer, P., Woolf, D., and Goddijn-  
2417 Murphy, L.: Revised estimates of ocean-atmosphere CO<sub>2</sub> flux accounting for near-surface temperature and salinity  
2418 deviations from 1985-01-01 to 2019-12-31 (NCEI Accession 0301544), NOAA National Centers for Environmental  
2419 Information, Dataset, <https://doi.org/10.25921/2dp5-xm29>, 2025.

2420 Wilkinson, M. D., Dumontier, M., Aalbersberg, I. J., Appleton, G., Axton, M., Baak, A., Blomberg, N., Boiten, J.-  
2421 W., da Silva Santos, L. B., Bourne, P. E., Bouwman, J., Brookes, A. J., Clark, T., Crosas, M., Dillo, I., Dumon, O.,  
2422 Edmunds, S., Evelo, C. T., Finkers, R., Gonzalez-Beltran, A., Gray, A. J. G., Groth, P., Goble, C., Grethe, J. S.,  
2423 Heringa, J., Hoen, P., Hooft, R., Kuhn, T., Kok, R., Kok, J., Scott J. Lusher, S. J., Martone, M. E., Mons, A., Packer,  
2424 A. L., Persson, B., Rocca-Serra, P., Roos, M., van Schaik, R., Sansone, S.-A., Schultes, E., Sengstag, T., Slater, T.,  
2425 Strawn, G., Swertz, M. A., Thompson, M., van der Lei, J., van Mulligen, E., Velterop, J., Waagmeester, A.,  
2426 Wittenburg, P., Wolstencroft, K., Zhao, J., Mons, B.: The Fair Guiding Principles for Scientific Data Management  
2427 and Stewardship, *Scientific Data*, 3(1), <https://doi.org/10.1038/sdata.2016.18>, 2016.

2428 Winn, C. D., MacKenzie, F. T., Carrillo, C. J., Sabine, C. L., and Karl, D. M.: Air–sea carbon dioxide exchange in  
2429 the North Pacific Subtropical Gyre: Implications for the global carbon budget, *Global Biogeochem Cycles*, 8, 157-  
2430 163, <https://doi.org/10.1029/94GB00387>, 1994.

2431 Winn, C. D., Li, Y.-H., Mackenzie, F. T., and Karl, D. M.: Rising surface ocean dissolved inorganic carbon at the

Deleted: sea-air

2433 Hawaii Ocean Time-series site, *Mar. Chem.*, 60, 33-47, [https://doi.org/10.1016/S0304-4203\(97\)00085-6](https://doi.org/10.1016/S0304-4203(97)00085-6), 1998.

2434 Wu, Z., Lu, W., Roobaert, A., Song, L., Yan, X.-H., and Cai, W.-J.: A machine-learning reconstruction of sea  
2435 surface  $p\text{CO}_2$  in the North American Atlantic Coastal Ocean Margin from 1993 to 2021, *Earth Syst. Sci. Data*.  
2436 <https://doi.org/10.5194/essd-17-43-2025>, 2025.

2437 Zeng, J., Iida, Y., Matsunaga, T., Shirai, T.: Surface ocean  $\text{CO}_2$  concentration and air–sea flux estimate by machine  
2438 learning with modelled variable trends, *Front. Mar. Sci.*, 9, 989233, <https://doi.org/10.3389/fmars.2022.989233>,  
2439 2022.

2440 Zeng, J.: NIES-ML3 ensemble product of surface ocean  $\text{CO}_2$  concentrations and air–sea  $\text{CO}_2$  fluxes reconstructed by  
2441 using three machine learning models with new  $\text{CO}_2$  trends, National Institute for Environmental Studies (NIES),  
2442 Japan, <https://doi.org/10.17595/20220311.001>, 2022.

2443 Zhang, H., Menemenlis, D., and Fenty, I. G.: ECCO LLC270 ocean-ice state estimate (Tech. Rep.), Jet Propulsion  
2444 Laboratory, California Institute of Technology, <http://hdl.handle.net/1721.1/119821>, 2018.

2445 Zhong, G., Li, X., Song, J., Qu, B., Wang, F., Wang, Y., ... & Duan, L. Reconstruction of global surface ocean  $p\text{CO}_2$   
2446 using region-specific predictors based on a stepwise FFNN regression algorithm. *Biogeosciences*, 19, 845-859,  
2447 <https://doi.org/10.5194/bg-19-845-2022>, 2022.

2448 Zhong, G., Li, X., Song, J., Qu, B., Wang, F., Wang, Y., Zhang, B., Cheng, L., Ma, J., Yuan, H., Duan, L., Li, N.,  
2449 Wang, Q., Xing, J., and Dai, J.: A global monthly 3D field of seawater pH over 3 decades: a machine learning  
2450 approach, *Earth Syst. Sci. Data*, 17, 719–740, <https://doi.org/10.5194/essd-17-719-2025>, 2025.

2451 Zweng, M. M., Reagan, J. R., Antonov, J. I., Locarnini, R. A., Mishonov, A. V., Boyer, T. P., Garcia, H. E.,  
2452 Baranova, O. K., Johnson, D. R., Seidov, D., and Biddle, M. M.: *World Ocean Atlas 2013, Volume 2: Salinity*,  
2453 edited by: Levitus, S. and Mishonov, A., NOAA Atlas NESDIS 74, 39 pp., 2013.

2454 Zweng, M. M., Reagan, J. R., Seidov, D., Boyer, T. P., Locarnini, R. A., Garcia, H. E., Mishonov, A. V., Baranova,  
2455 O. K., Weathers, K. W., Paver, C. R., Smolyar, I. V.: *World Ocean Atlas 2018, Volume 2: Salinity*, edited by  
2456 Mishonov, A., NOAA Atlas NESDIS 82, 2019.